UNIVERSITY OF CALIFORNIA, SAN DIEGO

Patterning of the cardiac inflow tract in zebrafish

A dissertation submitted in partial satisfaction of the
requirements for the degree Doctor of Philosophy

in

Biology

by

Hannah Knight

Committee in charge:

Professor Deborah Yelon, Chair
Professor Neil Chi
Professor Kimberly Cooper
Professor Sylvia Evans
Professor David Traver

2017

The Dissertation of Hannah Knight is approved, and it is acceptable

in quality and form for publication on microfilm and electronically:

_____

_____

_____

_____

_____

Chair

University of California, San Diego
2017

TABLE OF CONTENTS

Signature Page ……...iii

Table of Contents …….....iv

List of Figures ……..v

List of Tables …….....vii

Acknowledgments …..…….....viii

Vita ……..…….....x

Abstract of the Dissertation ……..xi

Chapter 1: Inflow tract development ……..……...1

Chapter 2: Patterning and differentiation of the cardiac inflow tract in zebrafish ……..39

Chapter 3: Hedgehog signaling restricts formation of the cardiac inflow tract in zebrafish ……76

Chapter 4: Future directions toward understanding inflow tract patterning ...118

References ……..138

Appendix: Utilizing zebrafish to understand second heart field development ……161

LIST OF FIGURES

Figure 1.1. Location and molecular marker signature of the zebrafish IFT ….31

Figure 1.2. Cells located in the IFT are responsible for pacemaking activity ..32

Figure 1.3. Schematic of the pacemaker gene regulatory network ...……...33

Figure 1.4. Murine pacemaker cells originate from the lateral edges of the heart fields ……..……...34

Figure 1.5. Schematic of the Hh signaling pathway 35

Figure 1.6. Hh signaling promotes production of cardiomyocytes in both chambers ……..…….36

Figure 1.7. Schematic of the Bmp signaling pathway …..……..37

Figure 1.8. Bmp signaling promotes production of atrial cardiomyocytes …..38

Figure 2.1. IFT cardiomyocytes express a set of pacemaker markers ……69

Figure 2.2. A biography of IFT cardiomyocytes …….70

Figure 2.3. IFT progenitors originate from a ventral portion of the lateral margin ……..71

Figure 2.4. IFT progenitors reside in lateral portions of the heart fields ..……72

Figure 2.5. IFT cardiomyocytes emerge by 23 somites and append to the venous pole of the heart tube ...……..73

Figure 2.6. IFT cardiomyocytes differentiate after atrial chamber cardiomyocytes ……...……..74

Figure 3.1. The IFT is expanded in *smoothened* mutants ...……103

Figure 3.2. Enlarged IFT arises by 24 hpf in *smo* mutants ...…...……...104

Figure 3.3. Hh signaling acts during gastrulation and early somitogenesis to limit IFT cell production and promote atrial cell production …….105

Figure 3.4. IFT cell number is unaffected by increased Hh signaling ……107

Figure 3.5. Expression of *ltbp3* in outflow tract progenitors responds to Hh signaling ……..…..……108

Figure 3.6. Intensity of *nkx2.5* expression is reduced in the Hh-deficient anterior lateral plate mesoderm ……..……..…..……109

Figure 3.7. Overexpression of *nkx2.5* can partially rescue the expansion of the IFT in Hh-deficient embryos ……..…..……...110

Figure 3.8. Bmp activity promotes production of IFT cardiomyocytes ……...112

Figure 3.9. Bmp activity promotes establishment and maintenance of IFT cardiomyocytes ……..…..……...113

Figure 3.10. IFT cell number is partially rescued in *smo;laf* double mutants 114

LIST OF TABLES

Table 3.1. Heart rate is abnormal in *smo* mutants at 48 hpf …….....115

Table 3.2. Antibodies used for immunofluorescence …….....116

ACKNOWLEDGMENTS

I would like to acknowledge several individuals who contributed to this work. First, I would like to thank Debbie for being my graduate advisor. Debbie is a superb scientist, and she has generously imparted her wisdom, scientific acumen, and attention to detail over the past several years. Debbie's mentorship is unparalleled, and I am so grateful for her guidance and support. Second, I would like to thank my committee members for their insightful feedback on my work, through all its iterations. Finally, I would like to thank all the members of the Yelon lab, both past and present. My lab colleagues have provided scientific insight, technical assistance, and invaluable friendship.

A modified version of Chapter 2 will be submitted for publication as a Resource Article in *Developmental Biology* (Knight, Hannah; Ren, Jie; Chi, Neil; Yelon, Deborah. "Patterning and differentiation of the cardiac inflow tract in zebrafish"). Please note that a portion of the material presented in Chapter 2 is redundant with a portion of the introductory content presented in Chapter 1. Hannah Knight and Jie Ren designed and performed the experiments presented in Chapter 2, interpreted the data, and coauthored the manuscript. Neil Chi and Deborah Yelon designed experiments, interpreted the data, and contributed to the editing of the manuscript. Hannah Knight was the primary investigator and author of this material.

A modified version of Chapter 3 will be submitted for publication as a Research Article in *Development* (Knight, Hannah; Ren, Jie; Chi, Neil; Yelon,

Deborah. “Hedgehog signaling restricts formation of the cardiac inflow tract in zebrafish”). Hannah Knight designed and performed the experiments presented in Chapter 3, with assistance from Jie Ren, Tina Vajdi, and Wei Gordon. Hannah Knight analyzed and interpreted the data and wrote the manuscript. Jie Ren and Neil Chi shared reagents, assisted with data analysis, and provided thoughtful feedback and insight throughout the project and during the editing of the manuscript. Deborah Yelon designed experiments, interpreted the data, and contributed to the editing of the manuscript. Hannah Knight was the primary investigator and author of this material.

The appendix, in full, is a reformatted reprint of the following book chapter: Knight, H.G., Yelon, D., 2016. “Utilizing Zebrafish to Understand Second Heart Field Development,” in: Nakanishi, T., Markwald, R.R., Baldwin, H.S., Keller, B.B., Srivastava, D., Yamagishi, H. (Eds.), Etiology and Morphogenesis of Congenital Heart Disease: From Gene Function and Cellular Interaction to Morphology. Springer Japan, Tokyo, pp. 193–199. Hannah Knight was the primary investigator and author of this paper.

VITA

2007 – 2011 Bachelor of Science, University of California, Los Angeles

2011 – 2017 Doctor of Philosophy, University of California, San Diego

ABSTRACT OF THE DISSERTATION

Patterning of the cardiac inflow tract in zebrafish

by

Hannah Knight

Doctor of Philosophy in Biology

University of California, San Diego, 2017

Professor Deborah Yelon, Chair

The mature heart is comprised of multiple types of specialized cardiomyocytes, each with distinct functional attributes. However, the mechanisms that specify discrete populations of cardiac progenitors are not well understood. For example, it is clear that cardiac pacemaking activity is

confined to a specialized population of cells in the cardiac venous pole, but the signals that create the appropriate number of pacemaker cardiomyocytes remain unknown. We have therefore sought to understand how pacemaker cells develop in the zebrafish embryo. First, we have investigated pacemaker cells in the inflow tract (IFT) of wild-type zebrafish embryos. We have observed that IFT cardiomyocytes express a suite of molecular markers that are reminiscent of mammalian pacemaker cells and that confer attributes specific to this population. Furthermore, we have determined that IFT progenitors are localized to discrete areas at the edges of the heart fields, prior to their differentiation. Next, we have shown that the specification of this IFT progenitor population is influenced by opposing inputs from two signaling pathways: Hedgehog (Hh) signaling and Bmp signaling. Given our prior finding that Hh signaling promotes cardiomyocyte production, we were surprised to discover that Hh signaling also acts to delimit the number of IFT cardiomyocytes. Using both genetic and pharmacological manipulations of the Hh pathway, we have shown that loss of Hh signaling results in dramatically expanded expression of IFT markers. Conversely, Bmp signaling drives IFT formation, as embryos with reduced Bmp signaling have a diminished IFT. Timed manipulations of Hh and Bmp activity have demonstrated that both signals act during early steps of cardiac patterning to define IFT size. Intriguingly, reducing both Hh and Bmp signaling restores a nearly normal number of IFT cells. We therefore propose a model in which IFT specification

relies on both limited amounts of Hh signaling and robust levels of Bmp signaling, which together set appropriate boundaries for the IFT progenitor population. Our findings reveal novel mechanisms of cardiac patterning; in the long term, these studies could contribute to our understanding of congenital heart disease and improve efforts to generate pacemaker cells in vitro for use in regenerative medicine.

Chapter 1: Inflow tract development

The inflow tract contains specialized cardiomyocytes

In order to create a functional heart, cardiac progenitor cells must give rise to a diverse array of specialized cardiac cell types. These distinct populations arise during cardiac patterning, a process that incorporates multiple signals in order to specify a variety of lineages in the appropriate ratios and locations. This patterning process occurs very early in embryonic development, yet it is the foundation of a lifetime of efficient circulation. Though the field has made remarkable progress in understanding multiple aspects of cardiac development, early cardiac patterning remains relatively mysterious.

As part of our ongoing efforts to understand cardiac patterning, we have investigated the mechanisms responsible for establishing one specific cardiac cell type: the pacemaker cell. Pacemaker cells initiate the action potentials that generate the heartbeat, and they are further distinguished from other cardiomyocytes by both their location and their expression of molecular markers (Liang et al., 2017; van Weerd and Christoffels, 2016). The unique conductive properties of pacemaker cells allow them to control conduction in the rest of heart (Choudhury et al., 2015; Monfredi et al., 2010). As a result, pacemaker cells are responsible for maintaining synchronized, rhythmic contractions of the cardiac chambers.

In mammals, pacemaker cells are located in a tight bundle of cells known as the sinoatrial node (SAN). Located at the junction of the right atrium

with the sinus venosus, the SAN spontaneously generates action potentials that set the pace for the entire cardiac conduction system (Mangoni and Nargeot, 2008). SAN action potentials are rapidly conducted through the atria, then delayed at the atrioventricular node before moving into the ventricular conduction system (Mangoni and Nargeot, 2008).

When pacemaker cells malfunction due to congenital malformation, disease, or aging, it can result in arrhythmia, insufficient circulation, or even sudden cardiac death (Choudhury et al., 2015; Dobrzynski et al., 2007). Currently, the only effective treatment is costly implantable electronic pacemakers (Mulpuru et al., 2017). The search for biological alternatives is in progress and has focused on generating pacemaker-like cells through directed differentiation of stem cells or through reprogramming of quiescent cardiomyocytes (Bakker et al., 2012; Hu et al., 2014; Jung et al., 2014; Kapoor et al., 2013; Nam et al., 2014; Protze et al., 2017; Scavone et al., 2013). However, these approaches have failed to yield efficient induction of pacemaker cells that are functionally equivalent to endogenous pacemaker cardiomyocytes (Boink et al., 2015; Nam et al., 2014). To improve the efficacy of these efforts, additional insight is necessary; in particular, it would be highly informative to elucidate the genetic regulation of pacemaker cells development in vivo so that this can be recapitulated in vitro. Furthermore, understanding how the pacemaker population develops during embryonic stages may shed light on the etiology of congenital arrhythmias. Therefore, it is worthwhile to

investigate open questions that concern the specification and differentiation of SAN cardiomyocytes.

It is unclear how pacemaker cells are specified in the early embryo, when pacemaker specification occurs, and where pacemaker progenitors arise. Fate mapping experiments in avian embryos suggest that pacemaker progenitors reside in a location posterior to the heart fields (Bressan et al., 2013). However, these data are inconsistent with genetic lineage tracing studies in mice that suggest that the SAN originates from the lateral portion of the heart fields (Christoffels, 2006; Mommersteeg et al., 2007b; Wiese et al., 2009), so the location of pacemaker progenitors cannot yet be precisely defined. Additional fate mapping could help resolve open questions regarding the origins of pacemaker cells, but the technical limitations of mammalian fate mapping have precluded investigation into the spatial organization of SAN progenitors at very early stages.

Furthermore, it is unclear how SAN differentiation is regulated: what initiates differentiation of SAN progenitors, and what refines this population as the embryonic heart matures? Here, many studies have made significant inroads in understanding the genetic network that functions during SAN differentiation (Blaschke et al., 2007; Christoffels, 2006; Espinoza-Lewis et al., 2009; Hoogaars et al., 2007; Liang et al., 2015; Mommersteeg et al., 2007b; Mori et al., 2006; Wiese et al., 2009). However, the upstream signals that

initiate the pacemaker genetic network are not yet understood and are worthy of further exploration.

The goal of this dissertation is to use the zebrafish embryo as a model organism to examine open questions regarding pacemaker development. Where do pacemaker cells originate? How does the embryo generate the appropriate number of pacemaker cells, rather than too many or too few? In zebrafish, pacemaker cells are located in the cardiac inflow tract (IFT), and we have studied the IFT in the context of both normal and abnormal cardiac patterning. Specifically, this dissertation explores three topics: characterization of the wild-type IFT, analysis of the role of Hedgehog (Hh) signaling in IFT development, and analysis of the role of Bone morphogenetic protein (Bmp) signaling in IFT development. As an introduction to this work, I will first review the characteristics of the zebrafish IFT in comparison to mammalian pacemaker cells. Then, I will discuss literature investigating the regulation of pacemaker cell development and the origin of pacemaker cells. Next, I will review the components of the Hh signaling pathway and the roles of Hh signaling during cardiac development. Finally, I will review the components of the Bmp signaling pathway and discuss its roles during cardiac development. This review will provide context for the novel data presented in Chapters 2 and 3.

The zebrafish inflow tract

The zebrafish embryo has emerged as an ideal model in which to investigate the specification and differentiation of pacemaker cardiomyocytes. In the zebrafish heart, the myocardium at the sinoatrial junction, which we refer to as the IFT, acts as a functional equivalent to the mammalian SAN (Tessadori et al., 2012). Early stages of IFT development can be examined using zebrafish because external fertilization allows convenient access to the early embryo from the onset of its development (Poon and Brand, 2013). Additionally, the optical transparency of zebrafish embryos allows direct visualization of the differentiation of pacemaker cardiomyocytes as it occurs (Staudt and Stainier, 2012). Furthermore, cardiac conduction can be easily analyzed in live embryos (Chi et al., 2008), revealing the functional consequences of IFT abnormalities. Most importantly, there is a growing body of research that has laid the groundwork for investigating the zebrafish IFT and its pacemaker activity (Arrenberg et al., 2010; Chi et al., 2008; Tessadori et al., 2012), so the zebrafish community is currently poised to contribute substantial information on the development of pacemaker cardiomyocytes.

Within the IFT of adult zebrafish, a population of pacemaker cells was recently identified and rigorously evaluated for homology to the mammalian SAN (Tessadori et al., 2012). This population is located at the junction between the atrium and the sinus venosus (Tessadori et al., 2012), as is the mammalian SAN (Anderson et al., 1979; Mangoni and Nargeot, 2008;

Sánchez-Quintana et al., 2005). Cardiomyocytes in the IFT initiate action potentials spontaneously, unlike the neighboring chamber myocardium (Tessadori et al., 2012), and the electrophysiological properties of these action potentials mimic mammalian pacemaker cells (Bleeker et al., 1980; Mangoni and Nargeot, 2008; Verheijck et al., 2001). Indeed, IFT cells express the pacemaker channel *hcn4* (Tessadori et al., 2012), which is enriched in the SAN and required to establish the unique electrophysiological properties of pacemaker cardiomyocytes (Garcia-Frigola et al., 2003; Moosmang et al., 2001; Stieber et al., 2003). Furthermore, it was observed that the zebrafish IFT cells express the markers *isl1, bmp4,* and *tbx2b* along with the myocardial marker *myl7* (Tessadori et al., 2012), all of which are expressed in the mammalian SAN as well (Christoffels, 2006). Isl1 serves as a useful marker of this population, since it is expressed specifically in the adult pacemaker population, but not in the adjacent chamber myocardium (Tessadori et al., 2012). Thus, the population of Isl1+ pacemaker cardiomyocytes in the adult zebrafish IFT is similar to the adult mammalian SAN in its location, molecular marker expression, and function, providing strong evidence for homology between these structures.

In fact, these similarities in anatomical structure, gene expression, and electrophysiological function between the zebrafish adult IFT and murine SAN are preserved from the characteristics of the zebrafish IFT during embryonic stages. In the zebrafish embryo, differentiated IFT cardiomyocytes are located

at the sinoatrial junction, and it has been demonstrated that pacemaker function is confined to this location. Embryos carrying the transgene *Tg(cmlc2:gCaMP),* which expresses a fluorescent calcium indicator in cardiomyocytes, have been utilized for optical mapping of calcium flux, which reveals that cardiac conduction originates in the venous pole (Chi et al., 2008). Furthermore, when IFT cells are hyperpolarized using transgenic light-gated ion channels, the heartbeat ceases, indicating that this region is required to initiate the heartbeat (Arrenberg et al., 2010). This pacemaking activity is present in a broad ring at the venous pole at 24 hours post fertilization (hpf), becomes refined to the IFT at 48 hpf, and is then further whittled down to the inner curvature of the IFT by 72 hpf (Figure 1.2 and (Arrenberg et al., 2010). Cardiomyocytes in the embryonic IFT also express the molecular marker Isl1, along with a group of pacemaker markers that includes *bmp4, tbx18, hcn4,* and *shox2* (Begemann et al., 2002; Blaschke et al., 2007; Chin et al., 1997; Poon et al., 2016; Witzel et al., 2012). These functional attributes and molecular markers establish the IFT as the primary cardiac pacemaker in the zebrafish embryo and demonstrate its functional and developmental homology to the mammalian SAN.

Regulation of IFT development

The molecular markers expressed in the IFT have been studied extensively during murine cardiac development, and these factors form the

basis of a genetic network that is required for formation of a functional SAN (Figure 1.3). In this network, several transcription factors promote expression of the pacemaker genetic program, including Tbx18, Tbx2, Tbx3, Isl1, and Shox2. In adjacent non-pacemaker cardiomyocytes, which we refer to as chamber cardiomyocytes, the transcription factor Nkx2.5 represses the pacemaker program and promotes chamber identity. It remains to be seen whether this entire genetic network plays a conserved role in the zebrafish IFT. Here, we compare the role of each factor in development of the mammalian SAN and the zebrafish IFT. Isl1 and Shox2 have been studied in zebrafish IFT development and are indeed required for normal pacemaker function, but Tbx18 and other Tbx factors warrant further study to evaluate their function in the context of the zebrafish.

Shared requirement for Isl1 and Shox2 in zebrafish and mammalian pacemaker cells

Isl1 has been used as a marker for the zebrafish IFT and is required in both zebrafish and mouse for normal pacemaker cell development. In mouse, *Isl1* is thought to be transiently expressed in nearly all cardiac progenitors (Prall et al., 2007), but its expression is lost during cardiac differentiation in most populations and retained only in specific populations of differentiated cardiomyocytes, including in the SAN (Cai et al., 2003; Sun et al., 2007). In zebrafish, *isl1* is initially expressed in a broad region that overlaps with the

heart fields (Witzel et al., 2012), but after cardiac differentiation, the only cardiomyocytes that express *isl1* are in the IFT (Tessadori et al., 2012). This suggests that Isl1 might play an important role during IFT differentiation. Indeed, zebrafish *isl1* mutants add fewer cells to the venous pole, lack *bmp4* expression in the IFT, and exhibit bradycardia (de Pater et al., 2009). At later stages, these *isl1* mutants display a sinus block, indicating defective pacemaking activity (Tessadori et al., 2012). This function of ISL1 is conserved in mammals: when *Isl1* is knocked out in the pacemaker lineage, mouse embryos display arrhythmia, reduced SAN cell number, and embryonic lethality (Liang et al., 2015). These conditional knockouts also have reduced expression of SAN markers such as *Bmp4*, *Shox2*, and *Hcn4* (Liang et al., 2015). Interestingly, Isl1 is capable of limiting its own expression to regulate the number of cardiac progenitors that contribute to the IFT. When Isl1 is bound to the RA-responsive transcription factor Ajuba, it delimits the number of IFT cells added to the zebrafish venous pole, and when Ajuba is knocked down, the number of IFT cells increases dramatically (Witzel et al., 2012). Thus, Isl1 is crucial both for establishing an appropriate number of IFT cells and for directing their differentiation into functional pacemaker cardiomyocytes.

The transcription factor gene *shox2* is also required for formation of pacemaker cells in both zebrafish and mouse. In mouse embryos with mutations in *Shox2*, the SAN is hypoplastic and fails to fully differentiate, resulting in bradycardia and embryonic lethality (Blaschke et al., 2007;

Espinoza-Lewis et al., 2009). SHOX2 directly activates transcription of both *Bmp4* and *Isl1* in pacemaker cells (Hoffmann et al., 2013; Puskaric et al., 2010). In zebrafish embryos, Shox2 deficiency results in severe bradycardia (Blaschke et al., 2007), but this can be rescued by increased *isl1* expression (Hoffmann et al., 2013). SHOX2 also represses NKX2.5: murine *Shox2* mutants aberrantly express *Nkx2.5* in the SAN, and *shox2* overexpression in Xenopus embryos results in a strong downregulation of *nkx2.5* in all cardiac tissue (Blaschke et al., 2007; Espinoza-Lewis et al., 2009). In fact, SHOX2 repression of *Nkx2.5* is a crucial element in SAN differentiation, as *Nkx2.5* overexpression can recapitulate the SAN defects caused by loss of *Shox2* (Espinoza-Lewis et al., 2011). Interestingly, SHOX2 and NKX2.5 bind many of the same gene regulatory elements, indicating that the interaction of these factors determines whether cardiomyocytes adopt a pacemaker genetic signature (Ye et al., 2015). Altogether, the requirements for both Isl1 and Shox2 appear well conserved between mammals and fish, suggesting that similar genetic networks are at play in the development of the murine SAN and the zebrafish IFT.

Tbx factors may function in zebrafish IFT development

Factors in the Tbx family are essential for mammalian pacemaker cell development and deserve further study in the zebrafish IFT. The transcription factor TBX18 is expressed in the myocardium of the murine sinus venosus,

which encompasses and gives rise to the SAN (Christoffels, 2006; Mommersteeg et al., 2010). Mice deficient in TBX18 have sinus venosus abnormalities and a small, deformed SAN (Christoffels, 2006; Wiese et al., 2009), indicating that TBX18 function is required for normal development of pacemaker tissues. *tbx18* is expressed in the zebrafish IFT (Begemann et al., 2002), but it remains to be seen whether loss of Tbx18 alters IFT development in zebrafish. TBX2 and TBX3 are expressed in the murine cardiac conduction system, including in the SAN, and they repress the differentiation of chamber myocardium in these tissues (Christoffels et al., 2004; Hoogaars et al., 2004; Hoogaars et al., 2007; Mommersteeg et al., 2007b). In particular, *Tbx3* overexpression is sufficient to repress atrial chamber genes and drive formation of ectopic, functional pacemaker cells even in differentiated atrial chamber cardiomyocytes (Hoogaars et al., 2007). In zebrafish, the function and expression of Tbx3 homologues in IFT development have not been investigated. However, *tbx2b* is expressed in the IFT of adult zebrafish (Tessadori et al., 2012), and Tbx2b and Tbx3b have been found to repress the chamber genetic program and promote the conduction system genetic program in the atrioventricular canal (AVC; Ribeiro et al., 2007), indicating that the roles of these factors are likely conserved from zebrafish to mammals. It will be satisfying to investigate the function of Tbx family transcription factors in the zebrafish IFT in future studies. Furthermore, zebrafish will be an

excellent model in which to identify factors that act upstream of Tbx factors during cardiac specification and patterning.

Early origins of IFT progenitors remain unknown

Though many studies have focused on describing the gene regulatory network acting in the mature SAN, little is known about the origin of these important cells during early embryonic development. Identification of IFT progenitor cells will aid in studies of their specification. For example, understanding the physical location of IFT progenitors allows us to develop hypotheses about how diffusible factors act on this population during its patterning and can provide insight into the lineage relationships between IFT progenitors and other cardiac populations.

Previous studies in mouse and chick embryos have identified potential locations for IFT progenitors during somitogenesis stages, after gastrulation is complete. In mouse embryos, Cre-mediated lineage tracing has shown that cells of the SAN derive from lineages that express *Tbx18* and *Isl1* (Christoffels, 2006; Mommersteeg et al., 2010; Sun et al., 2007; Wiese et al., 2009). By examining the expression patterns of these markers prior to SAN formation, it was shown that SAN progenitors are located in the caudal and lateral edges of the heart fields (Mommersteeg et al., 2010). In chick embryos, fate mapping has been used to show that pacemaker progenitor cells reside posterior to the heart fields (Bressan et al., 2013). This posterior area, termed

the tertiary heart field, lacks expression of *ISL1* (Bressan et al., 2013), calling into question whether the tertiary heart field correlates with the *Isl1*-expressing SAN progenitor territory described in mouse embryos. Perhaps this discrepancy indicates that pacemaker progenitors only activate *isl1* expression upon migration toward the heart tube from the tertiary heart field. In both species, SAN progenitors seem to reside at the periphery of the heart fields, suggesting that a similar arrangement may be conserved in zebrafish during somitogenesis stages. However, the origin of pacemaker cell progenitors prior to gastrulation has not yet been addressed in any species. Previous fate mapping studies have shown that atrial, ventricular, and outflow tract (OFT) progenitor populations are each located in defined territories within the lateral margin of the zebrafish blastula and the heart fields of the zebrafish gastrula (Hami et al., 2011; Keegan et al., 2004; Schoenebeck et al., 2007), raising the possibility that IFT progenitors may also reside in a specific territory. In Chapter 2, we define the location of IFT progenitors in the zebrafish embryo, which provides clues as to which factors influence IFT patterning.

It also remains unclear exactly how cardiac progenitor cells in the early embryo are assigned to a pacemaker fate. This process seems to rely in part on canonical Wnt signaling. In chick embryos, Wnt ligands are expressed near the presumptive pacemaker progenitor population during early somitogenesis (Bressan et al., 2013). Increasing Wnt activity in cardiac progenitors causes cells to adopt electrophysiological properties reminiscent of pacemaker cells,

whereas reducing Wnt activity in pacemaker progenitors results in ectopic expression of the chamber marker *NKX2.5* (Bressan et al., 2013). These data suggest that Wnt signaling acts during early somitogenesis to promote pacemaker specification at the periphery of the heart fields, but the broad expression patterns of Wnt ligands suggests that other signals must also refine this population (Bressan et al., 2013). What other factors cooperate with canonical Wnt signaling to insure that the proper number of pacemaker progenitors is specified? It will be interesting to uncover factors that regulate IFT specification upstream of transcription factors such as Tbx18 and Shox2, and the zebrafish model is uniquely poised to provide insight on these topics. In Chapter 3, we present data investigating the roles of both Hh and Bmp signaling in this context.

Roles of Hh signaling during cardiac development

The Hh signaling cascade

Since its initial discovery as a key pattern formation pathway in Drosophila embryos, Hh signaling has emerged as a crucial regulator of embryo formation and organogenesis. Hh signaling activity relies on a family of Hedgehog ligands, including Sonic hedgehog (Shh), Indian hedgehog (Ihh), and Desert hedgehog (Dhh) (Ingham and McMahon, 2001). These ligands are secreted and bind to the membrane-bound Hh receptor, Patched (Ptc) (Bumcrot et al., 1995; Ramsbottom and Pownall, 2016). Once bound to a Hh

ligand, Ptc de-represses the membrane-bound Hh effector protein, Smoothened (Smo) (Ramsbottom and Pownall, 2016). Smo activity allows Gli transcription factors to be processed into an activator form, resulting in active transcription of Hh-responsive genes (Figure 1.5). Conversely, in the absence of Hh ligands, Ptc represses Smo activity, Gli transcription factors are processed primarily into a repressor form, and Hh-responsive genes are expressed only at basal levels (Robbins et al., 2012).

Hh ligands form a family with three branches: Shh, Ihh, and Dhh (Ingham and McMahon, 2001). Due to an ancestral genome duplication in teleosts, zebrafish have duplicate versions of both Shh and Ihh, creating a total of five ligands (Ingham and McMahon, 2001). In early embryogenesis, these ligands show an overlapping pattern with high expression in the dorsal portion of the gastrula followed by strong expression in the midline (Currie and Ingham, 1996; Ekker et al., 1995; Krauss et al., 1993). These ligands are highly similar to each other, with Shh and Ihh showing the strongest similarity and Dhh showing the most divergence (Kumar et al., 1996). While Shh and Ihh are generally more potent than Dhh, all three ligands activate the Ptc receptor (Pathi et al., 2001).

The Ptc receptor is a transmembrane protein that sits at the cell membrane when Hh signaling is inactive (Robbins et al., 2012). In vertebrates, there are two members of the Ptc family, Ptc1 and Ptc2 (Marigo et al., 1996; Motoyama et al., 1998). These genes are upregulated in response to Hh

activity, which means that elevated Ptc expression can be used as a readout for where Hh signaling is active. Ptc1 also serves as a negative regulator of Hh signaling, allowing Hh to limit its own activity (Ingham, 1998). Because of this Hh-dampening effect, embryos with mutations in Ptc1 and Ptc2 show excess Hh activity (Koudijs et al., 2008). Ptc function is defined by its interaction with the main transducer of the Hh signaling cascade, Smo.

Smo is a transmembrane protein that is classified as a member of the G protein-coupled receptor superfamily (Ayers and Thérond, 2010). Smo is expressed both maternally and zygotically in a ubiquitous expression pattern (Varga 2001, Chen 2001). When Hh signaling is inactive, Smo is located in intracellular vesicles; Smo is transferred to the cell surface of the primary cilium upon its activation (Robbins et al., 2012). At the cell membrane, phosphorylation of the Smo C-tail finalizes its activation (Ayers and Thérond, 2010). Activated Smo initiates intracellular changes that alter processing of Gli transcription factors (Ayers and Thérond, 2010; Hui and Angers, 2011; Robbins et al., 2012). Thus, in embryos with mutations in *smo*, Hh activity is absent (Chen et al., 2001; Varga et al., 2001; Zhang et al., 2001). In zebrafish, *smo* mutants lack *ptc1* expression, indicating that there is no Hh activity in these embryos (Chen et al., 2001; Varga et al., 2001). Furthermore, injection of *shh* mRNA has no effect on *smo* mutant embryos (Chen et al., 2001). These embryos show defects across multiple organ systems, including the brain, spinal cord, muscle, blood, and heart (Chen et al., 2001; Varga et al.,

2001). These embryos also show increased apoptosis and decreased proliferation globally (Chen et al., 2001). Because Gli factors are not processed into an active form in *smo* mutants, Hh target genes are not transcribed in *smo.*

Gli factors are zinc finger transcription factors that can act as either repressors or activators. Full-length, unmodified Gli factors have very limited activation activity and result in only basal expression of Hh target genes (Robbins et al., 2012). However, in the absence of Hh ligand, the majority of Gli proteins in the cell are processed into a repressive form by cleavage of the activation domain (Hui and Angers, 2011; Robbins et al., 2012). When Hh signaling is active, cleavage of the activation domain ceases, and Gli factors are instead processed into a potent activator form (Hui and Angers, 2011; Robbins et al., 2012). In zebrafish, there are four Gli factors, known as Gli1, Gli2a, Gli2b, and Gli3. As in mammals, *gli1* is highly expressed in tissues where Hh signaling is active, and its expression is reduced in *smo* (Karlstrom et al., 2003). It primarily functions as an activator (Karlstrom et al., 2003). Both Gli2a and Gli2b can act as activators in response to Hh activity or as Hh-independent repressors (Karlstrom et al., 2003, 1999, Ke et al., 2008, 2005). Similarly, Gli3 can act as an activator or a repressor; however, Gli3 is most abundant in its repressor form as Hh activity represses Gli3 expression (Tyurina et al., 2005). In *smo* mutants, *gli3* expression is expanded (Tyurina et

al., 2005). Together, these factors mediate Hh activity throughout most tissues and organs in the developing embryo.

Hh activity has been well characterized in several tissues in zebrafish through analysis of *ptc1* expression, an established output of Hh activity. In early embryogenesis, *ptc1* is expressed highly in the dorsal mesoderm during gastrulation and then in the midline mesoderm and neural tube after gastrulation (Concordet et al., 1996; Huang et al., 2012; Lewis et al., 1999), indicating that Hh signaling is highly active in those tissues. The *ptc1* promoter has been used to generate a Hh reporter line in zebrafish, *Tg(ptc1:kaede)* (Huang et al., 2012). This transgene is also highly expressed in the midline tissues (Huang et al., 2012), supporting a large role for Hh signaling in patterning the midline tissues, including both mesodermal structures and the nervous system.

Hh signaling in cardiac development

Hh signaling is particularly well known for its role in patterning the central nervous system, but it has also emerged as a crucial factor in heart development. Mouse embryos with mutations in *Smo* have a small heart that cannot progress pass the linear heart tube stage (Zhang et al., 2001). In zebrafish, *smo* mutant embryos have hearts that are small with fewer cardiomyocytes in both chambers (Figure 1.6 and Thomas et al., 2008). Timed chemical manipulations of Hh activity have shown that Hh signaling is required

during gastrulation and early somitogenesis to promote specification of cardiac progenitor cells (Thomas et al., 2008). Although cardiac progenitors are not immediately adjacent to tissues that express Hh ligands, mosaic analyses in zebrafish have shown that Hh signaling is required cell autonomously (Thomas et al., 2008). Similarly, murine cardiac progenitors can be marked with a Hh-responsive Gli1 lineage tracer, suggesting that cell autonomous reception of Hh activity is conserved between species (Thomas et al., 2008). Taken together, these data support a model in which Hh signaling acts early in embryonic development to maximize the number of mesodermal cells that adopt a cardiac progenitor fate. In these previous studies, neither the murine SAN nor the zebrafish IFT were specifically investigated to determine whether Hh signaling also promotes specification of pacemaker progenitors.

In addition to this early requirement for Hh signaling, many studies suggest that Hh signaling is also important for the development of late-differentiating cardiac progenitors in the second heart field (SHF). In anterior SHF cells that give rise to the OFT, Hh signaling is a key regulator of proliferation and cell survival (Dyer et al., 2010; Dyer and Kirby, 2009; Goddeeris et al., 2007; Lin et al., 2006), and reduced Hh signaling results in abnormal OFT development. Embryos with mutations in the Hh ligand *shh* display a single, small OFT and both atrial and ventricular septal defects (Washington Smoak et al., 2005). Likewise, embryos lacking *Smo* in the SHF have a small OFT that lacks septation (Goddeeris et al., 2007; Lin et al.,

2006). These phenotypes can be reproduced when *Shh* is excised specifically from the pharyngeal endoderm, indicating that the pharyngeal endoderm is a source of ligand for Hh signaling in the anterior SHF (Goddeeris et al., 2007). Likewise, in chick embryos, Hh signaling in the anterior SHF has been shown to drive proliferation that is required for normal OFT development (Dyer and Kirby, 2009). Importantly, this function of Hh seems to be conserved in zebrafish. Zebrafish *smo* mutant embryos seem to lack the OFT entirely and show severely reduced incorporation of SHF cells into the heart (Hami et al., 2011). These data reveal a well-conserved requirement for Hh signaling in late stages of cardiac development.

At these later stages, Hh signaling is also required in the posterior SHF cells that give rise to the atrial and atrioventricular septa in mouse. *Shh* mutants frequently exhibit atrioventricular septation defects (Goddeeris et al., 2008). This arises due to limited Hh activity in the SHF, as conditional deletion of *Smo* in the SHF reproduces these atrioventricular septation defects (Goddeeris et al., 2008). Indeed, SHH ligand from the pulmonary endoderm signals to the posterior SHF, inducing migration of SHF cells into the atrial septum (Hoffmann et al., 2009). Although the SHF contribution to the atrial and atrioventricular septa has now been studied in depth, the SHF contribution to the atrium has been less well examined. More specifically, it remains unknown whether Hh signaling plays any role in development of pacemaker cardiomyocytes in the murine SAN or the zebrafish IFT. In Chapter 3 of this

dissertation, I present novel findings indicating that Hh signaling is required for normal development of the zebrafish IFT.

Roles of Bmp signaling during cardiac development

The Bmp signaling cascade

Bmp signaling is widely known for its importance in axis formation and its reiterative use in organogenesis. Ligands in the Bmp family are secreted into the extracellular space (Wharton and Serpe, 2013), where they bind to Bmp receptors in order to activate a signaling cascade that phosphorylates Smad transcription factors, resulting in Smad-mediated transcriptional regulation (Figure 1.7 and (Katagiri and Watabe, 2016). Bmp ligands are known to act as morphogens, but their gradients are heavily modified by Bmp antagonists such as Chordin, Follistatin, and Noggin (Brazil et al., 2015). The interplay between these ligands and their antagonists forms the foundation of axis formation and then resurfaces at later stages, such as during neural tube patterning (Hegarty et al., 2013; Schier and Talbot, 2005).

Bmp ligands are a large family of secreted proteins that are dynamically expressed throughout the embryo (Katagiri and Watabe, 2016). For example, the ligand *bmp4* is originally expressed throughout the zebrafish blastula before being confined to ventral tissues during gastrulation (Chin et al., 1997; Nikaido et al., 1997). Just after gastrulation, *bmp4* expression is present in both the anterior and posterior poles of the embryo (Chin et al., 1997;

Martinez-Barbera et al., 1997). By the second day of development, *bmp4* expression is detectable in specific portions of the developing limb, neural tube, heart tube, and somites (Chin et al., 1997; Martinez-Barbera et al., 1997). Though Bmp ligands are expressed broadly and dynamically in many tissues, the best-studied role for Bmp ligands is in axis formation. Embryos with mutations in Bmp ligand genes generally show dorsalization, or loss of ventral structures, reflecting the requirement for these ligands for promoting ventral fates (Schier and Talbot, 2005). Zebrafish embryos with mutations in *bmp4* show variable dorsalization with abnormal tail patterning (Lenhart et al., 2013; Stickney et al., 2007). Likewise, zebrafish embryos with mutations in *bmp2*, known as *swirl,* are highly dorsalized (Hammerschmidt et al., 1996; Kishimoto et al., 1997). However, these phenotypes are likely limited by the redundancy between Bmp ligands. For example, restoration of *bmp2* during only early development is sufficient to produce healthy, fertile adult fish, indicating that *bmp2* has no specific role during late development or adulthood (Kishimoto et al., 1997). To substantially decrease Bmp activity, manipulation of Bmp receptors is a more effective strategy.

Bmp receptors fall into two subtypes, known as type I and type II (Yadin et al., 2016). These two subtypes come together to form heterotetrameric receptor complexes that act as serine/threonine kinases (Yadin et al., 2016). Because of the nature of these complexes, a mutation in one Bmp receptor gene is sufficient to reduce Bmp activity but will not eliminate it. For example,

zebrafish with mutations in the type I receptor *alk8* show a relatively mild dorsalized phenotype (Mintzer et al., 2001; Mullins et al., 1996). These embryos are known as *lost-a-fin (laf),* reflecting the fact that embryos lack a ventral tail fin (Mintzer et al., 2001; Mullins et al., 1996). This phenotype can be reproduced by injection of a dominant negative *alk8* construct (Payne et al., 2001). Because *alk8* is maternally supplied, maternal-zygotic *laf* mutants show much more severe dorsalization (Mintzer et al., 2001). Conversely, injection of a constitutively active *alk8* construct creates excess Bmp signaling, resulting in marked loss of dorsal structures and expansion of ventral structures, referred to as ventralization (Payne et al., 2001). This phenotype is reminiscent of embryos in which Bmp antagonists are nonfunctional.

Many Bmp antagonists exist, including well-known examples such as Chordin and Noggin (Brazil et al., 2015). In zebrafish, Bmp antagonists are expressed on the dorsal side of the embryo during gastrulation and then their expression is maintained in various midline structures during somitogenesis stages (Bauer et al., 1998; Fürthauer et al., 1999; Miller-Bertoglio et al., 1997). Embryos with mutations in Bmp antagonists generally show a ventralized phenotype (Dal-Pra et al., 2006; Schier and Talbot, 2005). For example, the *chordino* mutant, which has a mutation in *chordin,* is highly ventralized (Hammerschmidt et al., 1996; Schulte-Merker et al., 1997). Zebrafish also have three homologs of *noggin,* and all three function as dorsalizers (Fürthauer et al., 1999). The interplay between these antagonists in dorsal

tissues and Bmp ligands in ventral tissues creates an activity gradient that is necessary for normal gastrulation and mesoderm patterning.

The primary downstream effectors of Bmp activity are Smad factors, specifically Smad1, Smad5, and Smad8 (Katagiri and Watabe, 2016). Smad proteins are capable of moving into the nucleus to activate or repress transcription, but their nuclear translocation is inhibited when Bmp signaling is inactive (Sieber et al., 2009). In the presence of a Bmp ligand, Smad1/5/8 are phosphorylated by Bmp receptors and released from the receptor complex, allowing them to alter transcription (Sieber et al., 2009). Mutation of Smad factors causes a reduction in Bmp activity, resulting in dorsalization (Hild et al., 1999). Antibody staining for the active, phosphorylated form of Smad1/5/8 can be used to detect active Bmp signaling (Kurata et al., 2001). Bmp activity has also been visualized through fluorescent reporters. For example, a fluorescent reporter known as *Tg(bre:egfp)* uses a Bmp-responsive promoter element to drive expression of GFP in areas where Bmp signaling is active (Collery and Link, 2011; Laux et al., 2011). *Tg(bre:egfp)* is first visible in the tailbud starting at 6 somites, and its expression is highly dynamic after that (Collery and Link, 2011; Laux et al., 2011). *Tg(bre:egfp)* expression indicates that Bmp activity occurs in various cardiac populations. *Tg(bre:egfp)* is present in cardiomyocytes at 19 hpf, as they differentiate shortly before heart tube formation (de Pater et al., 2012; Strate et al., 2015). At 48 hpf, *Tg(bre:egfp)* is highly expressed in the AVC and weakly expressed in the IFT (Laux et al.,

2011). This expression pattern corresponds to known roles for Bmp signaling in early cardiac patterning, AVC patterning, and atrial development.

Bmp signaling in cardiac development

Interestingly, Bmp signaling seems to influence multiple aspects of cardiac development, with a special impact on atrial cardiomyocytes. Previous work in the Yelon lab has shown that *laf* mutants have fewer atrial cardiomyocytes due to reduced atrial specification (Marques and Yelon, 2009). Overexpression of the Bmp antagonist *noggin* during cardiac patterning results in a very dramatic reduction in atrial cell number relative to a smaller reduction in ventricular cell number (de Pater et al., 2012). Similarly, chemical or genetic inhibition of Bmp activity during gastrulation strongly diminishes the number of atrial cardiomyocytes, with a more modest effect on the ventricular population (Marques and Yelon, 2009). Conversely, injection of constitutively active *alk8* mRNA results in a dramatically enlarged atrium and a modestly enlarged ventricle (Marques and Yelon, 2009). These data support a model in which Bmp activity promotes production of atrial cardiomyocytes, with a notable but less potent effect on ventricular cardiomyocytes.

The requirement for Bmp activity changes markedly across different stages of cardiac development. In experiments where Bmp activity is chemically inhibited, reduced Bmp signaling during gastrulation results in a small atrial population, but reduced Bmp signaling at later stages has no effect

(Marques and Yelon, 2009). In similar experiments, *noggin* overexpression at the end of gastrulation reduces production of both atrial and ventricular cardiomyocytes, whereas *noggin* overexpression in mid-somitogenesis specifically reduces production of atrial cardiomyocytes (de Pater et al., 2012). Interestingly, transplantation experiments were used to show that Bmp signaling is required cell autonomously to promote cardiomyocyte formation, but that fine-tuning the level of Bmp activity is crucial: either very high or very low levels of Bmp activity disrupt cardiomyocyte specification (Marques and Yelon, 2009). Indeed, the inhibitory factor Smad6a is expressed in cardiac progenitors at the onset of differentiation, indicating that the level of Bmp activity is moderated in order to allow cardiac differentiation. Increasing Bmp activity, either though Smad6a knockdown or through ectopic expression of *bmp2b*, results in reduced differentiation of ventricular cardiomyocytes and ectopic expression of atrial chamber markers (De Pater 2012). Taken together, these data support the following model: during early stages of cardiac patterning, high levels of Bmp activity promote cardiac specification, with a preference for atrial rather than ventricular specification, and then during cardiac differentiation stages, moderate levels of Bmp activity promote atrial differentiation and prevent ventricular differentiation.

The requirement for Bmp activity in early cardiac development is well conserved in other species. In Xenopus, *bmp4* and *alk3* are expressed in the heart fields, and injection of dominant negative Bmp receptors into the embryo

results in production of far fewer cardiac cells (Shi et al., 2000). Similarly, inhibition of Bmp activity in chick embryos reduces expression of cardiac markers (Schlange et al., 2000). In mouse embryos, deletion of the Bmp receptor *BmpR1a* in the mesoderm results in reduced specification of cardiac progenitors in the cardiac crescent (Klaus et al., 2007). Bmp activity also seems to be dynamically regulated in mouse: while early Bmp activity promotes cardiac specification and expression of *Nkx2.5* (Klaus et al., 2007), NKX2.5 limits Bmp activity in specified cardiac cells by repressing expression of *Bmp2* (Prall et al., 2007). During the proliferative period between cardiac specification and differentiation, Bmp activity must be attenuated, because high Bmp activity limits proliferation of cardiac progenitors and instead pushes those cells toward premature differentiation (Prall et al., 2007; Tirosh-Finkel et al., 2010).

After cardiac differentiation has commenced, Bmp signaling remains important for late-differentiating cardiomyocytes of the SHF. In zebrafish, cells in the SHF-derived arterial pole contain phosphorylated Smad, an indicator of active Bmp signaling (Hami et al., 2011). Furthermore, decreasing Bmp activity beginning at 24 hpf reduces OFT cardiomyocyte addition and expands OFT smooth muscle (Hami et al., 2011). Conversely, elevated Bmp activity in *gpc4* mutants prevents cardiomyocyte accretion after linear heart tube formation, indicating that suppressed levels of Bmp activity are required for SHF cardiomyocyte differentiation (Strate et al., 2015). These data support the

idea that moderate levels of Bmp activity are required for addition of late-differentiating cardiomyocytes to the zebrafish ventricle, rather than very high or very low levels. In mouse embryos, deletion of the Bmp receptor *AcvR1* in the SHF results in a malformed OFT with septal defects (Thomas et al., 2014); abnormal OFT morphogenesis and septal defects are also seen upon deletion of *Bmp4* in the SHF (McCulley et al., 2008). Furthermore, reduced Bmp activity in the SHF results in abnormalities at the venous pole, including atrioventricular septal defects and reduced proliferation (Briggs et al., 2013). Given that Bmp signaling promotes formation of atrial cardiomyocytes and is active in the murine venous pole, it seems likely that Bmp activity could promote production of IFT cardiomyocytes in the zebrafish venous pole. In Chapter 3 of this dissertation, I will present novel data indicating that IFT cardiomyocytes depend on both initial and ongoing Bmp activity for their development.

Summary

In this chapter, we have argued that investigating the patterning of pacemaker cardiomyocytes is a valuable endeavor that will advance the field's understanding of cardiac development. We have shown that the zebrafish IFT is homologous to the mammalian SAN and is an excellent model in which to study pacemaker cell development. We have reviewed the factors involved in regulating development of pacemaker cells and examined the developmental

origin of this population. We have discussed the roles of Hh and Bmp signaling in cardiac development, and we have proposed that both Hh and Bmp signaling are important for IFT patterning. In Chapter 2, I will characterize the wild-type inflow tract and examine its origin in zebrafish embryos. In Chapter 3, I will investigate the roles of Hh and Bmp signaling in IFT patterning. In Chapter 4, I will comment on the significance of this work and propose future directions.

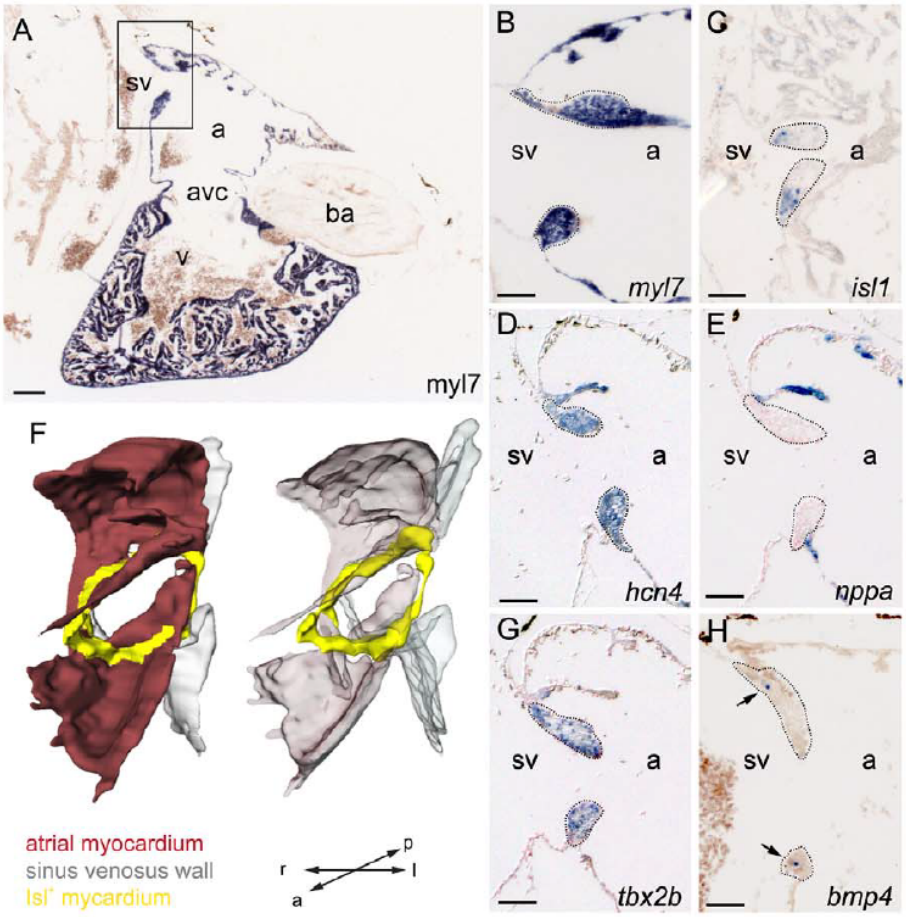

Figure 1.1.
Location and molecular marker signature of the zebrafish IFT.
(A) This section through an adult zebrafish heart shows the IFT region, which is boxed here and then enlarged in panels B-E,G-H. The IFT is located at the junction between the atrium and the sinus venosus. This heart is labeled with the myocardial marker *myl7.* (B-E,G-H) The IFT is characterized by a *myl7*+, *isl1*+, *hcn4*+, *nppa*- *tbx2b*+, *bmp4*+ molecular signature. (F) This 3D reconstruction of the sinoatrial junction shows that Isl1 (yellow) is expressed around the entire sinoatrial junction, forming a ring. This Isl1-expressing ring is defined as the IFT. a, atrium; avc, atrioventricular canal; ba, bulbus arteriosus; sv, sinus venosus; v, ventricle; l, left; r, right; a, anterior; p, posterior. Scale bars represent 50 µm. Reproduced from Tessadori et al., 2012.

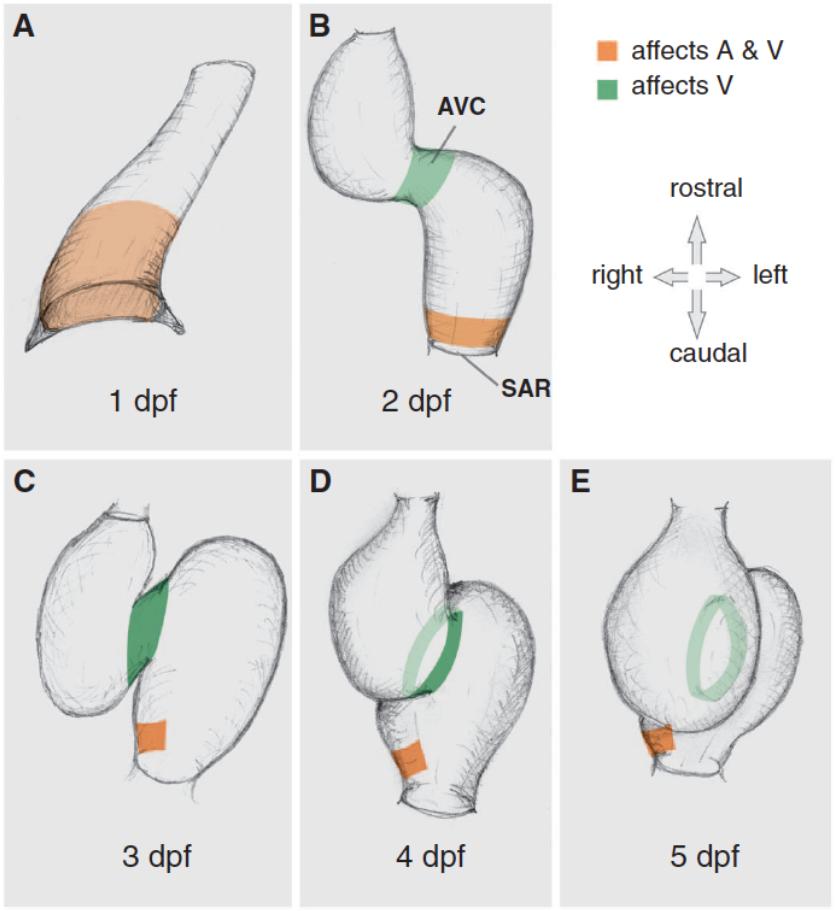

Figure 1.2.
Cells located in the IFT are responsible for pacemaking activity.
(A-E) Schematic drawings depict areas sensitive to hyperpolarization at the inflow and atrioventricular canal regions of wild-type zebrafish hearts. Optogenetic methods were used to hyperpolarize cells in different regions of the heart, thus ceasing their conductive activity. Hyperpolarization of cells in the orange region ceases contractions in both the atrium and ventricle, indicating that the orange region contains pacemaker cells. (B) The orange pacemaker region aligns with the territory referred to as the IFT. dpf, days post fertilization; avc, atrioventricular canal; sar, sinoatrial region; a, atrium; v, ventricle. Reproduced from Arrenberg et al., 2010.

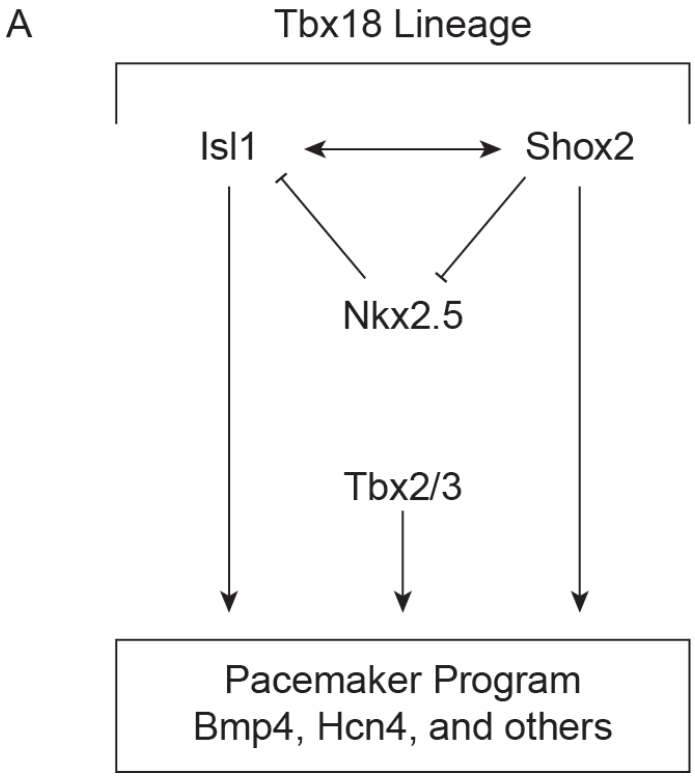

Figure 1.3.
Schematic of the pacemaker gene regulatory network.
(A) This schematic depicts a simplified version of the gene regulatory network that controls pacemaker cell differentiation. Cells arise from a Tbx18-expressing lineage and express transcription factors such as Isl1, Shox2, Tbx2, and Tbx3. These transcription factors activate expression of other pacemaker markers, including ion channels such as Hcn4. Meanwhile, transcription factors that are associated with a chamber identity, such as Nkx2.5, are excluded from pacemaker cells and retained only in non-pacemaker cells.

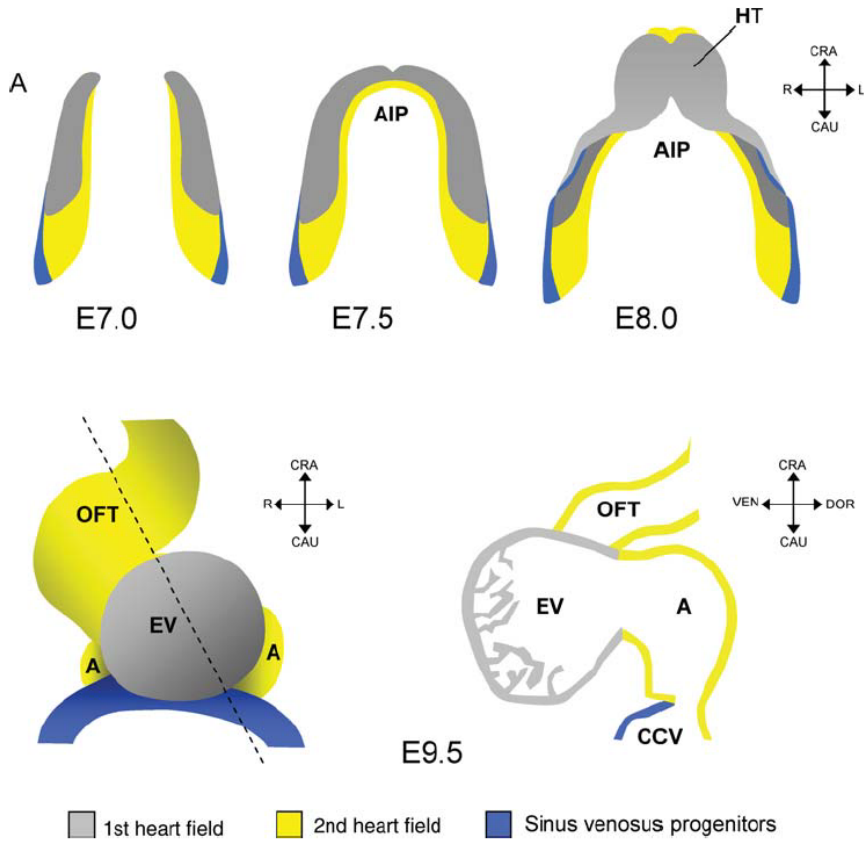

Figure 1.4.
Murine pacemaker cells originate from the edges of the heart fields.
(A) This schematic shows the fate maps of the heart fields (top row) that give rise to the mammalian heart (bottom row). The sinus venosus progenitor population, shown in blue, originates in the caudal and lateral portion of the heart fields. These progenitors give rise to the SAN and surrounding tissues in the sinus venosus. a, atrium; aip, anterior intestinal portal; ccv, common cardinal vein; ev, embryonic ventricle; ht, heart tube; oft, outflow tract; ven, ventral; dor, dorsal; cra, cranial; cau, caudal; l, left; r, right. Reproduced from Mommersteeg et al., 2010.

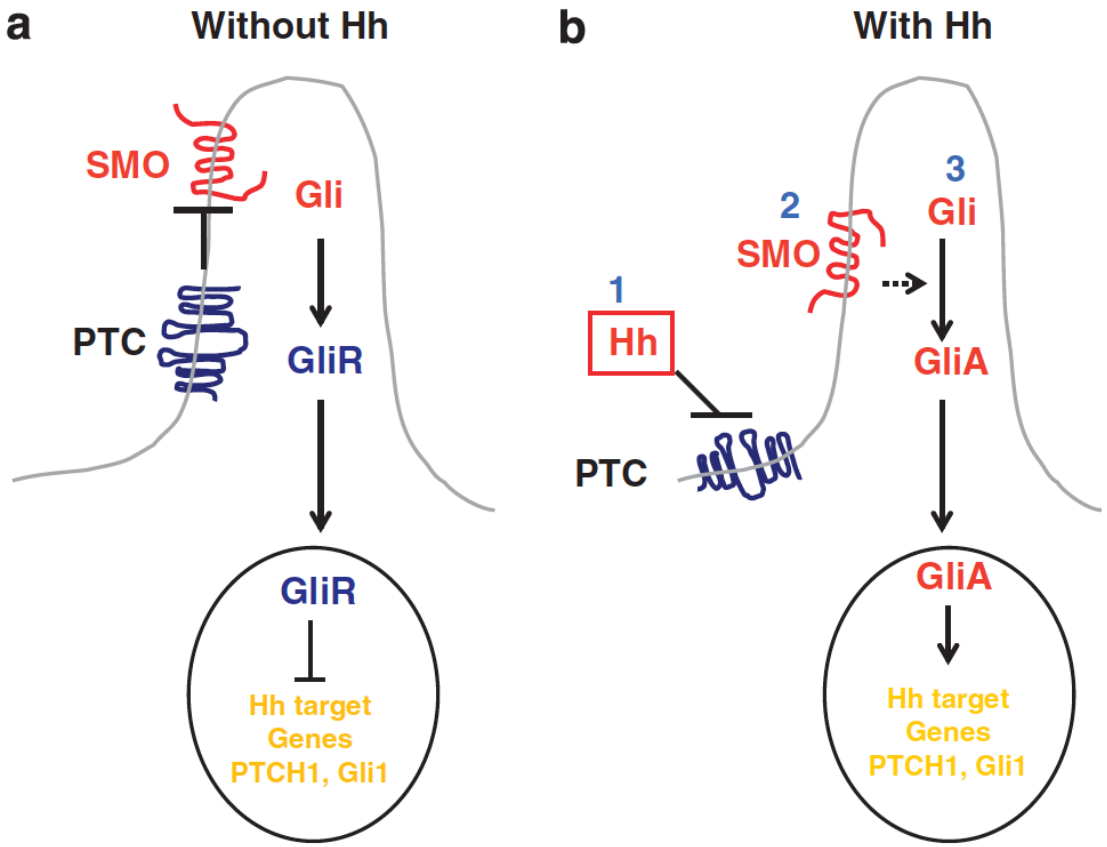

Figure 1.5.
Schematic of the Hh signaling pathway.
(A) When Hh ligands are absent, the Hh receptor Ptc continuously inhibits activity of Smo. Gli molecules are cleaved to create their repressor forms (GliR), which translocate into the nucleus and repress transcription of Hh target genes such as Ptch1 and Gli1. (B) When Hh ligands are present, Ptc binds to Hh ligands and ceases inhibition of Smo. Smo undergoes conformational changes and becomes active. Gli molecules are no longer cleaved and are instead processed into active forms (GliA), which activate transcription of Hh target genes. Reproduced from Yang et al., 2010.

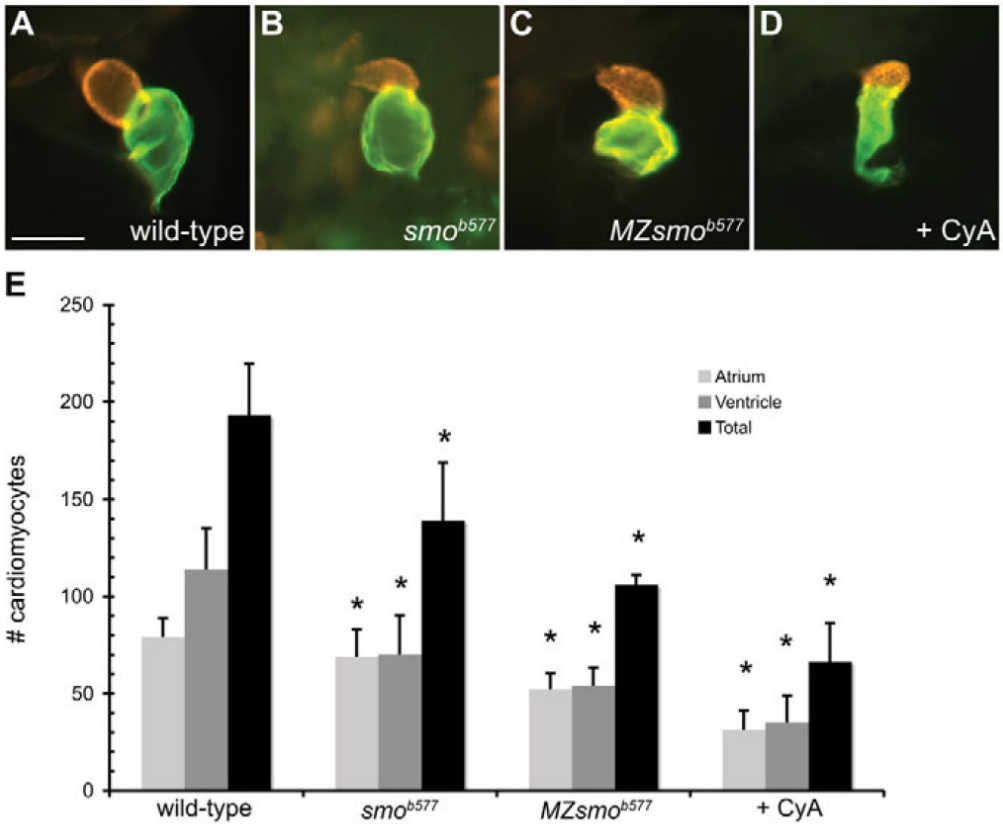

Figure 1.6.
Hh signaling promotes production of both ventricular and atrial cardiomyocytes.
(A-D) Zebrafish hearts at 48 hpf show the ventricle in red and the atrium in green. Scale bar represents 100 µm. (A) A wild-type heart shows the typical size. (B-D) Hh-deficient embryos have small hearts in which both the atrium and the ventricle are diminished. Here, Hh signaling has been reduced through zygotic mutation of *smo* (B), maternal and zygotic mutation of *smo* (C), and cyclopamine treatment (D). (E) Quantification shows that there are fewer cardiomyocytes in Hh-deficient hearts relative to wild-type controls at 52 hpf. Asterisks indicate statistically significant differences from wild-type. Reproduced from Thomas et al., 2008.

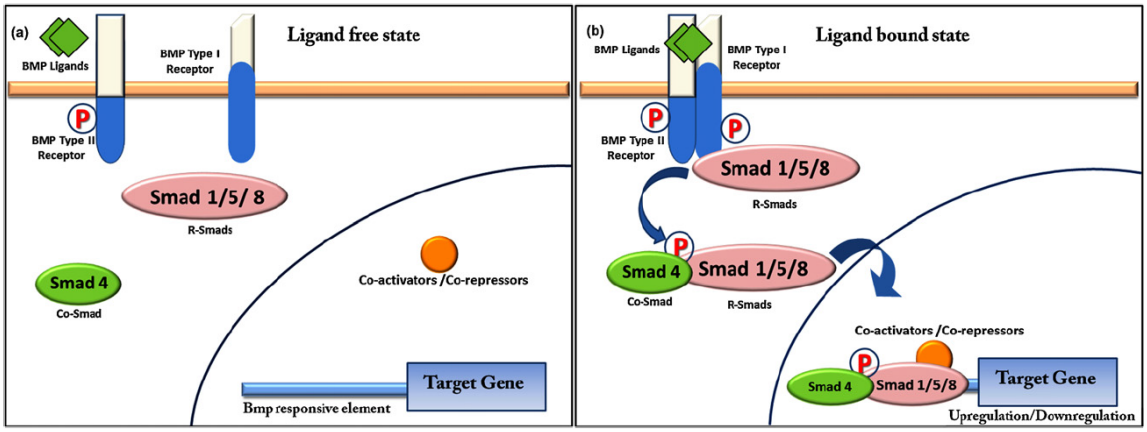

Figure 1.7.
Schematic of the Bmp signaling pathway.
(A) In the absence of Bmp ligands, the Bmp Type I and Type II receptors do not form an active complex. Smad1/5/8 factors are not activated, and they do not translocate to the nucleus to regulate transcription of Bmp target genes. (B) In the presence of Bmp ligands, Bmp Type I and Type II receptors form a complex and act as serine-threonine kinases. Smad1/5/8 factors are activated via phosphorylation, allowing them to bind to Smad4 and translocate to the nucleus. In concert with cofactors, Smad1/5/8 regulates expression of Bmp target genes. Reproduced from Bandyopadhyay et al., 2013.

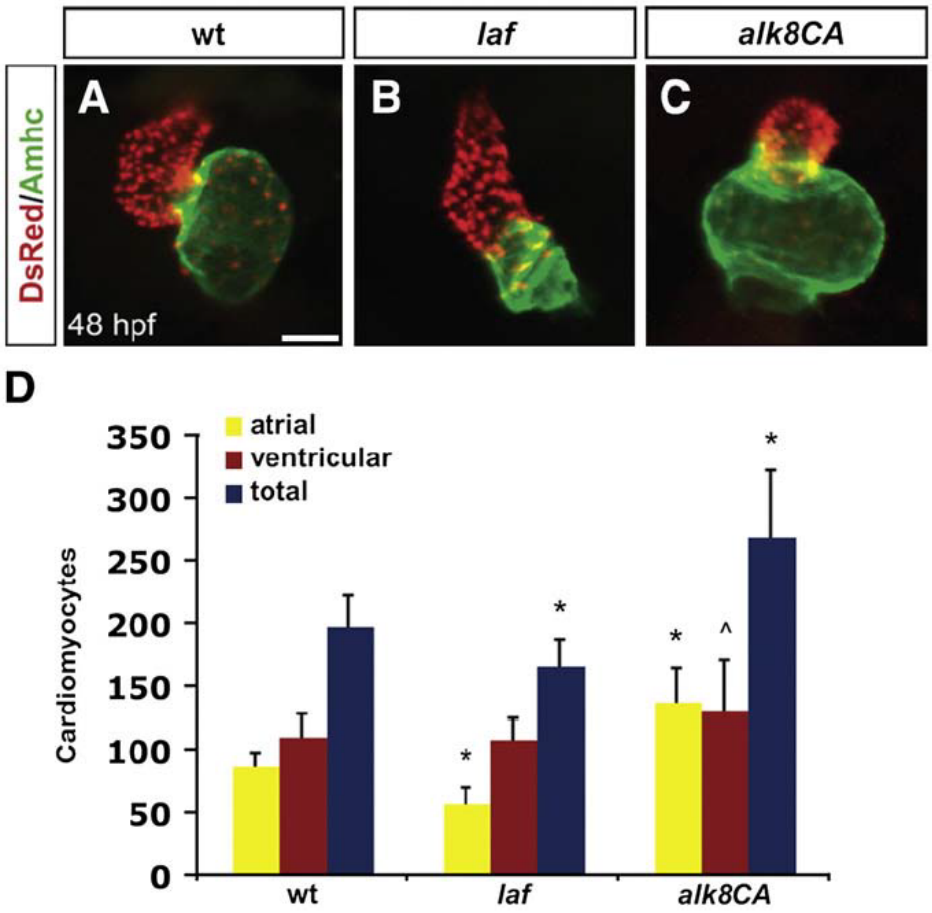

Figure 1.8.
Bmp signaling promotes production of atrial cardiomyocytes.
(A-C) Zebrafish hearts at 48 hpf show all cardiomyocytes in red with the atrium marked in green. Scale bar represents 50 µm. (A) A wild-type heart shows the typical size and shape. (B) In a *laf* mutant heart, which has reduced Bmp activity, the atrium is abnormally small. (C) In embryos expressing *alk8CA*, which constitutively activates Bmp signaling, the hearts are enlarged. Notably, the atrium is particularly outsized relative to the ventricle. (D) Quantification shows that there are fewer atrial cardiomyocytes in *laf* relative to wild-type controls at 48 hpf. Conversely, there are more cardiomyocytes in *alk8CA*-expressing embryos relative to wild-type controls at 48 hpf, with a striking increase in atrial cell number. Statistically significant differences from wild-type are indicated by asterisks and carets. Reproduced from Marques et al., 2009.

Chapter 2: Patterning and differentiation of the cardiac inflow tract in zebrafish

ABSTRACT

The rhythmic and synchronous beating of cardiomyocytes, which is essential for efficient circulation, relies on pacemaking activity that originates in the cardiac inflow tract (IFT). The specialized function of cardiac pacemaker cells has been well documented, but open questions remain regarding the origins of the pacemaker lineage and the regulation of pacemaker differentiation. The zebrafish embryo presents valuable opportunities to study early phases of pacemaker development in depth. Here, we review the evidence for homology between the zebrafish IFT and the mammalian sinoatrial node, examining their functional attributes, expression of molecular markers, and dependence on key transcription factors. We integrate this information with new data indicating how zebrafish IFT progenitor cells are organized within the heart fields and demonstrating when and where these cells differentiate into IFT cardiomyocytes. Together, these results illuminate the biography of the zebrafish IFT and provide an important resource for future studies that can elucidate the genetic pathways controlling specification and differentiation of pacemaker progenitor cells.

INTRODUCTION

In the mammalian heart, the sinoatrial node (SAN) is crucial for maintaining synchronized, rhythmic contractions of the cardiac chambers. Located at the junction between the right atrium and the sinus venosus, the SAN is a tight bundle of pacemaker cells that spontaneously generate action potentials to set the pace for the entire cardiac conduction system (Mangoni and Nargeot, 2008). SAN action potentials are rapidly conducted through the atria, then delayed at the atrioventricular node before moving into the ventricular conduction system (Mangoni and Nargeot, 2008).

When the pacemaker cells in the SAN malfunction due to congenital malformation, disease, or aging, it can result in arrhythmia, insufficient circulation, or even sudden cardiac death (Choudhury et al., 2015; Dobrzynski et al., 2007). Currently, the only effective treatment is costly implantable electronic pacemakers (Mulpuru et al., 2017). The search for biological alternatives is in progress and has focused on generating pacemaker-like cells through directed differentiation of stem cells or through reprogramming of quiescent cardiomyocytes (Bakker et al., 2012; Hu et al., 2014; Jung et al., 2014; Kapoor et al., 2013; Mandel et al., 2012; Nam et al., 2014; Protze et al., 2017; Scavone et al., 2013). However, these approaches have failed to yield efficient induction of pacemaker cells that are functionally equivalent to endogenous pacemaker cardiomyocytes (Boink et al., 2015; Nam et al., 2014). To improve the efficacy of these efforts, additional insight is necessary; in

particular, it would be highly informative to elucidate the genetic networks that regulate pacemaker development in vivo so that these can be recapitulated in vitro. Furthermore, understanding how the pacemaker population develops during embryonic stages may shed light on the etiology of congenital arrhythmias. Therefore, it is worthwhile to investigate open questions that concern the specification and differentiation of pacemaker cells.

It is unclear how pacemaker cells are specified in the early embryo, when pacemaker specification occurs, and where pacemaker progenitors arise. Fate mapping experiments in avian embryos suggest that pacemaker progenitors reside in locations posterior to the heart fields (Bressan et al., 2013). However, these data are inconsistent with genetic lineage tracing studies in mice that suggest that the SAN originates from caudal and lateral territories located at the edges of the heart fields (Christoffels, 2006; Mommersteeg et al., 2007b; Wiese et al., 2009), so a precise understanding of the requirements for pacemaker specification remains elusive. Furthermore, it is unclear how pacemaker differentiation is regulated: what triggers the differentiation of pacemaker progenitors, and what refines this population as the embryonic heart matures? Although many studies have made significant inroads in understanding the genetic network that functions during SAN differentiation (Blaschke et al., 2007; Christoffels, 2006; Espinoza-Lewis et al., 2009; Hoogaars et al., 2007; Liang et al., 2015; Mommersteeg et al., 2007b; Mori et al., 2006; Wiese et al., 2009), the upstream signals that initially activate

the pacemaker network have not yet been fully elucidated and the temporal dynamics of this process are not completely understood.

The zebrafish embryo has emerged as an ideal model in which to investigate the specification and differentiation of pacemaker cardiomyocytes. In the zebrafish heart, the myocardium at the sinoatrial junction, which we refer to as the inflow tract (IFT), acts as a functional equivalent to the mammalian SAN (Tessadori et al., 2012). Early stages of IFT development can be examined using zebrafish because external fertilization allows convenient access to the early embryo from the onset of its development (Poon and Brand, 2013). Additionally, the optical transparency of zebrafish embryos allows direct visualization of the differentiation of pacemaker cardiomyocytes as it occurs (Staudt and Stainier, 2012). Furthermore, cardiac conduction can be easily analyzed in live embryos (Chi et al., 2008), revealing the functional consequences of IFT abnormalities. Most importantly, there is a growing body of research that has laid the groundwork for investigating the zebrafish IFT and its pacemaker activity (Arrenberg et al., 2010; Chi et al., 2008; Tessadori et al., 2012), so the zebrafish community is currently poised to contribute substantial information regarding the mechanisms regulating pacemaker development.

In this resource paper, we first review the evidence for homology between the zebrafish IFT and the mammalian SAN. Next, we integrate the analysis of new data that indicate how zebrafish IFT progenitor cells are

organized within the embryonic heart fields and demonstrate when and where these cells initiate their differentiation into IFT cardiomyocytes. Taken together, this information comprises a biography of the zebrafish IFT and provides a framework for future studies investigating the regulation of pacemaker specification and differentiation.

UTILITY OF THE ZEBRAFISH FOR ANALYSIS OF INFLOW TRACT DEVELOPMENT

Within the IFT of adult zebrafish, a population of pacemaker cells was recently identified and rigorously tested for homology to the mammalian SAN (Tessadori et al., 2012). This population is located at the junction between the atrium and the sinus venosus (Tessadori et al., 2012), as is the mammalian SAN (Anderson et al., 1979; Mangoni and Nargeot, 2008; Sánchez-Quintana et al., 2005). Cardiomyocytes in the IFT initiate action potentials spontaneously, unlike the neighboring chamber myocardium (Tessadori et al., 2012), and the electrophysiological properties of these action potentials mimic mammalian pacemaker cells (Bleeker et al., 1980; Mangoni and Nargeot, 2008; Verheijck et al., 2001). Indeed, IFT cells express the pacemaker channel *hcn4* (Tessadori et al., 2012), which is enriched in the SAN and is required to establish the unique electrophysiological properties of pacemaker cardiomyocytes (Garcia-Frigola et al., 2003; Moosmang et al., 2001; Stieber et al., 2003). Furthermore, it was observed that the zebrafish IFT cells express the markers *isl1, bmp4,* and *tbx2b* along with the myocardial marker *myl7* (Tessadori et al., 2012), all of which are expressed in the mammalian SAN as well (Christoffels, 2006). Isl1 serves as a useful marker of this population, since it is expressed specifically in the adult pacemaker population, but not in the adjacent chamber myocardium (Figure 1.1 and Tessadori et al., 2012). Thus, the population of Isl1+ pacemaker cardiomyocytes in the adult zebrafish

IFT is similar to the adult mammalian SAN in its location, molecular marker expression, and function, providing strong evidence for homology between these structures.

In fact, these similarities in anatomical structure, gene expression, and electrophysiological function between the zebrafish adult IFT and murine SAN are preserved from the characteristics of the zebrafish IFT during embryonic stages. In the zebrafish embryo, differentiated IFT cardiomyocytes are located at the sinoatrial junction (Figure 2.1A), and it has been demonstrated that pacemaker function is confined to this location. Embryos carrying the transgene *Tg(cmlc2:gCaMP),* which expresses a fluorescent calcium indicator in cardiomyocytes, have been utilized for optical mapping of calcium flux, which reveals that cardiac conduction originates in the venous pole (Chi et al., 2008). Furthermore, when IFT cells are hyperpolarized using transgenic light-gated ion channels, the heartbeat ceases, indicating that this region is required to initiate the heartbeat (Arrenberg et al., 2010). This pacemaking activity is present in a broad ring at the venous pole at 24 hours post fertilization (hpf), becomes refined to the IFT at 48 hpf, and is then further whittled down to the inner curvature of the IFT by 72 hpf (Arrenberg et al., 2010). Cardiomyocytes in the embryonic IFT also express the molecular marker Isl1 (Figure 2.1G-H; Witzel et al., 2012), along with a group of pacemaker markers that includes *bmp4, tbx18, shox2,* and *hcn4* (Figure 2.1 A-E; Begemann et al., 2002; Blaschke et al., 2007; Chin et al., 1997; Poon et al.,

2016). These functional attributes and molecular markers establish the IFT as the primary cardiac pacemaker in the zebrafish embryo and demonstrate its functional and developmental homology to the mammalian SAN.

REGULATION OF IFT DEVELOPMENT

The molecular markers expressed in the IFT have been studied extensively during murine cardiac development, and these factors form the basis of a genetic network that is required for formation of a functional SAN. In this network, several transcription factors promote expression of the pacemaker genetic program, including Tbx18, Tbx2, Tbx3, Isl1, and Shox2 (van Weerd and Christoffels, 2016). In adjacent non-pacemaker cardiomyocytes, which we refer to as chamber cardiomyocytes, the transcription factor Nkx2.5 represses the pacemaker program and promotes chamber identity (van Weerd and Christoffels, 2016). It remains to be seen whether this entire genetic network plays a conserved role in the zebrafish IFT. Here, we compare the role of each factor in development of the mammalian SAN and the zebrafish IFT. Isl1 and Shox2 have been studied in zebrafish IFT development and are indeed required for normal pacemaker function, but Tbx18 and other Tbx factors warrant further study to evaluate their function in the context of the zebrafish.

Shared requirement for Isl1 and Shox2 in zebrafish and mammalian pacemaker cells

Isl1 has been used as a marker for the zebrafish IFT and is required in both zebrafish and mouse for normal pacemaker cell development. In mouse, *Isl1* is thought to be transiently expressed in nearly all cardiac progenitors

(Prall et al., 2007), but its expression is lost during cardiac differentiation in most populations and retained only in specific populations of differentiated cardiomyocytes, including in the SAN (Cai et al., 2003; Sun et al., 2007). In zebrafish, *isl1* is initially expressed in a broad region that overlaps with the heart fields (Witzel et al., 2012), but after cardiac differentiation, the only cardiomyocytes that express *isl1* are in the IFT (Tessadori et al., 2012). This suggests that Isl1 might play an important role during IFT differentiation. Indeed, zebrafish *isl1* mutants add fewer cells to the venous pole, lack *bmp4* expression in the IFT, and exhibit bradycardia (de Pater et al., 2009). At later stages, these *isl1* mutants display a sinus block, indicating defective pacemaking activity (Tessadori et al., 2012). This function of ISL1 is conserved in mammals: when *Isl1* is knocked out in the pacemaker lineage, mouse embryos display arrhythmia, reduced SAN cell number, and embryonic lethality (Liang et al., 2015). These conditional knockouts also have reduced expression of SAN markers such as *Bmp4*, *Shox2*, and *Hcn4* (Liang et al., 2015). Interestingly, Isl1 is capable of limiting its own expression to regulate the number of cardiac progenitors that contribute to the IFT. When Isl1 is bound to the RA-responsive transcription factor Ajuba, it delimits the number of IFT cells added to the zebrafish venous pole, and when Ajuba is knocked down, the number of IFT cells increases dramatically (Witzel et al., 2012). Thus, Isl1 is crucial both for establishing an appropriate number of IFT cells and for directing their differentiation into functional pacemaker cardiomyocytes.

The transcription factor gene *shox2* is also required for formation of pacemaker cells in both zebrafish and mouse. In mouse embryos with mutations in *Shox2*, the SAN is hypoplastic and fails to fully differentiate, resulting in bradycardia and embryonic lethality (Blaschke et al., 2007; Espinoza-Lewis et al., 2009). SHOX2 directly activates transcription of both *Bmp4* and *Isl1* in pacemaker cells (Hoffmann et al., 2013; Puskaric et al., 2010). In zebrafish embryos, Shox2 deficiency results in severe bradycardia (Blaschke et al., 2007), but this can be rescued by increased *isl1* expression (Hoffmann et al., 2013). SHOX2 also represses NKX2.5: murine *Shox2* mutants aberrantly express *Nkx2.5* in the SAN, and *shox2* overexpression in Xenopus embryos results in a strong downregulation of *nkx2.5* in all cardiac tissue (Blaschke et al., 2007; Espinoza-Lewis et al., 2009). In fact, SHOX2 repression of *Nkx2.5* is a crucial element in SAN differentiation, as *Nkx2.5* overexpression can recapitulate the SAN defects caused by loss of *Shox2* (Espinoza-Lewis et al., 2011). Interestingly, SHOX2 and NKX2.5 bind many of the same gene regulatory elements, indicating that the interaction of these factors determines whether cardiomyocytes adopt a pacemaker genetic signature (Ye et al., 2015). Altogether, the requirements for both Isl1 and Shox2 appear well conserved between mammals and fish, suggesting that similar genetic networks are at play in the development of the murine SAN and the zebrafish IFT.

Tbx factors may function in zebrafish IFT development

Factors in the Tbx family are essential for mammalian pacemaker cell development and deserve further study in the zebrafish IFT. The transcription factor TBX18 is expressed in the myocardium of the murine sinus venosus, which encompasses and gives rise to the SAN (Christoffels, 2006; Mommersteeg et al., 2010). Mice deficient in TBX18 have sinus venosus abnormalities and a small, deformed SAN (Christoffels, 2006; Wiese et al., 2009), indicating that TBX18 function is required for normal development of pacemaker tissues. *tbx18* is expressed in the zebrafish IFT (Begemann et al., 2002), but it remains to be seen whether loss of Tbx18 alters IFT development in zebrafish. TBX2 and TBX3 are expressed in the murine cardiac conduction system, including in the SAN, and they repress the differentiation of chamber myocardium in these tissues (Christoffels et al., 2004; Hoogaars et al., 2004; Hoogaars et al., 2007; Mommersteeg et al., 2007b). In particular, *Tbx3* overexpression is sufficient to repress atrial chamber genes and drive formation of ectopic, functional pacemaker cells even in differentiated atrial chamber cardiomyocytes (Hoogaars et al., 2007). In zebrafish, the function and expression of Tbx3 homologues in IFT development have not been investigated. However, *tbx2b* is expressed in the IFT of adult zebrafish (Tessadori et al., 2012), and Tbx2b and Tbx3b have been found to repress the chamber genetic program and promote the conduction system genetic program in the atrioventricular canal (AVC; Ribeiro et al., 2007), indicating that

the roles of these factors are likely conserved from zebrafish to mammals. It will be satisfying to investigate the function of Tbx family transcription factors in the zebrafish IFT in future studies. Furthermore, zebrafish will be an excellent model in which to identify factors that act upstream of Tbx factors during progenitor specification.

EARLY ORIGINS OF IFT PROGENITORS

Though many studies have focused on describing the gene regulatory network acting in the mature SAN, little is known about the origin of these important cells during early embryonic development. Identification of IFT progenitor cells will aid in studies of their specification. For example, understanding the physical location of IFT progenitors allows us to develop hypotheses about how diffusible factors act on this population during its patterning and can provide insight into the lineage relationships between IFT progenitors and other cardiac populations.

Previous studies in mouse and chick embryos have identified potential locations for IFT progenitors during somitogenesis stages, after gastrulation is complete. In mouse embryos, Cre-mediated lineage tracing has shown that cells of the SAN derive from lineages that express *Tbx18* and *Isl1* (Christoffels, 2006; Mommersteeg et al., 2010; Sun et al., 2007; Wiese et al., 2009). By examining the expression patterns of these markers prior to SAN formation, it was shown that SAN progenitors are located in the caudal and lateral edges of the heart fields (Mommersteeg et al., 2010). In chick embryos, fate mapping has been used to show that pacemaker progenitor cells reside posterior to the heart fields (Bressan et al., 2013). This posterior area, termed the tertiary heart field, lacks expression of *ISL1* (Bressan et al., 2013), calling into question whether the tertiary heart field correlates with the *Isl1*-expressing SAN progenitor territory described in mouse embryos. Perhaps this

discrepancy indicates that pacemaker progenitors only activate *isl1* expression upon migration toward the heart tube from the tertiary heart field. In both species, SAN progenitors seem to reside at the periphery of the heart fields, suggesting that a similar arrangement may be conserved in zebrafish during somitogenesis stages. However, the origin of pacemaker cell progenitors prior to gastrulation has not yet been addressed in any species.

Previous studies in zebrafish have employed fate mapping to determine that atrial, ventricular, and outflow tract (OFT) progenitor populations are each located in defined territories within the early embryo (Hami et al., 2011; Keegan et al., 2004; Schoenebeck et al., 2007), raising the possibility that IFT progenitors may also reside in a specific territory. In the late blastula, cardiac progenitors are located in two bilateral territories, near the embryonic margin and about midway between the dorsal and ventral poles of the embryo. More specifically, atrial progenitors are found in a relatively ventral position within this territory, primarily between 90 and 140 degrees from dorsal, in the third and fourth cell tier relative to the margin (Keegan et al., 2004; Figure 2.2A). Ventricular progenitors are located in a more dorsal portion of this territory, between 60 and 125 degrees from dorsal, in the first through third cell tiers (Keegan et al., 2004; Figure 2.2A). OFT progenitors are positioned closest to the dorsal side of the territory, between 55 and 105 degrees from dorsal, in the first or second cell tiers (Hami et al., 2011; Figure 2.2A). During gastrulation, these cardiac progenitor populations are rearranged into two bilateral heart

fields within the anterior lateral plate mesoderm (ALPM). In the ALPM, cardiac progenitors are spatially organized such that ventricular progenitors are found in more medial positions and atrial progenitors are found in more lateral positions within the heart fields (Schoenebeck et al., 2007; Figure 2.2B). OFT progenitors localize in relatively medial and anterior portions of the heart fields (Hami et al., 2011; Figure 2.2B). Importantly, none of these studies specifically evaluated the location of IFT progenitors.

To evaluate the fate map for IFT progenitor cells in the early zebrafish embryo, we revisited our previously reported data sets, in combination with additional data that had not been included in our prior publications. First, we examined our data from previous experiments performed at 40% epiboly (Keegan et al., 2005, 2004, and unpublished data). In these studies, we generated a high-resolution fate map of cardiac progenitor cells by using a photoactivatable lineage tracer to label a small number of blastomeres just prior to gastrulation, recording the initial position of the labeled cells, and then subsequently recording the locations of their progeny within the heart at 48 hours post fertilization (hpf). In these original experiments, a group of atrial progenitors was identified, and that group included labeled cells that contributed to the IFT or to the non-IFT portion of the atrium, which we refer to as the atrial chamber (AC); here, we have separated those two populations. In this data set, we identified eight examples in which labeled cells contributed to the IFT myocardium, plus an additional three examples in which labeled cells

contributed to both the IFT and the (AC; Figure 2.3). In all 11 examples, the labeled cells were initially located in tiers 2-4, between 92 and 160 degrees from dorsal (Figure 2.3). Thus, IFT progenitor cells seem to be reside in the upper tiers and the ventral portion of the cardiogenic territory at 40% epiboly, suggesting that IFT progenitors are a discrete and spatially organized subset of cells located near the ventral edge of the atrial progenitor population. Combining this new finding with previously published fate maps (Hami et al., 2011; Keegan et al., 2004), we conclude that cardiac progenitors are located in four overlapping territories in the late blastula: atrial and ventricular progenitors are flanked by IFT progenitors on the ventral side and OFT progenitors on the dorsal side (Figure 2.2A).

We next asked where IFT progenitors are located reside relative to the heart fields in the ALPM. For this analysis, we examined our data from previous experiments performed between the 6 somite and 9 somite stages (Schoenebeck et al., 2007). In these studies, we labeled small clusters of cells within the ALPM, generating a fate map of cardiac progenitors with slightly broader resolution relative to our map at 40% epiboly. As in our other studies, we originally scored contributions to the atrium but did not distinguish between contribution to the IFT and the AC. Reexamining these data, we found 48 examples in which labeled cells became IFT cardiomyocytes (Figure 2.4). Of these 48 examples, 43 were located in the lateral portion of the heart fields, where atrial progenitor cells typically reside. The other five examples were

found in the medial portion of the heart fields, and no examples were found in the anterior ALPM, which contains blood and vessel progenitors are located (Figure 2.4). In half (24/48) of these examples, labeled cells were present in both the IFT and AC (Figure 2.4), indicating the proximity of IFT progenitors to AC progenitors. The broad resolution of this fate map does not allow us to distinguish the degree to which IFT and AC progenitors are intermingled; however, the trends reflected in our data make it appealing to consider that IFT progenitors could be positioned along the lateral edge of the progenitor field. Integrating this new information with previously published data (Hami et al., 2011; Schoenebeck et al., 2007), we propose a fate map of the ALPM in which IFT, AC, ventricular, and OFT progenitors are spatially organized, with a relatively lateral to medial distribution within the heart fields (Figure 2.2B). This arrangement echoes the spatial organization of cardiac progenitors observed prior to gastrulation (Figure 2.2A). This fate map also suggests conservation with the mammalian sinus venosus fate map, in which sinus venosus progenitors reside on the lateral edges of the murine heart fields (Mommersteeg et al., 2010).

Together, these results provide a framework for further studies of IFT progenitor specification in the context of the zebrafish embryo. Bearing in mind the relatively ventral and lateral locations of the IFT progenitors, we can begin to create and test hypotheses regarding the signals that might influence IFT fate. Such future studies would benefit from the identification of molecular

markers that are specifically expressed in pacemaker progenitor cells. Whereas the mammalian SAN has been shown to arise from a progenitor population that expresses Tbx18 and Isl1 (Christoffels, 2006; Mommersteeg et al., 2007b, 2010; Wiese et al., 2009), no molecular markers have been identified that clearly distinguish this progenitor population prior to its differentiation in avian or zebrafish embryos. Characterization of the gene expression profile of IFT progenitor cells would be a key step toward the elucidation of factors at play during IFT patterning.

DIFFERENTIATION OF IFT MYOCARDIUM

Another interesting avenue for further study is investigation into the factors that initiate the differentiation of IFT cardiomyocytes. However, before pursuing this analysis in depth, we must first ascertain when and where IFT differentiation occurs. In zebrafish, myocardial differentiation begins during mid-somitogenesis stages, as ventricular and atrial cardiomyocytes migrate toward the midline, eventually forming a ring-shaped cardiac cone (Yelon et al., 1999; Figure 2.2C). Differentiation occurs in two phases: an initial wave that begins with differentiation of ventricular cardiomyocytes followed by differentiation of atrial cardiomyocytes, and a second wave in which OFT cells differentiate at the arterial pole of the ventricle (de Pater et al., 2009; Figure 2.2D-E). Previous experiments using developmental timing assays have suggested that cardiomyocytes at the venous pole of the atrium differentiate later than the rest of the atrial myocardium, but prior to the second wave of OFT differentiation (de Pater et al., 2009). However, these studies did not utilize molecular markers to distinguish IFT and AC cells, so they did not resolve how late-differentiating cardiomyocytes at the venous pole relate to the pacemaking territory of the IFT.

To investigate when and where the IFT myocardium differentiates, we chose to employ Isl1 as a molecular marker. By examining Isl1 localization in embryos carrying the transgene *Tg(myl7:egfp)*, we can determine when Isl1 first appears in *myl7*-expressing differentiated cardiomyocytes. At the 18

somite stage, no Isl1+ cardiomyocytes could be detected (Figure 2.5A-C), suggesting the IFT progenitor cells have not yet begun to differentiate. At the 21 somite stage, a small population of Isl1+ cardiomyocytes could be detected at the periphery of the cardiac cone (Figure 2.5D-F), suggesting that a few IFT progenitors begin to differentiate between 18 and 21 somites. At the 23 somite stage, we observed many Isl1+ cardiomyocytes along the outer circumference of the cardiac cone (Figure 2.5G-I), suggesting that IFT differentiation is well underway by this time. At 24 hpf, after the linear heart tube has formed, Isl1+ cardiomyocytes form a ring at the IFT (Figure 2.5J-L). At this point, cardiac contraction has commenced, and pacemaking activity is present in a ring-shaped region at the venous pole of the heart tube (Arrenberg et al., 2010), which likely encompasses the Isl1+ IFT.

We next wondered how these IFT differentiation dynamics relate to differentiation in the rest of the atrium. To investigate this, we revisited previously-published developmental timing assays that revealed late-differentiating cells at the venous pole (de Pater et al., 2009) and we added simultaneous analysis of an IFT marker. Isl1 localization was examined in embryos carrying the transgenes *Tg(myl7:egfp)* and *Tg(myl7:dsred)*. In this assay, differential protein folding dynamics between eGFP and DsRed result in fluorescence of eGFP but not DsRed in newly-differentiated cardiomyocytes (de Pater et al., 2009). At 36 hpf, Isl1 is present in the majority of the eGFP+ and DsRed- cells at the venous pole of the heart (Figure 2.6), indicating that

the pacemaker cardiomyocytes in the IFT are late-differentiating relative to the remainder of the atrium and the ventricle. However, these data and others suggest that IFT cells differentiate earlier than SHF-derived OFT cells (de Pater et al., 2009), which proliferate for an extended period after heart tube formation prior to their differentiation (de Pater et al., 2009; Hami et al., 2011; Zeng and Yelon, 2014; Zhou et al., 2011). It will be interesting to determine whether additional IFT cells are appended to the venous pole at later stages in future studies.

These data pinpoint the timeframe and location during which IFT differentiation occurs, providing a foundation for future studies investigating open questions regarding the regulation of this process. For example, future experiments could evaluate which signaling pathways are active in and around IFT progenitor cells during this critical time period, leading to new hypotheses regarding the signals that trigger IFT differentiation. Extensions of these studies could probe the interesting question of why IFT cardiomyocytes differentiate later than the rest of the atrial population. Furthermore, it would be intriguing to examine the dynamics of the IFT as the heart continues to grow, as it is unclear whether the cells appended to the IFT prior to 24 hpf remain in the IFT or get taken up into the atrium and replaced by other pacemaker cardiomyocytes at later stages.

FUTURE DIRECTIONS FOR STUDIES OF THE ZEBRAFISH INFLOW TRACT

Taken together, the synthesis of these findings creates a dynamic biography of the zebrafish IFT (Figure 2.2). In our proposed timeline of IFT development, IFT progenitor cells originate in the ventral portion of the cardiogenic territory in the late blastula (Figure 2.2A). During gastrulation, the IFT progenitor cells come to reside in the lateral portion of the heart fields within the ALPM (Figure 2.2B). Then, together with the rest of the cardiac mesoderm, the IFT progenitors migrate toward the midline, retaining their relative position at the periphery of the field and initiating their differentiation along the outer circumference of the cardiac cone (Figure 2.2C). As the heart tube forms, IFT cardiomyocytes are appended to the venous pole of the atrium where they begin to function as pacemaker cells (Arrenberg et al., 2010). The IFT is retained as the heart tube matures (Figure 2.2E), and it continues to function as the primary pacemaker in the adult zebrafish heart (Tessadori et al., 2012).

Given the ease of studying the zebrafish IFT and its remarkable similarity to the murine SAN, the zebrafish can serve as a valuable model for studies aiming to provide new insight into the development of pacemaker cells. For example, it will be important for future studies to investigate exactly how cardiac progenitor cells in the early embryo are assigned to a pacemaker fate. This process seems to rely in part on canonical Wnt signaling. In chick

embryos, Wnt ligands are expressed near the presumptive pacemaker progenitor population during early somitogenesis (Bressan et al., 2013). Increasing Wnt activity in cardiac progenitors causes cells to adopt electrophysiological properties reminiscent of pacemaker cells, whereas reducing Wnt activity in pacemaker progenitors results in ectopic expression of the chamber marker *NKX2.5* (Bressan et al., 2013). These data suggest that Wnt signaling acts during early somitogenesis to promote pacemaker specification at the periphery of the heart fields, but the broad expression patterns of Wnt ligands suggest that other signals must also refine this population (Bressan et al., 2013). What other factors cooperate with canonical Wnt signaling to insure that the proper number of pacemaker progenitors is specified? It will be interesting to uncover factors that regulate IFT specification upstream of transcription factors such as Tbx18 and Shox2, and the zebrafish model is uniquely poised to provide insight on these topics.

Future studies in the zebrafish could also be used to answer open questions about the heart fields and their differentiation dynamics. Studies in mammalian and avian embryos have been inconclusive about whether the pacemaker population originates from the second heart field or from a distinct tertiary heart field. Populations within the venous pole have been shown to originate from a common second heart field lineage that also gives rise to the arterial pole (Bertrand et al., 2011; Domínguez et al., 2012; Lescroart et al., 2012; Rana et al., 2014; van den Berg et al., 2009). However, pacemaker cells

may be considered a discrete population from the posterior second heart field because they originate from a Tbx18+ Nkx2-5- population that arises after second heart field cells have already incorporated into the heart (Christoffels, 2006; Mommersteeg et al., 2010; Wiese et al., 2009). In zebrafish, it seems unlikely that IFT and OFT cardiomyocytes share a common lineage because the progenitor populations are located on opposite sides of the heart fields (Figure 2.2A-B). However, the clonal relationship between these cell populations has not yet been tested and deserves more rigorous study. Also, it remains to be seen whether there is plasticity within the OFT or IFT populations that could tie portions of these two late-differentiating structures to a common cellular lineage. On the other hand, future studies in zebrafish may determine that pacemaker cardiomyocytes originate in a tertiary heart field, defined as a discrete area in the ALPM that expresses neither Isl1 nor Nkx2.5 (Bressan et al., 2013). Alternatively, perhaps the notion of separate heart fields will prove to be inappropriate: cardiac progenitors may in fact differentiate in a continuous wave rather than in discrete phases, and live imaging of differentiating cardiomyocytes in zebrafish embryos could be used to address this possibility.

Finally, investigation of the zebrafish IFT could shed light on what regulates the differentiation of pacemaker cardiomyocytes, both during their initial differentiation phase and at later stages as the heart matures. One particularly interesting open question is how the pacemaker activity is confined

to a small territory within the heart. In zebrafish, the primary pacemaking activity is initially spread over a large territory that encompasses much of the atrium, but it becomes restricted to the IFT by 48 hpf and to a specific group of cells on the inner curvature of the sinoatrial junction at later stages (Arrenberg et al., 2010). This refinement process is conserved in chick embryos (Bressan et al., 2013; Kamino et al., 1981), but the mechanisms underlying refinement remain unknown. This refinement incorporates two processes: extinguishing pacemaking activity in unnecessary pacemaker cells, and imposing left-right asymmetry on the venous pole. It has been shown that left-right asymmetry relies on the homeobox transcription factor Pitx2, which represses SAN formation on the left side of the heart (Ammirabile et al., 2012; Mommersteeg et al., 2007b; Wang et al., 2010). However, even on the correct side of the heart, it remains unclear how pacemaking activity is refined from a broad territory to a small group of cells. This process of refinement affects some molecular markers of the IFT. For example, Bmp4, Hcn4, and a transgenic reporter linked to Fhf2a are initially broadly expressed and are then progressively refined in the venous pole (Chin et al., 1997; Poon et al., 2016; Vicente-Steijn et al., 2011). It will be interesting to identify factors that act upstream of these factors to restrict pacemaking activity within the IFT. Further study of the zebrafish IFT will provide novel insights into the patterning and regulation of pacemaker cardiomyocytes. Identifying the regulatory network that controls IFT differentiation in zebrafish is likely to be useful for

devising novel strategies for in vitro differentiation of pacemaker cardiomyocytes. Finally, it will be exciting to test whether zebrafish can be used to model diseases that affect the IFT, such as congenital arrhythmias, which would allow high-throughput testing of potential therapeutics.

MATERIALS AND METHODS

Zebrafish

We used the following zebrafish strains: *Tg(myl7:egfp)*^{twu277} (Huang et al., 2003) and *Tg(myl7:dsredt4)*^{sk74} (Garavito-Aguilar et al., 2010). All zebrafish husbandry and experiments followed IACUC-approved protocols.

In situ hybridization

In situ hybridization was performed as previously described (Schindler et al., 2014) using probes for *bmp4* (ZDB-GENE-980528-2059), *tbx18* (ZDB-GENE-020529-2), *shox2* (ZDB-GENE-040426-1457), *hcn4* (ZDB-GENE-050420-360), and *isl1* (ZDB-GENE-980526-112).

Immunofluorescence

Immunofluorescence was performed as previously described (Schindler et al., 2014) using the monoclonal antibody MF20 (Developmental Studies Hybridoma Bank) and a polyclonal antibody against Islet1 (GeneTex; GTX128201L). The secondary antibodies used were goat anti-mouse IgG2 TRITC (Southern Biotech 1090-03), goat anti-rabbit Alexa Fluor 488 (Life Technologies A11008), and goat anti-rabbit Alexa Fluor 568 (Life Technologies A11011).

Imaging

In situ images were captured using a Zeiss Axioplan and Axiocam and processed using Zeiss Axiovision and Adobe Creative Suite software. Immunofluorescence images were captured using a Leica SP5 confocal laser-scanning microscope and analyzed using Imaris software (Bitplane) and ImageJ. All confocal images shown are 3D reconstructions.

Fate map analysis

Previously generated data sets were analyzed to approximate the locations of IFT progenitor cells in the early embryo. These include several sets of previously published experiments (Keegan et al., 2005, 2004; Schoenebeck et al., 2007), as well as additional unpublished data from prior experiments. For each experimental embryo, available data indicate the initial position of the labeled cells and the subsequent location of the labeled progeny within the MF20-labeled heart at 48 hpf. Because IFT molecular markers were not used when generating these data sets, we used morphological criteria to score contribution of labeled progeny to the IFT. Specifically, we scored cardiomyocytes as IFT if they were located in the bottom 30% of the atrium, close to the venous pole rather than the atrioventricular canal. Instances in which the available information was insufficient to judge IFT contribution were excluded from this analysis.

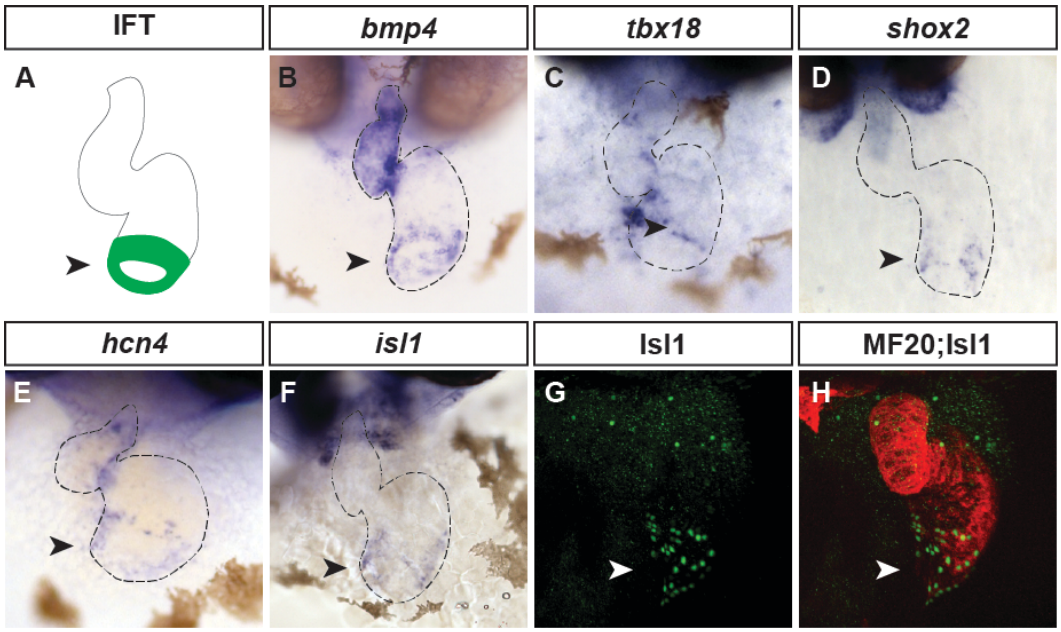

Figure 2.1.
Inflow tract cardiomyocytes express a set of pacemaker markers.
(A-H) Frontal views depict the embryonic zebrafish heart at 48 hours post fertilization (hpf); arrowheads indicate the inflow tract (IFT).
(A) Schematic outlines the embryonic ventricle and atrium; green territory highlights the IFT, a ring of tissue at the base of the atrium.
(B-F) *In situ* hybridization reveals expression of the pacemaker markers *bmp4* (B), *tbx18* (C), *shox2* (D), *hcn4* (E), and *isl1* (F) in the IFT; dashed lines outline the cardiac chambers. (G-H) Immunofluorescence indicates Isl1 localization in the nuclei of the IFT cardiomyocytes (green in G,H). The MF20 antibody marks the myocardium (red, H). Quantification of Isl1+ nuclei in the IFT yields an average of 31.5 IFT cells in wild-type embryos at 48 hpf (n=14; standard deviation=5.5).

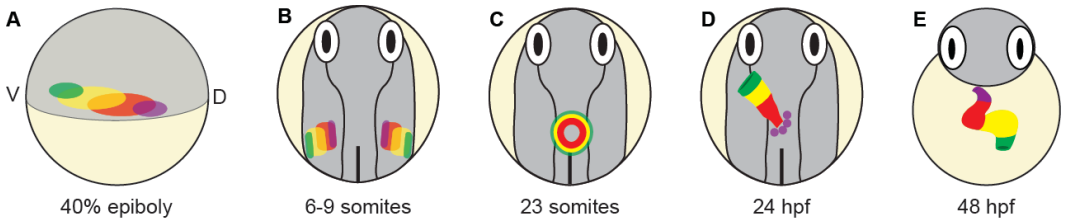

Figure 2.2.
A biography of IFT cardiomyocytes.
(A-E) Schematics depict the regions in the zebrafish embryo that give rise to the myocardium of the IFT (green), the atrial chamber (AC, yellow), the ventricular chamber (red), and the OFT (purple).
(A) Lateral view of the blastula at 40% epiboly, before gastrulation begins; D and V indicate the dorsal and ventral (V) sides of the embryo. Ovals indicate the territories that have been shown to contain ventricular and atrial progenitor cells (Keegan et al., 2004), as well as progenitors of the OFT lineage (Hami et al., 2011). The ventral location of the IFT progenitors is derived from the data presented here (Fig. 2.3).
(B) Dorsal view of the gastrula at 6-9 somites, highlighting the territories within the anterior lateral plate mesoderm (ALPM) that have been shown to contain ventricular and atrial progenitors (Schoenebeck et al., 2007)and OFT progenitors (Hami et al., 2011). The lateral location of the IFT progenitors is derived from the data presented here (Fig. 2.4).
(C) Dorsal view at 23 somites illustrates how differentiated ventricular and atrial cardiomyocytes form the cardiac cone at the embryonic midline (Berdougo et al., 2003). The location of the differentiating IFT precursors around the periphery of the cone reflects the data presented here (Fig. 2.5).
(D) Dorsal view at 24 hpf shows the position of the elongating heart tube, with OFT progenitors located near the arterial pole (Lazic and Scott, 2011; Zeng and Yelon, 2014; Zhou et al., 2011). At this stage, IFT cardiomyocytes are appended to the venous pole of the atrium and begin initiating the heartbeat (Arrenberg et al., 2010; de Pater et al., 2009).
(E) Frontal view at 48 hpf. As the heart loops and matures, OFT cells append to the arterial pole (de Pater et al., 2009). IFT cells remain at the base of the atrium and continue to serve as the primary cardiac pacemaker (Arrenberg et al., 2010).

A

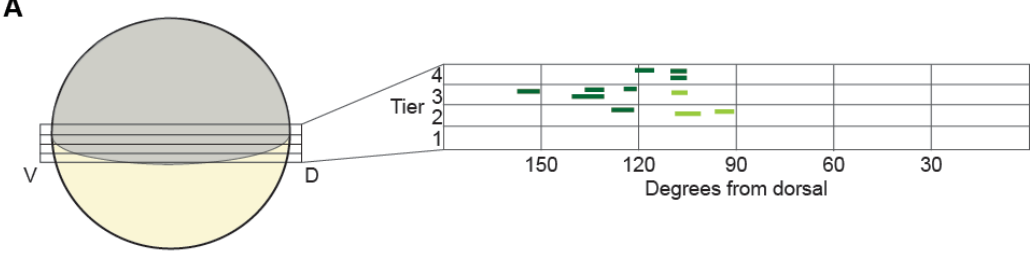

B

Tier	Degrees	Side	Progeny
2	92-98	L	AC and IFT
2	101-109	L	AC and IFT
2	122-129	L	IFT
3	105-110	L	AC and IFT
3	121-125	L	IFT
3	130-136	R	IFT
3	130-140	R	IFT
3	153-160	L	IFT
4	105-110	L	IFT
4	105-110	L	IFT
4	115-121	R	IFT

Figure 2.3.
IFT progenitors originate from a ventral portion of the lateral margin.
(A) In previous experiments (Keegan et al., 2005, 2004), fate mapping of cardiac progenitors was performed by injecting a caged fluorescein-dextran lineage tracer at the single-cell stage, followed by uncaging in small groups of cells at 40% epiboly and subsequent analysis of cell fates at 48 hpf. For each set of labeled cells, their location at 40% epiboly was recorded in terms of latitude, using cell tiers to measure distance from the margin, and longitude, using degrees from the dorsal midline. By revisiting previously published fate mapping data (Keegan et al., 2005, 2004) and unpublished data, we identified eight examples (dark green) in which labeled cells contributed to the IFT. We also found an additional three examples (light green) in which labeled cells contributed to both the IFT and the AC. In all 11 examples, IFT progenitors were located in tiers 2-4, between 92 and 160 degrees from dorsal.
(B) Table lists each instance of IFT labeling, indicating the cell tier, degrees from dorsal, and side (left or right indicated by L or R, respectively) at 40% epiboly, as well as the final myocardial contribution of the labeled progeny at 48 hpf.

A

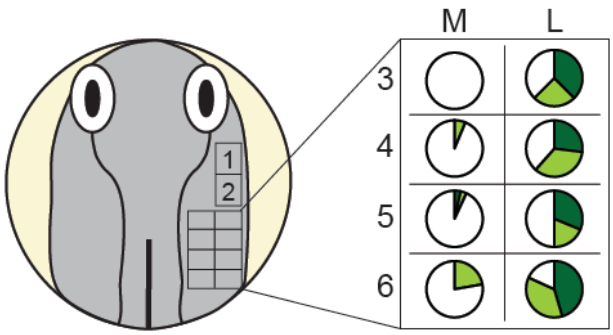

B

Zone	Medial				Lateral			
	IFT	IFT & AC	Total	%	IFT	IFT & AC	Total	%
3	0	0	20	0%	6	4	16	62.5%
4	0	1	16	6.3%	7	9	26	61.5%
5	1	1	26	7.7%	5	3	16	50%
6	0	2	9	22.2%	5	4	11	81.8%

Figure 2.4.
IFT progenitors reside in lateral portions of the heart fields.
(A) In previous experiments (Schoenebeck et al., 2007), fate mapping of cardiac progenitors was performed by uncaging a caged fluorescein-dextran lineage tracer in small groups of cells within the ALPM at 6-9 somites, followed by analysis of cell fates at 48 hpf. For each set of labeled cells, their location in the ALPM was categorized into one of six zones, with zone 1 in the anterior and zone 6 in the posterior portion of the ALPM, using the tip of the notochord as a landmark along the anterior-posterior axis. Zones 3-6 were further subdivided into medial and lateral portions based on distance from the midline. By revisiting previously published fate mapping data (Schoenebeck et al., 2007) and unpublished data, we identified 24 examples in which labeled cells contributed to the IFT, plus an additional 24 examples in which labeled cells contributed to both the IFT and the AC. Pie charts represent the proportion of experiments that labeled IFT myocardium (dark green), IFT and AC myocardium (light green), or non-IFT myocardium (white) for each zone of the ALPM.
(B) Table indicates the frequency of IFT labeling, organized by zone. The “total” column lists the total number of experiments in which myocardium was labeled, and the “percentage” column lists the percentage of these experiments in which either the IFT or the IFT and AC were labeled. Experiments that did not result in any myocardial labeling were excluded in this analysis.

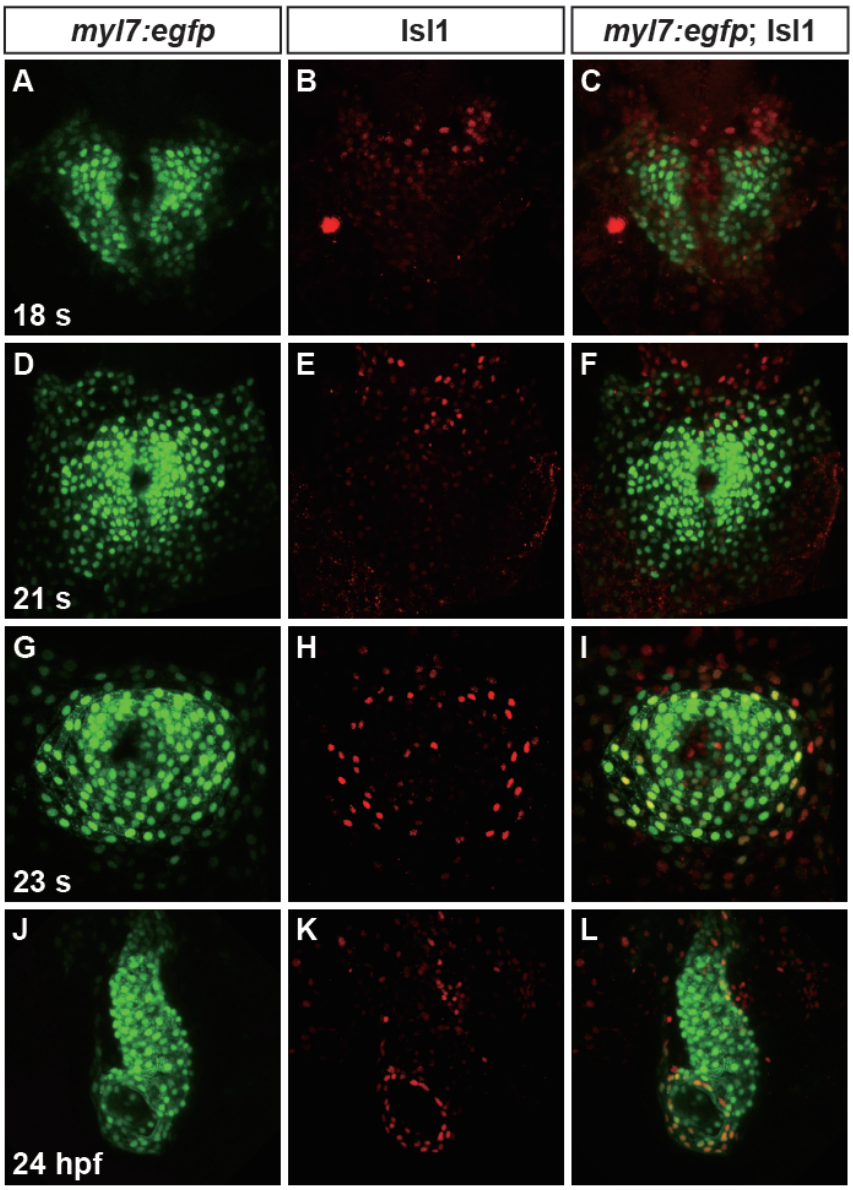

Figure 2.5.
IFT cardiomyocytes emerge by 23 somites and append to the venous pole of the heart tube.
(A-L) Immunofluorescence in *Tg(myl7:egfp)* embryos indicates nuclear localization of Isl1 (red) in cells within and near the differentiated myocardium (green). (A-I) Dorsal views, anterior toward the top. Examination of Isl1 localization at 18 somites (A-C), 21 somites (D-F), and 23 somites suggests that the differentiation of IFT cardiomyocytes commences between 21 and 23 somites, when these cells are positioned at the periphery of the cardiac cone. **(J-L)** Lateral view of the heart tube, arterial pole toward the top. By 24 hpf, IFT cardiomyocytes are present in the venous pole of the heart tube.

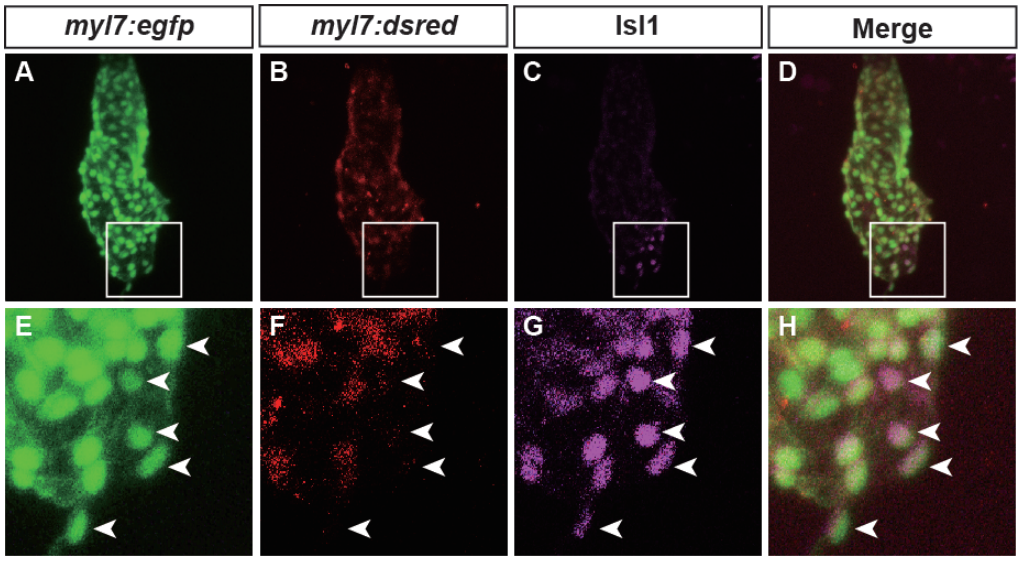

Figure 2.6.
IFT cardiomyocytes differentiate after atrial chamber cardiomyocytes.
(A-H) Immunofluorescence with an antibody against Isl1 combined with visualization of native eGFP and DsRed in *Tg(myl7:egfp);Tg(myl7:dsred)* embryos indicates the location of late-differentiating cells (eGFP+/DsRed-; (de Pater et al., 2009; Lepilina et al., 2006) and Isl1+ cells (purple) within the heart at 36 hpf. Frontal views, arterial pole toward the top. Panels E-H are enlarged versions of the boxed areas in panels A-D; arrowheads indicate eGFP+/DsRed-/Isl1+ cardiomyocytes. (A,E) eGFP becomes visible rapidly after the *myl7* promoter becomes active in differentiated cardiomyocytes. (B,F) DsRed becomes visible approximately 24 hours after the *myl7* promoter becomes active in differentiated cardiomyocytes, due to slower protein folding. (C,D,G,H) Most Isl1+ cardiomyocytes are eGFP+ and DsRed- at 36 hpf, indicating that they are late-differentiating.

ACKNOWLEDGMENTS

A modified version of Chapter 2 will be submitted for publication as a Resource Article in *Developmental Biology* (Knight, Hannah; Ren, Jie; Chi, Neil; Yelon, Deborah. “Patterning and differentiation of the cardiac inflow tract in zebrafish”). Please note that a portion of the material presented in Chapter 2 is redundant with a portion of the introductory content presented in Chapter 1. Hannah Knight and Jie Ren designed and performed the experiments presented in Chapter 2, interpreted the data, and coauthored the manuscript. Neil Chi and Deborah Yelon designed experiments, interpreted the data, and contributed to the editing of the manuscript. Hannah Knight was the primary investigator and author of this material.

Chapter 3: Hedgehog signaling restricts formation of the cardiac inflow tract in zebrafish

ABSTRACT

Cardiac pacemaking activity is confined to a specialized population of cells in the cardiac inflow tract (IFT), but the patterning processes that establish IFT dimensions remain unknown. Here, we demonstrate that Hedgehog (Hh) signaling has a potent effect on limiting the number of IFT cells in the embryonic zebrafish heart. Using both genetic and pharmacological manipulations of the Hh pathway, we find that loss of Hh signaling results in a significantly expanded IFT. Conversely, reduction of Bmp signaling dramatically diminishes IFT production and hinders IFT maintenance. Through temporal inhibition of each pathway, we show that Hh and Bmp signaling are both required in the same timeframe, prior to cardiac differentiation, to establish the normal number of IFT cardiomyocytes. Remarkably, simultaneous reduction of both Hh and Bmp signaling restores the IFT population to a relatively normal size, suggesting that these pathways act in opposition during IFT patterning. We therefore propose a model in which IFT specification relies on both low levels of Hh signaling and high levels of Bmp signaling, which together set appropriate boundaries for the IFT progenitor population.

INTRODUCTION

The mature heart is comprised of multiple types of specialized cardiomyocytes, each with distinct functional attributes. However, the patterning mechanisms that specify discrete populations of cardiac progenitors are not well understood. For instance, it is known that pacemaking activity is confined to a small population of specialized cardiomyocytes located in a discrete region at the sinoatrial junction (Monfredi et al., 2010), but it is unclear which factors regulate the allocation of an appropriate proportion of pacemaker cells (Chapter 2). As a step toward understanding the complex genetic networks that underlie cardiac patterning, we have sought to elucidate which signaling pathways control specification of the pacemaker progenitor population.

Pacemaker cells originate from late-differentiating cardiac progenitors that are appended to the venous pole after the primitive atrium has formed (Christoffels, 2006; Mommersteeg et al., 2010). In this *Tbx18*-expressing lineage, several transcription factors, including Tbx18, Tbx2, Tbx3, Isl1, and Shox2, drive pacemaker differentiation (van Weerd and Christoffels, 2016). The signals that lie upstream of this genetic program remain relatively mysterious, although a few pathways have been implicated in the process. For example, Wnt signaling has been identified as a positive regulator of pacemaker development (Bressan et al., 2013). Furthermore, it is known that venous pole development is positively regulated by retinoic acid signaling via

Tbx5 activation (Niederreither et al., 2001). However, we do not yet have a complete picture of how signaling pathways interact to create a population of pacemaker cells that is sufficiently large but also restricted to the right size and location.

We have chosen to use zebrafish as a model organism in which to study the early patterning processes that ultimately give rise to pacemaker cells. In the embryonic zebrafish heart, pacemaker cells are located within a specific territory, referred to as the inflow tract (IFT), that appears to be the functional equivalent of the mammalian sinoatrial node (SAN; Chapter 2). Like the SAN, the zebrafish IFT initiates the heartbeat and demonstrates pacemaker activity at both embryonic and adult stages (Arrenberg et al., 2010; Tessadori et al., 2012), and cells in the IFT express genes in the pacemaker differentiation program, including *isl1*, *bmp4,* and *hcn4* (Chin et al., 1997; Poon et al., 2016; Witzel et al., 2012). Furthermore, zebrafish IFT development seems to depend on the transcription factor Isl1, as does SAN development; *isl1* mutant zebrafish lack expression of pacemaker genes in the IFT and also display bradycardia (de Pater et al., 2009). Thus, analysis of the regulation of zebrafish IFT formation has the potential to provide new insight into the genetic pathways that establish the pacemaker lineage.

Our work demonstrates a novel role for Hedgehog (Hh) signaling during IFT development. Prior studies have indicated that the Hh pathway promotes the initial specification of cardiac progenitor cells. In both mouse and

zebrafish, mutations in *smoothened (smo)*, which encodes the transmembrane protein responsible for Hh signal transduction, result in formation of a small heart (Thomas et al., 2008; Zhang et al., 2001). This phenotype arises due to defects in mesodermal patterning: in zebrafish, Hh signaling is required cell-autonomously during and shortly after gastrulation to maximize the number of mesodermal cells that adopt cardiac fate (Thomas et al., 2008). In addition, several studies suggest that Hh signaling is a key component in second heart field (SHF) development. Hh signaling promotes formation of the outflow tract (OFT) from progenitor cells within the SHF: in mouse, embryos with reduced Hh signaling (hereafter referred to as Hh-deficient embryos) have a diminished OFT with septal defects (Goddeeris et al., 2007; Lin et al., 2006; Washington Smoak et al., 2005), and, in zebrafish, *smo* mutant embryos show severely reduced incorporation of SHF cells into the OFT (Hami et al., 2011). Hh signaling is also required for the formation of septa by cells from the murine posterior SHF. Hh-deficient embryos have atrioventricular septation defects (Goddeeris et al., 2008), and Hh signaling is required for migration of SHF cells into the atrial septum (Hoffmann et al., 2009). Despite the attention paid to Hh signaling during venous pole septation, the involvement of Hh signaling in formation of the appropriate number of cardiac IFT or SAN cells at the venous pole has remained unstudied.

Here, we demonstrate that Hh signaling is required during early stages of cardiac patterning to define the size of the zebrafish IFT. In contrast to other

roles of the Hh pathway in promoting cardiomyocyte production, we find that Hh signaling restricts formation of IFT cardiomyocytes: reduced Hh activity results in an enlarged IFT. This phenotype arises due to Hh signaling prior to cardiac differentiation, suggesting an influence on the specification of IFT progenitor cells. Interestingly, Bmp signaling acts during a similar timeframe to promote formation of IFT cardiomyocytes: reduced Bmp activity results in a severely diminished IFT. Intriguingly, reducing both Hh and Bmp signaling restores the IFT to a nearly normal size, suggesting that Hh and Bmp signaling work together to set the dimensions of the IFT population. Synthesizing these data, we propose that Hh and Bmp signaling pattern cardiac progenitors in order to assign an appropriate proportion to an IFT fate.

RESULTS

Loss of Hh signaling causes expansion of the cardiac IFT

While analyzing the hearts of embryos with reduced Hh activity, we were intrigued to discover that *bmp4*, an IFT marker, is dramatically expanded in *smo* mutant embryos at 48 hours post fertilization (hpf) (Figure 3.1A-B). In contrast to the narrow ring of *bmp4* expression that marks the IFT at the venous pole of the wild-type atrium, *bmp4* is expressed in a larger territory at the venous pole of the *smo* mutant heart, beginning from the inlet at the base of the atrium and extending upward. Several other IFT markers are expressed in the same pattern: *hcn4, tbx18, shox2*, and Isl1 are similarly expanded in *smo* relative to wild-type siblings (Figure 3.1C-J). Using nuclear localization of Isl1 to quantify the number of IFT cardiomyocytes at 48 hpf, we observe that IFT cell number is roughly 50% higher in *smo* mutants than in wild-type (Figure 3.2G). This phenotype is particularly striking because the total number of atrial and ventricular cardiomyocytes is substantially smaller in *smo* mutants (Thomas et al., 2008), indicating that the expansion of the IFT cardiomyocyte population is present in the context of a general reduction in heart size. Thus, these data reveal a novel and unexpected requirement for Hh signaling in restricting the dimensions of the cardiac IFT.

Since cells in the IFT act as the cardiac pacemaker, we examined heart rate and rhythm in *smo* mutant embryos. *smo* mutants exhibit a significantly reduced heart rate at 48 hpf, compared to their wild-type siblings (Table 3.1,

$p<0.0001$). In addition to observing bradycardia, we also noted arrhythmia in some *smo* mutants (Table 3.1). Within this arrhythmic group, some embryos displayed an additional abnormal phenotype in which cardiac contraction occasionally initiates outside the IFT, contrasting with normal heartbeats in which the IFT initiates the contraction. It is unclear whether the abnormal heart rate and rhythm in *smo* mutants arise due to the expanded IFT or due to other defects in the chamber myocardium. However, in mouse, failure to restrict expression of pacemaker markers can result in atrial arrhythmia (Wang et al., 2010), suggesting that a similar mechanism may cause functional defects in *smo*. These data reveal that Hh signaling is required for normal cardiac function in addition to delimiting the size of the IFT.

Hh signaling limits IFT size prior to the onset of myocardial differentiation

We wondered whether Hh activity restricts IFT expansion after the heart tube forms, perhaps by preventing unchecked growth of the IFT population. In wild-type embryos*, bmp4* is initially expressed throughout the heart tube (Chin et al., 1997), with its restricted expression in the IFT becoming apparent by 32 hpf (Figure 3.2A). Intriguingly, as early as 32 hpf, *bmp4* is expressed in a broader area and at higher levels in *smo* mutants relative to their wild-type siblings (Figure 3.2A-B). This expansion in *bmp4* expression is maintained through at least 48 hpf (Figure 3.2C-F). In addition, we quantified the number

of Isl1+ IFT cardiomyocytes at 24 hpf, just after heart tube formation, as well as at 32 hpf. In wild-type embryos, we find that the number of IFT cells is quite consistent between 24 hpf and 48 hpf, indicating that this population is established prior to 24 hpf and then maintained as the heart matures (Figure 3.2G). In *smo* mutants, we observe an increase in the number of Isl1+ IFT cells at both 24 hpf and 32 hpf. Notably, these data indicate that the degree of IFT expansion in *smo* is maintained consistently from 24 hpf through at least 48 hpf (Figure 3.2G). This consistency suggests that Hh signaling suggests that Hh signaling acts prior to heart tube formation to restrict IFT cell number.

Next, we shifted our attention to earlier stages to ask when Hh activity is required to limit the size of the IFT. Prior work in zebrafish has suggested that the critical period for cardiac progenitor specification occurs during gastrulation and early somitogenesis (Marques et al., 2008; Thomas et al., 2008; Marques and Yelon, 2009; Keegan et al., 2005), prior to the onset of myocardial differentiation around the 13 somite stage (Yelon et al., 1999). To test whether Hh signaling delimits the IFT population during these cardiac specification stages, we utilized cyclopamine (CyA), a potent pharmacological inhibitor of Smo (Cooper et al., 1998). When CyA is added during gastrulation (at dome stage) or just after gastrulation (at tailbud stage or at 3 somites), loss of Hh signaling results in an increase in the number of Isl1+ cells in the IFT (Figure 3.3A). In these embryos, the size and morphology of both the IFT and cardiac chambers are comparable to what is observed in *smo* mutants (Figure

3.3A and data not shown). However, when CyA is applied during mid-somitogenesis stages (at 6 somites or beyond), there is no change in the number of IFT cardiomyocytes (Figure 3.3A) and the hearts appear comparable to controls (data not shown). Similarly, CyA treatment during or just after gastrulation results in expanded *bmp4* expression in the IFT (Figure 3.3F-G), as seen in *smo* (Figure 3.1F). However, application of CyA during mid-somitogenesis does not alter *bmp4* expression (Figure 3.3H and data not shown), resulting in a heart that is indistinguishable from controls (Figure 3.3F). These data indicate that Hh signaling acts prior to myocardial differentiation to restrict IFT cell number, potentially by setting limits on IFT progenitor specification.

Interestingly, Hh signaling acts during this same timeframe to promote production of ventricular cardiomyocytes (Thomas et al., 2008). In this prior study, we considered analysis of the ventricular population to be representative of both chambers, but our new IFT observations motivated us to explicitly test whether Hh signaling also promotes atrial cardiomyocyte production during this critical time period. We treated embryos with CyA and then counted *amhc*-expressing cells at 22 somites, a convenient stage for visualization of atrial cardiomyocytes prior to heart tube formation. We found that inhibition of Hh activity during or just after gastrulation reduces the number of *amhc*-expressing atrial cells, whereas CyA treatment during somitogenesis leaves the atrial population intact (Figure 3.3B-E). These data indicate that Hh

signaling plays contrasting roles during cardiac specification stages, simultaneously promoting production of atrial and ventricular cells while also limiting the number of IFT cells.

Increased Hh activity does not affect IFT size

Our data thus far suggested the hypothesis that Hh activity above a certain threshold could preclude specification of IFT progenitor cells. To test this, we next asked whether a heightened dose of Hh activity would reduce IFT size. To increase Hh activity, we overexpressed the Hh ligand *sonic hedgehog* (*shh*) throughout the embryo, via injection of *shh* mRNA (Ekker et al., 1995; Krauss et al., 1993). We have previously shown that *shh* overexpression results in production of more cardiomyocytes in both the ventricle and the atrium (Thomas et al., 2008). Here, in order to distinguish IFT cardiomyocytes from the rest of the atrium, we quantified Isl1+ IFT cells separate from Isl1- atrial cells. As expected from our prior studies, we observed an increase in the number of Isl1- atrial cells upon *shh* overexpression (Figure 3.4A-C). However, IFT size is unchanged in response to increased Hh activity (Figure 3.4A-E). Similarly, *bmp4* expression is retained in the IFT of embryos overexpressing *shh* (Figure 3.4F-G). Thus, while Hh activity is necessary to prevent IFT expansion, increased Hh activity is not sufficient to depress the IFT population beyond its usual size.

This finding contrasts sharply with the positive response to increased Hh activity in other cardiomyocyte populations. As mentioned above, *shh* overexpression expands the total number of ventricular and atrial cardiomyocytes (Thomas et al., 2008 and Figure 3.4A-C). In addition, *shh* overexpression results in an expansion of the expression of *ltbp3* (Figure 3.5A-B), which marks OFT progenitors in the SHF (Zhou et al., 2011). Since the OFT, ventricular, and atrial populations are also reduced in *smo* embryos (Hami et al., 2011; Thomas et al., 2008; Figure 3.5C), it seems that these three populations all respond in a reciprocal fashion to loss and gain of Hh activity. This is distinct from the response of the IFT population, which expands in response to reduced Hh signaling but appears unaffected by increased levels of Hh. Thus, we suggest that there may be two separable roles for Hh signaling during cardiac specification stages: in addition to its role in promoting production of atrial, ventricular, and OFT cells, Hh signaling also acts separately to inhibit production of IFT cells.

Nkx2.5 acts downstream of Hh signaling to restrict IFT development

We next asked how this novel role for Hh signaling fits into the genetic network that regulates IFT formation. We envision that the Hh pathway interacts with other factors in order to determine the dimensions of the IFT, including other signaling pathways and downstream transcription factors. Because Nkx2.5 is a well-established repressor of the pacemaker

differentiation program (Espinoza-Lewis et al., 2011; Mommersteeg et al., 2007a, 2007b; Ye et al., 2015), we hypothesized that Nkx2.5 may act downstream of Hh activity to restrict IFT size. Indeed, prior studies have observed altered *nkx2.5* expression in the anterior lateral plate mesoderm (ALPM) of both *smo* mutants and CyA-treated embryos (Zhang et al., 2001; Thomas et al., 2008). By revisiting this aspect of the phenotype, we have found that the distribution of *nkx2.5* expression is comparable in Hh-deficient embryos and their normal siblings, but that the intensity of *nkx2.5* expression is reduced in Hh-deficient embryos (Figure 3.6). These data suggest that low levels of *nkx2.5* expression in Hh-deficient embryos could contribute to the formation of an enlarged IFT.

We next asked whether increasing the levels of *nkx2.5* expression could prevent IFT expansion in Hh-deficient embryos. Recent studies have shown that overexpression of *nkx2.5* after IFT differentiation can inhibit *isl1* expression in the IFT (Kimara Targoff and Sophie Colombo, Columbia University Medical Center, personal communication), but it remains unknown whether *nkx2.5* also restricts IFT progenitor specification. To test this, we examined whether increasing *nkx2.5* expression prior to IFT differentiation could rescue the expanded IFT phenotype in CyA-treated embryos. In these experiments, we used the transgene *Tg(hsp70l:nkx2.5-EGFP)*, which drives expression of *nkx2.5* under control of a heat-inducible promoter and has been previously shown to rescue *nkx2.5* mutants (George et al., 2015). Both

transgenic embryos and non-transgenic siblings were treated with CyA at dome stage, and then all embryos were heat-shocked at 3 somites to induce transient *nkx2.5* overexpression (Figure 3.7A). We chose this stage for induction because endogenous *nkx2.5* expression begins at approximately 3 somites (Lee et al., 1996) and because this stage is within the timeframe when cardiac progenitor specification is underway. In wild-type embryos treated with CyA, the number of Isl1+ cells in the IFT is increased at 48 hpf relative to wild-type controls (Figure 3.7B-D), as previously observed (Figure 3.3A). *Tg(hsp70l:nkx2.5-EGFP)* embryos treated with CyA display an intermediate phenotype, in which the number of Isl1+ cells is lower than in nontransgenic CyA-treated siblings but still significantly elevated relative to wild-type controls ($p=0.045$, Figure 3.7B-D,F). Thus, *nkx2.5* overexpression can attenuate the IFT expansion in Hh-deficient embryos, but the limited degree of rescue observed suggests that Hh signaling relies on additional factors, beyond Nkx2.5, to regulate the size of the IFT.

Bmp signaling promotes IFT development

We next asked how Hh-mediated restriction of the IFT population is balanced during cardiac patterning. We envision that other signaling pathways promote IFT progenitor specification, counteracting Hh activity to result in the appropriate IFT dimensions. The Bmp pathway is an appealing candidate for this role. Prior work in zebrafish has shown that Bmp signaling acts during

cardiac specification stages to promote cardiomyocyte formation, with a particularly potent effect on promoting the production of atrial cardiomyocytes (de Pater et al., 2012; Marques and Yelon, 2009). Additionally, in the murine venous pole, Bmp signaling supports the proliferation of SHF cells and their contribution to atrioventricular septation (Briggs et al., 2013). However, it has not yet been determined whether Bmp activity is required for development of pacemaker cells at the venous pole.

Examination of the effects of a mutation in the type I Bmp receptor gene *alk8,* also known as *laf* (Bauer et al., 2001; Mintzer et al., 2001; Mullins et al., 1996)*,* revealed that reduction of Bmp signaling results in formation of a small atrium with a diminished IFT at 48 hpf (Figure 3.8, 3.9A). Whereas wild-type embryos exhibit discrete expression of *bmp4, tbx18,* and *shox2* in the IFT (Figure 3.8A,C,E), *laf* mutants do not display concentrated expression of these genes at the venous pole (Figure 3.8B,D,F). Similarly, *laf* mutant hearts typically contain very few Isl+ IFT cells at 48 hpf (Figure 3.8H, 3.9A). Quantification of the number of Isl1+ cells revealed that the IFT in *laf* embryos is already reduced at 24 hpf (Figure 3.9A), indicating that Bmp signaling promotes IFT cardiomyocyte production prior to heart tube formation. Interestingly, the *laf* mutant IFT continues to diminish between 24 hpf and 48 hpf (Figure 3.9A), suggesting that Bmp signaling may play an additional role in maintenance of the IFT population after it has already differentiated. These

data indicate that Bmp signaling is required for the establishment of an appropriately sized IFT.

In order to evaluate whether Bmp signaling, like Hh signaling, influences IFT size during cardiac specification stages, we utilized dorsomorphin (DM), a small molecule antagonist of type I Bmp receptors (Yu et al., 2008), to reduce Bmp activity at different timepoints. Addition of DM at dome stage reduces the IFT dramatically (Figure 3.9B), resulting in a heart and IFT that are comparable to *laf* mutants (data not shown). However, addition of DM at tailbud stage results in a more modest deficit in IFT cell number relative to wild-type (Figure 3.9B), suggesting that Bmp activity has a particularly potent effect on IFT specification during gastrulation. When DM is applied at 24 hpf, the IFT is mildly reduced by 48 hpf (Figure 3.9B), comparable to the loss of IFT cells that emerges during the same timeframe in *laf* (Figure 3.9A). Altogether, these data support a requirement for Bmp signaling both during IFT specification and IFT maintenance, with the major impact of Bmp activity occurring during early phases of cardiac patterning, when Bmp and Hh signaling may interact to define IFT size.

Bmp signaling acts in opposition to Hh signaling during IFT formation

We hypothesized that Hh and Bmp signaling may act in the same pathway to direct IFT specification. To test this, we generated *smo;laf* double mutant embryos that have reductions in both Hh and Bmp signaling. Classical

epistasis between *smo* and *laf* would result in *smo;laf* double mutants exhibiting either an expanded IFT, similar to *smo*, or a minimal IFT, similar to *laf.* Alternatively, a less direct interaction between the two pathways, such as convergence on the same target genes, could result in *smo;laf* double mutants displaying an intermediate phenotype, potentially reminiscent of the wild-type IFT. Indeed, the IFT in *smo;laf* double mutant embryos is fairly similar to the wild-type IFT. For example, in contrast to the enlarged IFT we observe in *smo* (Figure 3.1J, 3.2G) and the diminished IFT we observe in *laf* (Figure 3.8H, 3.9A)*, smo;laf* double mutants show an intermediate phenotype in which expression of *bmp4* is restored to a relatively normal pattern in the IFT (Figure 3.10A,D). Additionally, the number of Isl1+ IFT cells in *smo;laf* double mutants is more similar to the number of cells in wild-type siblings than to the number in either single mutant (Figure 3.10B-C, E-G). This phenotype is particularly remarkable because it occurs in the context of a very small heart in *smo;laf* double mutants (data not shown). Taken together, these data suggest that Hh and Bmp signaling act in opposition during cardiac patterning in order to generate an appropriately sized IFT population.

DISCUSSION

Taken together, our studies highlight novel roles for both Hh and Bmp signaling in defining the size of the cardiac IFT. Embryos with reduced Hh activity have an enlarged IFT, indicating that Hh activity is required to restrict IFT cell number. Conversely, embryos with reduced Bmp activity have a diminished IFT, indicating that Bmp signaling promotes production of IFT cells. These two pathways both exert their influence on the size of the IFT population prior to myocardial differentiation, presumably during specification of the IFT lineage. Furthermore, Hh and Bmp signaling seem to counteract each other, as reducing both signals results in a relatively normal IFT. Based on these findings, we propose that the restrictive influence of Hh signaling and the inductive influence of Bmp signaling converge to set appropriate boundaries for the IFT progenitor population.

The newly identified requirement for Hh activity during IFT patterning is notable for two reasons: its restrictive nature and its timing. The role of Hh signaling in limiting the production of IFT cardiomyocytes is in stark contrast to its role in promoting the formation of other cardiomyocyte populations, as in the zebrafish atrium and ventricle (Thomas et al., 2008), the zebrafish OFT (Hami et al., 2011), the murine heart tube (Zhang et al., 2001), the murine OFT (Goddeeris et al., 2007; Lin et al., 2006; Washington Smoak et al., 2005), and the murine atrial septum (Goddeeris et al., 2008; Hoffmann et al., 2009). Furthermore, in several of these contexts, Hh activity is required at later

stages in development, after myocardial differentiation has already begun, whereas we find that Hh signaling influences IFT formation during and just after gastrulation, before the onset of differentiation. We therefore favor the interpretation that Hh signaling acts to delimit the specification of IFT progenitor cells within the ALPM. Importantly, this idea has not yet been directly tested through fate mapping experiments or through analysis of an IFT progenitor marker. At present, no molecular markers specific to IFT progenitors within the ALPM have been identified. In future studies, it will be worthwhile to evaluate whether and how IFT specification is expanded in Hh-deficient embryos. These studies will also reveal precisely which other population is reduced in order to generate excess IFT cells in Hh-deficient embryos.

Our data also illuminate important roles for Bmp signaling during IFT formation. The proposed requirement for Bmp activity during IFT specification is consistent with our previous findings: our previous work has shown that Bmp signaling acts during cardiac specification stages to promote production of atrial cardiomyocytes (Marques and Yelon, 2009), just as it seems to do for production of IFT cells. Our finding that Bmp signaling is required for maintenance of IFT cardiomyocytes is novel, while also being consistent with previous studies showing that Bmp activity is required during differentiation stages to promote cardiomyocyte production in both the zebrafish atrium and the murine venous pole (Briggs et al., 2013; de Pater et al., 2009). Given that

the Bmp ligand *bmp4* is expressed within the IFT, we posit that paracrine Bmp signaling within the IFT is required for survival of this population or for reinforcement of IFT fate. Future experiments investigating how Bmp activity promotes specification and maintenance of the pacemaker cell population will extend our knowledge about this important cardiac population.

It is important to note that our data do not indicate where Hh and Bmp signaling are active during cardiac specification stages, relative to the locations of the IFT progenitor cells. During these stages, Bmp ligands are produced on the ventral side of the embryo, and Bmp activity is highest ventrally and low on the dorsal side (Chin et al., 1997; Nikaido et al., 1997; Tucker et al., 2008), whereas Hh ligands are produced on the dorsal side of the embryo, resulting in high Hh activity in dorsal tissues (Concordet et al., 1996; Currie and Ingham, 1996; Ekker et al., 1995; Krauss et al., 1993; Lewis et al., 1999). Cardiac progenitor cells arise in between these positions, at the lateral margin on both the left and right sides of the embryo (Keegan et al., 2004). Notably, our fate maps of the wild-type embryo suggest that IFT progenitor cells are located at the ventral edge of the lateral marginal zone, near the source of Bmp ligands and far from the source of Hh ligands (Chapter 2). This layout is consistent with a model in which IFT specification occurs in cells that experience robust Bmp activity and limited Hh activity. We also suspect that Bmp signaling could act cell autonomously in IFT progenitors, whereas Hh activity could act either autonomously or non-autonomously.

Previous studies have demonstrated that Hh and Bmp signaling each act cell autonomously to promote ventricular and atrial fate, respectively (Marques and Yelon, 2009; Thomas et al., 2008), and future mosaic analyses studies could be designed to explicitly test where Hh and Bmp signaling are required in the context of IFT specification. A complementary method would be to visualize the IFT progenitor population at early stages in combination with reporters of Hh or Bmp signal reception (Collery and Link, 2011; Huang et al., 2012; Laux et al., 2011); however, all currently known IFT markers are only expressed after differentiation (data not shown). In future studies, it would be worthwhile to identify molecular markers of the IFT progenitor population in order to visualize this population in the early heart fields, determine what signals are active, and analyze changes to IFT progenitors when signaling is altered.

Altogether, we propose a model in which specification of an appropriate number of IFT progenitor cells relies on two requirements: high Bmp activity and limited Hh activity. While Bmp activity promotes IFT specification, Hh activity sets a boundary for IFT specification. Together, these two signals result in IFT progenitor emergence only from a defined territory at the edge of the heart fields, thus creating an IFT population that is sufficient but not oversized. It seems feasible that Hh and Bmp activity could converge on downstream target genes that direct IFT identity, perhaps with Gli and Smad factors binding within the same enhancer but with different consequences. It is also possible that Hh and Bmp signaling act through different target genes,

potentially in different tissues. One interesting alternative could involve Hh activity regulating expression of Bmp signaling antagonists, such as *noggin* and *chordin*. Perhaps in the absence of Hh activity, diminished expression of these antagonists results in increased Bmp activity in the heart fields, resulting in excess IFT specification. Future experiments can test this possibility, as well as investigating downstream effectors of Hh and Bmp activity, in order to provide insight into the specific mechanisms of IFT patterning.

In future work, it will be interesting to investigate whether the roles for Hh and Bmp signaling during IFT development are conserved in other species. We posit that conservation is likely; however, because altering very early patterning in mammalian embryos generally results in lethality prior to SAN formation (Mishina et al., 1995; Zhang et al., 2001), the use of conditional alleles will be needed to illuminate how Hh and Bmp signaling affect mammalian SAN development. It will also be interesting to understand whether abnormalities in Hh signaling, Bmp signaling, or their downstream effectors are associated with congenital arrhythmias. Finally, it will be exciting to ask whether modulating Hh and Bmp activity can improve efforts to generate pacemaker-like cardiomyocytes in vitro (Protze et al., 2017; Vedantham, 2015). Perhaps limiting Hh activity can improve the efficiency of current protocols to generate pacemaker-like cells. Furthermore, it seems possible that introducing Bmp activity in differentiating cardiomyocytes could improve the maturation and/or survival of pacemaker-like cells. In the long

term, these data and extensions of this work will help elucidate the etiology of congenital arrhythmias and may help inform efforts to generate in vitro pacemaker cells for therapeutic purposes.

MATERIALS AND METHODS

Zebrafish

We used the following zebrafish strains: *smo*^{b577} (Varga et al., 2001), *laf*^{sk42} (Marques and Yelon, 2009), *Tg(myl7:H2A-mCherry)*^{sd12} (Schumacher et al., 2013), *Tg(nkx2.5:ZsYellow)*^{fb7} (Zhou et al., 2011), *Tg(hand2:EGFP)*^{pd24} (Kikuchi et al., 2011), and *Tg(hsp70l:nkx2.5-EGFP)*^{fcu1} (George et al., 2015). All zebrafish husbandry and experiments followed IACUC-approved protocols.

In situ hybridization and immunofluorescence

In situ hybridization and immunofluorescence were performed as previously described (Zeng and Yelon, 2014). In situ probes were used for *bmp4* (ZDB-GENE-980528-2059), *tbx18* (ZDB-GENE-020529-2), *shox2* (ZDB-GENE-040426-1457), *hcn4* (ZDB-GENE-050420-360), *amhc* (*myh6*; ZDB-GENE-031112-1), and *ltbp3* (ZDB-GENE-060526-130). Primary and secondary antibodies are outlined in Table 3.2.

Imaging

In situ images were captured using a Zeiss Axioplan and Axiocam and processed using Zeiss Axiovision and Adobe Creative Suite software. Immunofluorescence images were captured using a Leica SP5 confocal laser-scanning microscope and analyzed using Imaris software (Bitplane) and ImageJ. All confocal images shown are 3D reconstructions.

Heart rate observations

Heart rate was determined by counting the number of atrial contractions over a period of 30 seconds from videos of live embryos imaged at 21°C. Videos were recorded and processed using a Zeiss M2Bio microscope, an Optronics DEI750 video camera, and iMovie software.

Cell counting

To count Isl1+ IFT cardiomyocytes (Figures 3.2, 3.3, 3.7, 3.9, and 3.10), we employed immunofluorescence with an anti-Isl1 antibody. Isl1 localizes to the nucleus of IFT cardiomyocytes, and cardiomyocytes are distinguishable from other cardiac cell types based on MF20 staining. Though some pericardial Isl1 was observed, we only counted cells in which the Isl1+ nucleus was surrounded by MF20 staining. We occasionally observed embryos with poor quality anti-Isl1 staining, across all genotypes and without any discernible pattern; these samples were excluded from our analysis.

To count *amhc*-expressing cells at 22 somites in Figure 3.3, we used an established protocol for counting cells after in situ hybridization (Thomas et al., 2008). A cell was counted only if its nucleus was clearly outlined by *amhc* expression.

To count cardiomyocytes in the atrium in Figure 3.4, we used the transgene *Tg(myl7:H2A-mCherry)* to label the nuclei of all cardiomyocytes, an anti-Isl1 antibody to label the nuclei of all IFT cardiomyocytes, and the S46

antibody (anti-Amhc) to label all atrial cardiomyocytes. We counted atrial cardiomyocytes by visualizing native mCherry protein in Amhc+ cells. We subtracted the number of Isl1+ Amhc+ cells from the total number of atrial cardiomyocytes to determine the number of Isl1- atrial cardiomyocytes, which we define as the “atrial chamber.”

Drug treatments

Embryos were treated with CyA (Fisher Scientific 507605; dissolved in ethanol) at 25-75 μm or DM (Sigma-Aldrich P5499; dissolved in DMSO) at 10-20 μm in E3 embryo medium. Embryos treated with 25-75 μm CyA at dome stage resemble *smo* mutants based on their diminutive head, mild cyclopia, ventral body curvature, and U-shaped somites. Embryos treated with 10-20 μm DM at dome stage resemble *laf* mutants based on their mild dorsalization, including absence of the ventral tail fin. Control embryos were treated with an equal volume of the small molecule vehicle, either ethanol or DMSO.

Heat shock

For experiments depicted in Figure 3.7, embryos were incubated at 28.5°C and were treated with CyA at dome stage as described above. At 3 somites, embryos were transferred to an E3 solution pre-equilibrated to 37.5°C and containing either CyA or ethanol. Embryos were incubated at 37.5°C for 60 minutes and were then removed from the 37.5°C solution and replaced into

the 28.5°C solution. Embryos carrying *Tg(hsp70l:nkx2.5-EGFP)* were identified based on eGFP visualization, and nontransgenic siblings were used as controls. Embryos were maintained at 28.5°C continuously until fixation at 48 hpf.

Injection of RNA

Embryos were injected with 50 pg mRNA encoding zebrafish *shha* (referred to as *shh*) at the one-cell stage (Ekker et al., 1995).

Statistics and replicates

Figures show data representing at least two experiments from independent crosses. The only exceptions are Figure 3.8E and 3.8F, which are each based on one experiment. All statistical analyses of data were performed using GraphPad to conduct two-tailed, unpaired *t*-tests.

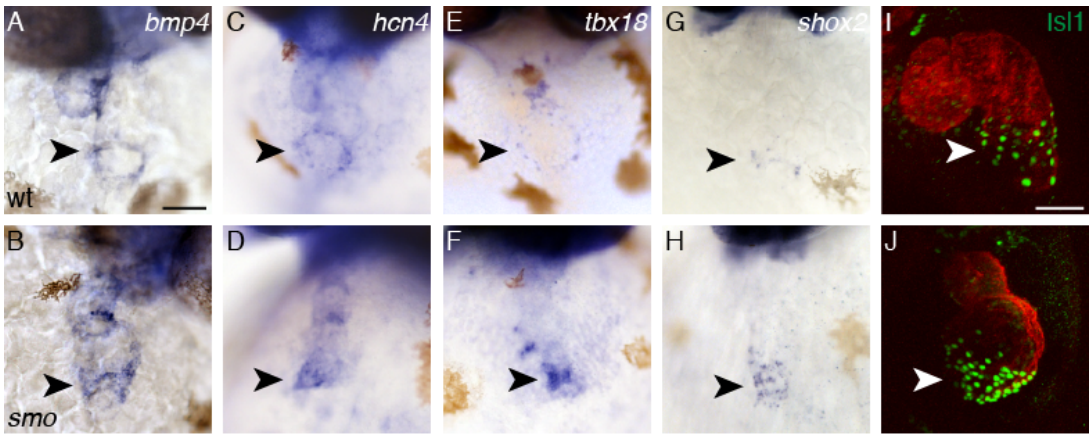

Figure 3.1.
The IFT is expanded in *smoothened* mutants.
(A-J) Wild-type (wt, top row) and *smoothened* mutant (*smo*, bottom row) embryos at 48 hpf are shown after in situ hybridization (A-H) or after immunofluorescence followed by confocal imaging (I-J). Frontal views; arrowheads indicate the IFT. (A-B) *bmp4* expression is expanded in the venous pole of *smo* mutants relative to wt siblings (n=8 wt, 12 *smo*). (C-H) *hcn4, tbx18,* and *shox2* are similarly expanded in the venous pole of *smo*, compared to wt (n=10 wt, 12 *smo* for *hcn4;* n=12 wt, 12 *smo* for *tbx18*; n=26 wt, 13 *smo* for *shox2*). (I-J) Isl1 (green) is present in the nuclei of IFT cardiomyocytes. More Isl1+ cells are observed in the IFT of *smo* mutants than in wt siblings (n=15 wt, 11 *smo*). 3D reconstruction shows the myocardium in red, labeled with MF20. Scale bars: 50 μm.

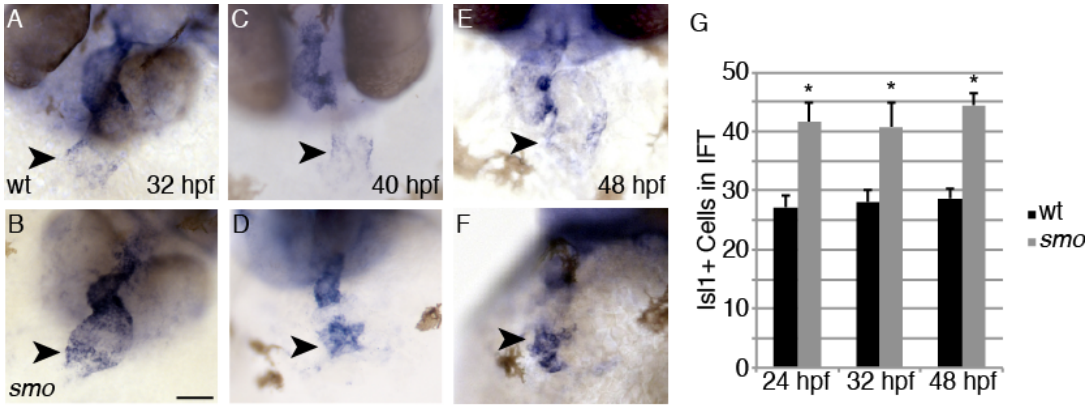

Figure 3.2.
Enlarged IFT arises by 24 hpf in *smo* mutants.
(A-F) In situ hybridization depicts *bmp4* expression in wt (top row) and *smo* (bottom row). Frontal views; arrowheads indicate the IFT. Expression of *bmp4* is already expanded in the IFT of *smo* mutants, relative to wt siblings, at 32 hpf (A-B, n=6 wt, 8 *smo*). This expansion is maintained at 40 hpf (C-D, n=8 wt, 10 *smo*) and 48 hpf (E-F, n=8 wt, 12 *smo*). Scale bar: 50 µm.
(G) Bar graph indicates the average number of Isl1+ cells in the IFT; error bars represent standard error, and asterisks indicate significant differences from wt ($p \leq 0.01$). See Materials and Methods for cell counting technique. The size of the IFT in *smo* mutants, relative to the IFT in wt siblings, is increased as early as 24 hpf (n=9 wt, 12 *smo*). This increase is maintained at 32 hpf (n=11 wt, 12 *smo*) and 48 hpf (n=15 wt, 11 *smo*). The number of Isl1+ cells in wt embryos is also steadily maintained throughout this timeframe.

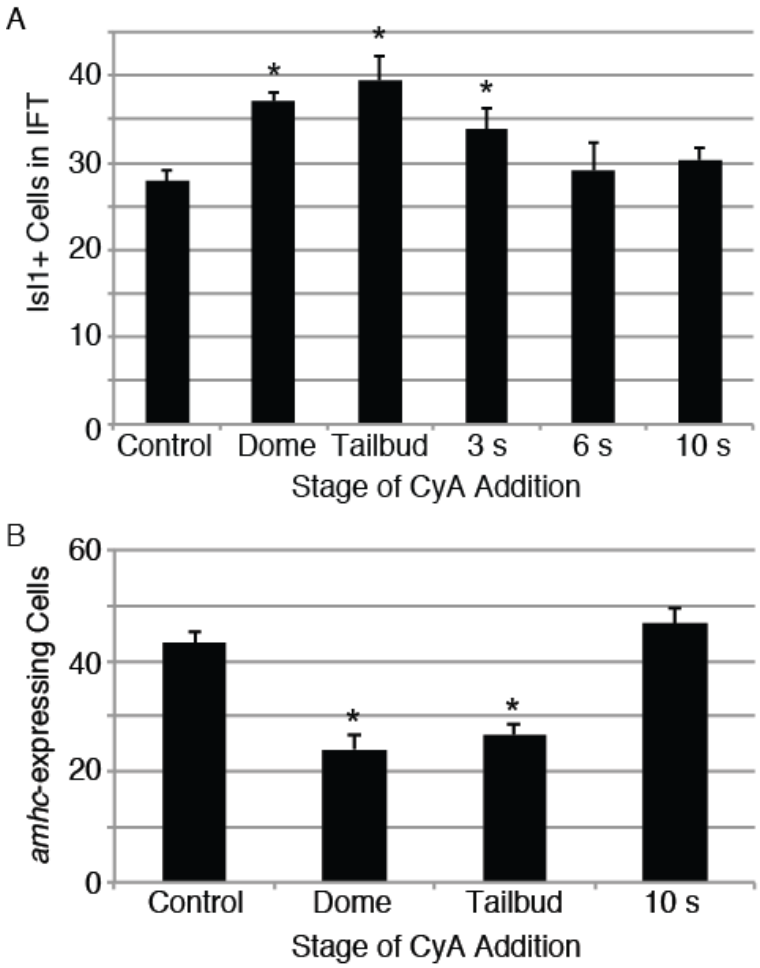

Figure 3.3.
Hh signaling acts during gastrulation and early somitogenesis to limit IFT cell production and promote atrial cell production.
(A) Bar graph indicates the average number of Isl1+ cells in the IFT at 48 hpf, as in Figure 3.2G; asterisks indicate significant differences from controls ($p<0.01$). Embryos treated with CyA beginning at dome (n=9), tailbud (n=13), or 3 somites (s, n=9) have higher numbers of Isl1+ cells in the IFT than ethanol-treated control embryos do (n=18). Embryos treated with CyA at 6 s (n=6) or 10 s (n=6) have the same number of IFT cells as found in controls.
(B) Bar graph indicates the average number of *amhc*-expressing cells at 22 s; error bars represent standard error, and asterisks indicate significant differences from controls ($p<0.01$). See Materials and Methods for cell counting technique. Embryos treated with CyA at dome (n=12) or tailbud (n=20) have lower numbers of *amhc*-expressing cells than control embryos do (n=37), whereas embryos treated at 10 s (n=14) have the same number of *amhc*-expressing cells as found in controls.

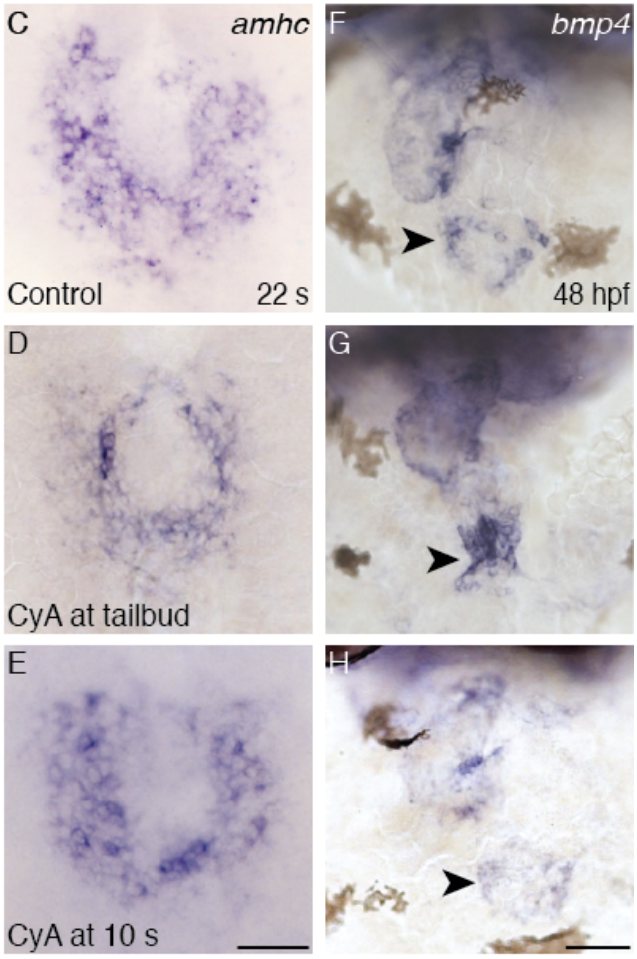

Figure 3.3, Continued.
Hh signaling acts during gastrulation and early somitogenesis to limit IFT cell production and promote atrial cell production.

(C-E) In situ hybridization depicts *amhc* expression at 22 s. Dorsal views; anterior toward the top. Embryos treated with CyA at tailbud stage (D) express *amhc* in fewer cells relative to controls (C). Embryos treated with CyA at 10 s exhibit normal *amhc* expression (E).
(F-H) In situ hybridization depicts *bmp4* at 48 hpf. Frontal views; arrowheads indicate the IFT. Embryos treated with CyA at tailbud stage (G, n=12) exhibit expanded *bmp4* expression relative to controls (F, n=44) whereas embryos treated at 10 s have a normal pattern of *bmp4* expression (H, n=24). Scale bars: 50 µm.

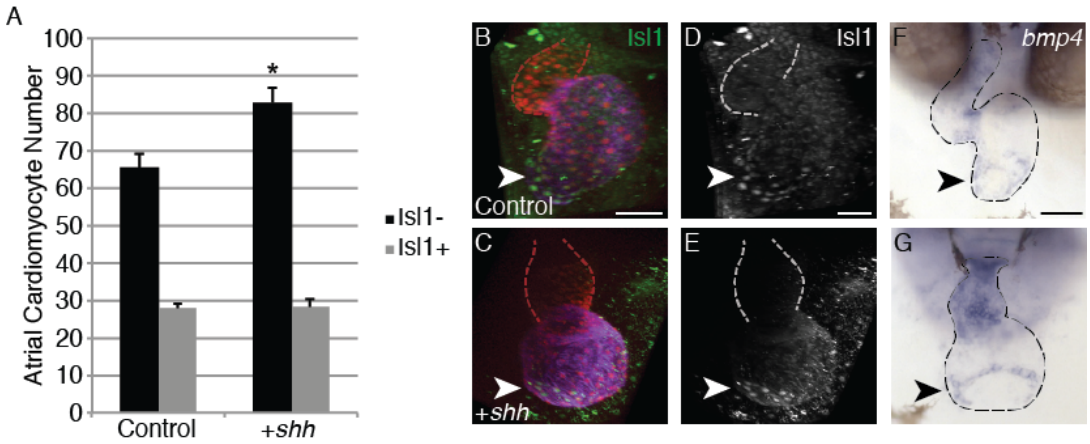

Figure 3.4.
IFT cell number is unaffected by increased Hh signaling.
(A) Bar graph indicates the average number of Isl1+ and Isl1- cardiomyocytes in the atrium at 48 hpf; error bars represent standard error, and asterisk indicates significant difference from controls ($p<0.03$). See Materials and Methods for cell counting technique. Injection of *shh* mRNA into wt embryos increases the number of Isl1- atrial cardiomyocytes but does not change in the number of Isl1+ IFT cardiomyocytes relative to uninjected control embryos (n=8 control, 5 +*shh*).
(B-C) In *Tg(myl7:H2A-mCherry)* embryos at 48 hpf, mCherry fluorescence (red) marks cardiomyocyte nuclei, and immunofluorescence reveals Amhc (purple) and Isl1 (green) localization. Frontal views; arrowheads indicate the IFT; red dotted lines indicate the ventricle. Although injection with *shh* mRNA alters cardiac morphology, the size of the IFT is comparable in injected embryos (C) and controls (B).
(D-E) Isl1 immunofluorescence from panels B-C is shown alone in white. Frontal views; arrowheads indicate the IFT; white dotted lines indicate the ventricle.
(F-G) In situ hybridization depicts *bmp4* expression at 48 hpf. Frontal views; arrowheads indicate the IFT. Embryos injected with *shh* mRNA retain *bmp4* expression in the IFT (E, n=12), in a narrow ring similar to that seen in uninjected controls (D, n=9). Scale bars: 50 µm.

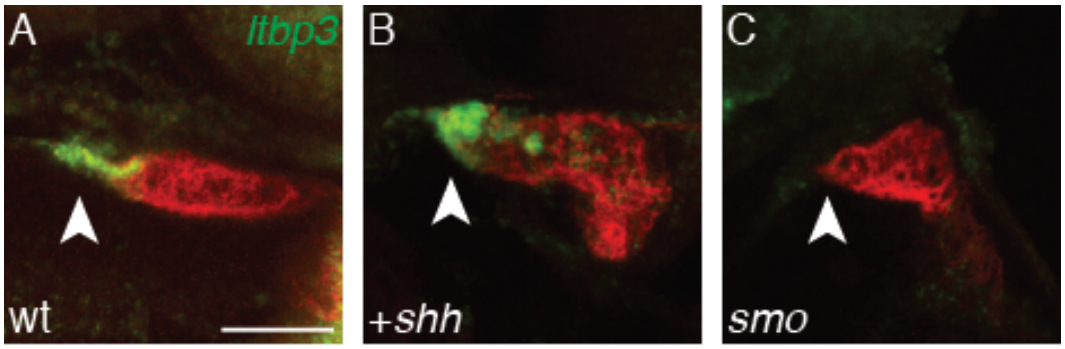

Figure 3.5.
Expression of *ltbp3* in outflow tract progenitors responds to Hh signaling.
(A-C) Fluorescent in situ hybridization indicating expression of *ltbp3* (green) is combined with MF20 immunofluorescence that marks the myocardium (red), followed by confocal imaging. Partial 3D reconstructions show lateral views at 26 hpf; arrowheads indicate the arterial pole of the heart. In wt embryos (A), *ltbp3* is expressed in OFT progenitor cells located at the arterial pole (n=13). In embryos injected with *shh* mRNA (B), *ltbp3* expression is expanded at the arterial pole (n=9). In most *smo* embryos, *ltbp3* expression is either absent (C, n=7/12) or reduced (n=4/12) at the arterial pole. Scale bar: 50 µm.

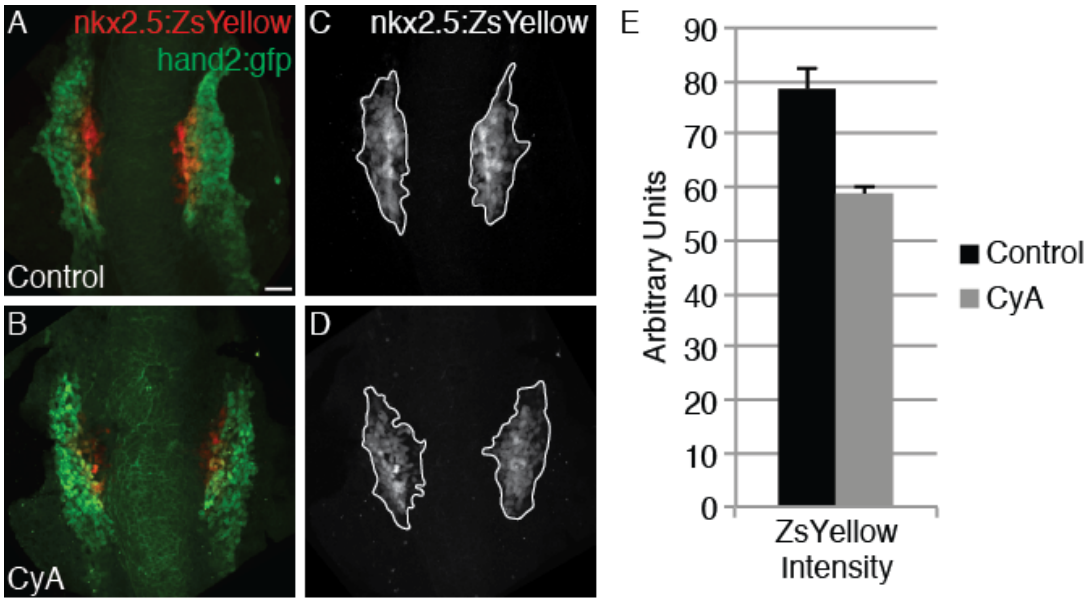

Figure 3.6.
Intensity of *nkx2.5* expression is reduced in the Hh-deficient anterior lateral plate mesoderm.
(A-D) In *Tg(hand2:eGFP);Tg(nkx2.5:ZsYellow)* embryos, immunofluorescence followed by confocal imaging allows visualization of eGFP (indicating *hand2* reporter expression) and ZsYellow (indicating *nkx2.5* reporter expression) at 10 s. Dorsal views of 3D reconstructions are shown, with both channels shown in A-B and ZsYellow shown alone in C-D. White outlines indicate the territory expressing detectable amounts of ZsYellow (C-D). (A,C) Ethanol-treated control embryos show normal distribution of *hand2* and *nkx2.5* reporter expression within the anterior lateral plate mesoderm (ALPM). (B,D) CyA-treated embryos show normal distribution of both *hand2* and *nkx2.5* reporter expression, but the intensity of *nkx2.5* expression within the ALPM is reduced. Scale bar: 50 μm.
(E) Bar graph indicates the average intensity at 10 s; error bars represent standard error, and asterisk indicates significant difference from controls ($p<0.0001$). Within its expression domain (as outlined in C and D), the intensity of *nkx2.5* reporter fluorescence is higher in control embryos (n=10) than in CyA-treated embryos (n=10).

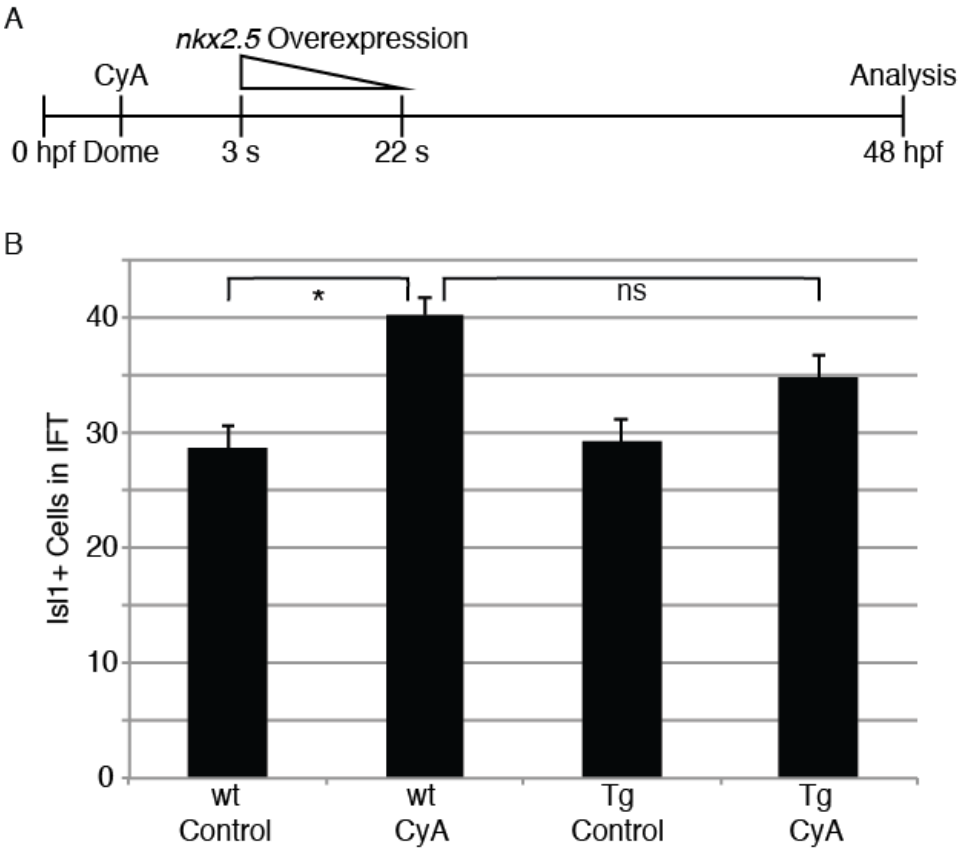

Figure 3.7.
Overexpression of *nkx2.5* can partially rescue the expansion of the IFT in Hh-deficient embryos.
(A) Schematic depicts timeline of the experiment performed: embryos were treated with CyA or ethanol (as a control) at dome, heat shocked to induce transient *nkx2.5* overexpression at 3 s, and then analyzed at 48 hpf. Transient expression of *nkx2.5* diminishes by 8 hours after heat shock administration (George et al., 2015), which corresponds to approximately 22 s in this experiment.
(B) Bar graph indicates the average number of Isl1+ cells in the IFT, as in Fig. 2G; error bars represent standard error; asterisk indicates a significant difference relative to wt controls ($p<0.01$), and ns indicates no significant difference. Treatment of wt embryos with CyA results in more Isl1+ IFT cells than in wt ethanol-treated controls (n=13 wt controls, 7 wt with CyA; $p=0.0011$). Transgenic (Tg) overexpression of *nkx2.5* beginning at 3 s slightly reduces the number of Isl1+ cells in the IFT of CyA-treated embryos (n=18 Tg with CyA; $p=0.1304$ relative to wt with CyA). Overexpression of *nkx2.5* at 3 s has no effect on IFT cell number in ethanol-treated control embryos (n=23 Tg controls; $p=0.861$ relative to wt controls).

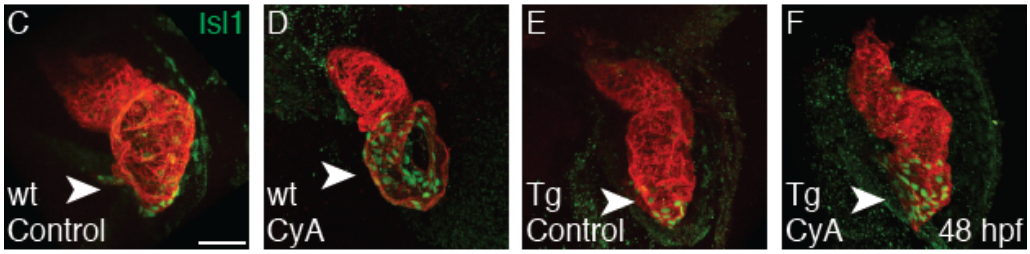

Figure 3.7, Continued.
Overexpression of *nkx2.5* can partially rescue the expansion of the IFT in Hh-deficient embryos.

(C-F) Frontal views of immunofluorescence at 48 hpf as in Fig. 1I,J; arrowheads indicate the IFT. Whereas wt control (C) and Tg control (E) embryos have a normal distribution of Isl1+ IFT cardiomyocytes, wt CyA-treated embryos show an increase in Isl1+ IFT cells (D). Tg CyA-treated embryos show an intermediate phenotype (F), in which the IFT is modestly expanded relative to Tg controls but also mildly restrained relative to wt CyA-treated siblings. Scale bar: 50 μm.

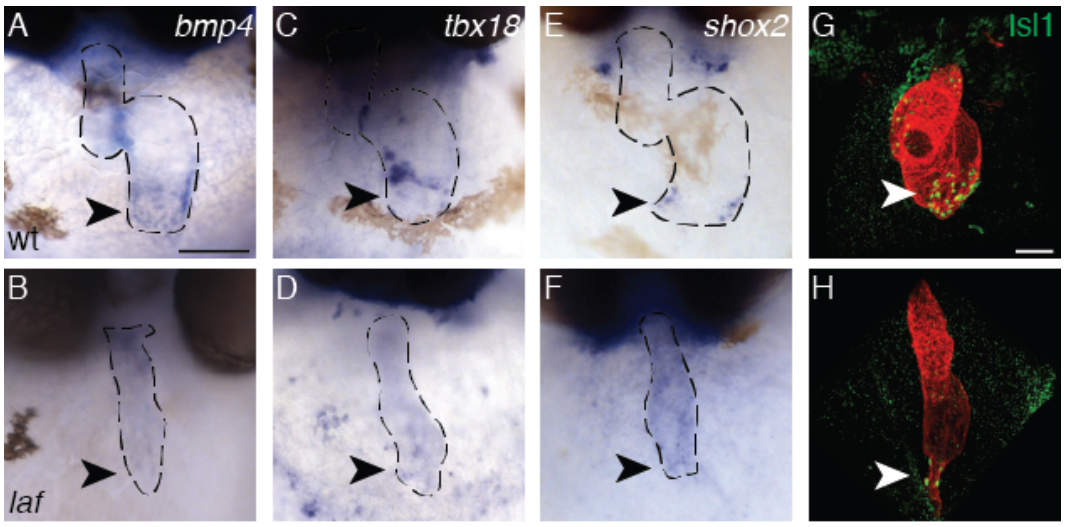

Figure 3.8.
Bmp activity promotes production of IFT cardiomyocytes.
(A-H) Wt (top row) and *laf* mutant (bottom row) embryos at 48 hpf are shown after in situ hybridization (A-F) or after immunofluorescence followed by confocal imaging (G-H). Frontal views; arrowheads indicate the venous pole. Whereas wt embryos (A,C,E) show discrete expression of IFT markers in the venous pole, concentrated expression of *bmp4* (B), *tbx18* (D), and *shox2* (F) is not evident at the venous pole of most *laf* embryos (n=44 wt, 29/52 *laf* for *bmp4;* n=11 wt, 10/11 *laf* for *tbx18;* n=13 wt, 14/14 *laf* for *shox2*). Likewise, Isl1 (green) is present in very few cells in *laf* mutants (G) compared to their wt siblings (H) (n=24 wt, 20 *laf*). 3D reconstruction shows the myocardium in red. Isl1 staining near wt ventricle (G) is outside the heart. Note that variability observed in the *laf* mutant phenotype may reflect a variable degree of maternal *alk8* contribution in individual embryos (Mintzer et al., 2001). Scale bars: 50 µm.

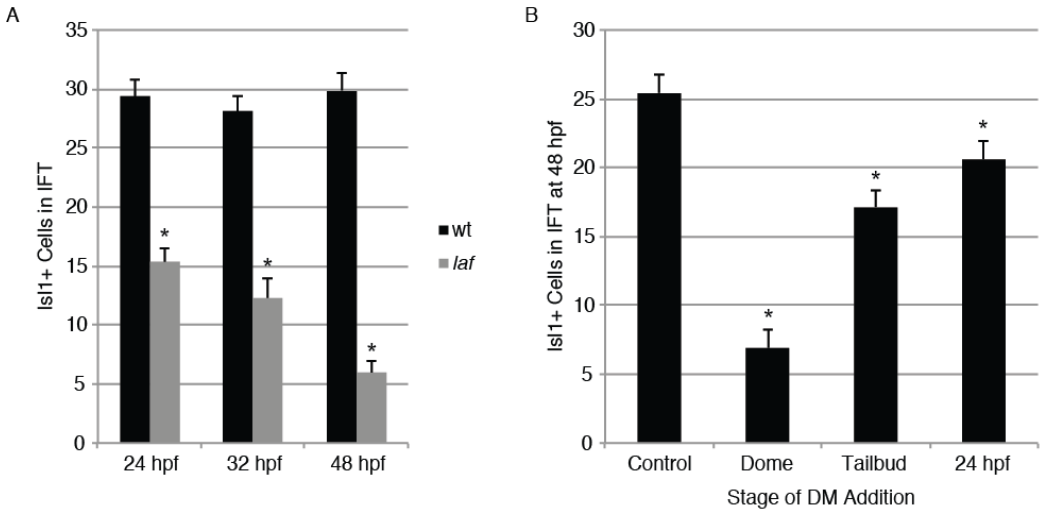

Figure 3.9.
Bmp activity promotes establishment and maintenance of IFT cardiomyocytes.
(A) Bar graph indicates the average number of Isl1+ cells in the IFT, as in Figure 3.2G; error bars represent standard error; asterisks indicate significant differences from controls ($p<0.0001$). Isl1+ IFT cell number is decreased at 24 hpf in *laf* compared to wt siblings (n=8 wt, 15 *laf*). This reduced IFT population is further diminished in *laf* at 32 hpf (n=26 wt, 10 *laf*) and again at 48 hpf (n=24 wt, 20 *laf*).
(B) Bar graph indicates the average number of Isl1+ cells in the IFT at 48 hpf, as in Figure 3.2G; error bars represent standard error; asterisks indicate significant differences from controls ($p<0.05$). Embryos treated with dorsomorphin (DM) at dome show a striking decrease in IFT cell number at 48 hpf relative to DMSO-treated controls (n=18 controls, 17 DM-treated; $p<0.0001$), comparable to *laf* embryos. Embryos treated at tailbud (n=14) or 24 hpf (n=14) show a modest decrease in IFT cell number ($p=0.0065$ and 0.0483, respectively).

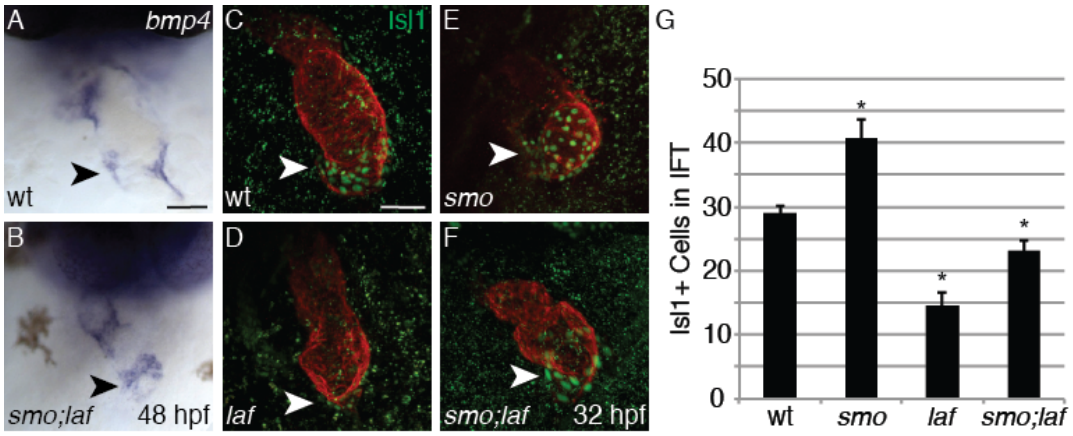

Figure 3.10.
IFT cell number is partially rescued in *smo;laf* double mutants.
(A-B) In situ hybridization depicts *bmp4* expression at 48 hpf. Frontal views; arrowheads indicate the IFT. *bmp4* expression is restored to a normal pattern and intensity in *smo;laf* double mutants (B, n=8), comparable to wt siblings (A, n=5). This contrasts with the expanded *bmp4* expression at the venous pole in *smo* mutants (Figure 3.1F) and the diminished *bmp4* expression at the venous pole in *laf* mutants (Figure 3.8E).
(C-F) Immunofluorescence depicts Isl1 (green) and MF20 (red) at 32 hpf. This timepoint was chosen because *smo;laf* embryos reliably survive to 32 hpf, whereas they have variable survival at later stages. Lateral views; arrowheads indicate the IFT. Scale bars: 50 µm.
(G) Bar graph indicates the average number of Isl1+ cells in the IFT at 32 hpf, as in Figure 3.2G; error bars represent standard error; asterisks indicate significant differences from controls ($p<0.008$). Isl1+ IFT cell number is increased in *smo* (E, n=12), decreased in *laf* (D, n=6), and partially rescued in *smo;laf* (F, n=17), relative to wt siblings (C, n=14).

Table 3.1.

Heart rate is abnormal in *smo* mutants at 48 hpf.
smo mutants exhibit a significantly reduced average heart rate (± standard error), compared to their wild-type siblings (wt: n=38, *smo*: n=36, $p<0.0001$).

Observations	wt	*smo*
Heart rate (beats per minute)	106 ± 2	52 ± 3
Normal heart rate and rhythm	38/38	0/36
Bradycardia	0/38	24/36
Bradycardia and arrhythmia	0/38	5/36
Bradycardia, arrhythmia, and abnormal conduction	0/38	7/36

Table 3.2.

Antibodies used for immunofluorescence.

	Antibody	Vendor	Product	Dilution
Primary antibodies	MF20	Developmental Studies Hybridoma Bank	supernatant	1:10
	S46	Developmental Studies Hybridoma Bank	supernatant	1:10
	rabbit anti-Isl1	GeneTex	128201L	1:2000
	rabbit anti-RCFP	Clontech	632475	1:250
	chicken anti-GFP	Abcam	13970	1:500
Secondary antibodies	goat anti-mouse IgG1 FITC	SouthernBiotech	1070-02	1:100
	goat anti-mouse IgG2b TRITC	SouthernBiotech	1090-03	1:100
	goat anti-rabbit Alexa Fluor 647	Invitrogen	21245	1:200
	goat anti-rabbit Alexa Fluor 488	Life Technologies	A11008	1:500
	goat anti-rabbit Alexa Fluor 594	Life Technologies	A11012	1:200
	goat anti-chicken Alexa Fluor 488	Invitrogen	A11039	1:200

ACKNOWLEDGMENTS

A modified version of Chapter 3 will be submitted for publication as a Research Article in *Development* (Knight, Hannah; Ren, Jie; Chi, Neil; Yelon, Deborah. “Hedgehog signaling restricts formation of the cardiac inflow tract in zebrafish”). Hannah Knight designed and performed the experiments presented in Chapter 3, with assistance from Jie Ren, Tina Vajdi, and Wei Gordon. Hannah Knight analyzed and interpreted the data and wrote the manuscript. Jie Ren and Neil Chi shared reagents, assisted with data analysis, and provided thoughtful feedback and insight throughout the project and during the editing of the manuscript. Deborah Yelon designed experiments, interpreted the data, and contributed to the editing of the manuscript. Hannah Knight was the primary investigator and author of this material.

Chapter 4: Future directions toward understanding inflow tract patterning

Introduction

In this dissertation, I have described a body of work that adds substantially to our understanding of inflow tract (IFT) development in the zebrafish embryo. In Chapter 2, we have characterized the wild-type IFT, including analysis of its origins and its differentiation dynamics. In Chapter 3, we have shown that the size of the IFT is determined through the interaction of two signaling pathways: Hh signaling restricts production of IFT cardiomyocytes, while Bmp signaling promotes IFT formation. In this chapter, I will discuss five open questions that can be addressed in future extensions of this work. Finally, I will comment on the potential biomedical significance of these contributions.

Where are IFT progenitors located?

In Chapter 2, we proposed a model in which IFT progenitors originate in the ventral portion of the cardiogenic territory in the late blastula and then come to reside in the lateral portion of the heart fields within the ALPM. This model was generated after analyzing previously published fate mapping data in which IFT progenitors were not originally classified separately from atrial chamber cardiomyocytes (Keegan et al., 2004; Schoenebeck et al., 2007). Since these original experiments did not incorporate a molecular marker for the IFT cardiomyocytes, we were only able to assess contribution to the IFT based on the gross anatomical location of labeled cells. In future experiments,

we could create a more definitive fate map of IFT progenitors by using traditional fate mapping techniques combined with an IFT molecular marker, such as *bmp4* or Isl1. This type of study would most likely provide a more refined, higher-resolution understanding of where IFT progenitors are located relative to other cardiac progenitor populations in the early embryo.

An alternative strategy for advancing our analysis of IFT progenitor cells would be to visualize expression of a molecular marker that is specific to the IFT progenitors. However, no IFT progenitor marker has yet been identified; presently, all known markers of cardiac progenitor cells are thought to be expressed more broadly than in only IFT progenitors. Isl1 specifically marks differentiated IFT cardiomyocytes, but prior to myocardial differentiation, it is expressed broadly in the heart fields and is present in multiple progenitor populations (Hans et al., 2004; Witzel et al., 2017, 2012). Furthermore, the IFT markers *tbx18* and *shox2* are not readily detectable in the zebrafish ALPM (data not shown), indicating that their robust expression only emerges at later stages, as IFT differentiation proceeds. Identification of a novel marker of IFT progenitors would be highly valuable to the field and warrants further study.

To identify a novel marker that would be specific to IFT progenitors, we could use either a candidate-based approach or an unbiased approach. A candidate-based approach could begin by determining whether any other markers of differentiated IFT cardiomyocytes are expressed in the ALPM. For example, *tbx2b* is expressed in the differentiated IFT, and *tbx2b* also seems to

be detectable in the ALPM (Tessadori et al., 2012; Thisse and Thisse, 2004). More detailed analysis of *tbx2b* expression relative to other markers would reveal whether it is indeed expressed in lateral portions of the heart fields, corresponding to the presumed location of the IFT progenitor cells. An alternative, unbiased approach could be to isolate tissue from different portions of the ALPM for gene expression profiling. Comparisons between the gene expression profiles of the lateral ALPM and medial ALPM could be used to generate a greater number of candidates, and then candidates can be screened for expression in IFT progenitors and IFT cardiomyocytes. Once a marker is identified, genetic lineage tracing studies would be valuable to confirm that the gene of interest is an IFT progenitor marker. This approach would be labor-intensive, but the data could yield meaningful insights into how different cardiac progenitor populations are arranged and patterned.

Importantly, these techniques could also be used to investigate how cardiac specification is altered in *smo* and *laf* mutant embryos. Fate mapping experiments could be used to compare the dimensions of the IFT progenitor populations in wild-type, *smo,* and *laf* embryos; these experiments would rigorously test whether IFT specification is expanded in *smo* and reduced in *laf,* and they would provide insight into exactly which cell fate decisions are regulated by Hh and Bmp signaling. For example, in *laf* mutants, it has been shown that the ALPM is more narrow than in wild-type siblings (Marques and Yelon, 2009); perhaps this reflects the loss of a lateral portion of the heart

field, with medial portions preserved, or perhaps the entire heart field has reduced dimensions along the medial-lateral axis. Fate mapping would distinguish between these possibilities. Similarly, if an early IFT marker were identified, it could be used to determine how the distribution of IFT progenitors is altered in *smo* and *laf* relative to other progenitor populations in the early embryo. For example, perhaps analysis of the expression pattern of an IFT progenitor marker in *smo* mutants would reveal that the IFT progenitor population expands medially into the area that typically gives rise to atrial chamber cardiomyocytes, or, alternatively, perhaps the excess IFT progenitors come from a lateral expansion, beyond the normal boundary of the heart field. Further studies in this vein would refine our understanding of how Hh and Bmp signaling function during cardiac patterning with respect to the IFT progenitor population as well as other types of cardiac progenitors.

How does Hh signaling restrict IFT specification?

In Chapter 3, we have shown that Hh signaling restricts the production of IFT cardiomyocytes. Based on the timeframe when Hh signaling is required, during gastrulation and early somitogenesis, we propose that Hh signaling restricts IFT progenitor specification. However, several topics remain mysterious, including one surprisingly elusive open question: where is Hh signaling required relative to the IFT progenitor population during this timeframe?

A straightforward approach toward answering this question is to first ask where Hh signaling is active in and near the embryonic heart fields, as we assume that Hh signaling will be required in a cell type that experiences the Hh signaling cascade. To analyze where Hh signaling is active, we can evaluate the expression patterns of Hh-responsive genes relative to the locations of the cardiac progenitors. It is well-established that Hh ligands are expressed in the dorsal portion of the gastrula and then in the midline after gastrulation (Currie and Ingham, 1996; Ekker et al., 1995; Krauss et al., 1993). As expected, the Hh-responsive gene Ptc1 is expressed at high levels near these regions of the embryo (Concordet et al., 1996; Huang et al., 2012; Lewis et al., 1999). However, cardiac progenitors are located at the lateral margin prior to gastrulation and in the ALPM after gastrulation (Keegan et al., 2004; Schoenebeck et al., 2007), calling into question whether cardiac progenitors are exposed to Hh activity. Hh ligands are secreted and may travel long distances (Gritli-Linde et al., 2001; Ramsbottom and Pownall, 2016), so it is possible that cardiac progenitors are actively responding to Hh signaling. Indeed, murine cardiac progenitors are marked with a Gli1-Cre reporter of Hh activity (Thomas et al., 2008). However, we have not yet been able to detect expression of *ptc1* in cardiac progenitors in zebrafish, either through in situ hybridization or through analysis of the Hh reporter *Tg(ptc1:kaede)* (Huang et al., 2012; data not shown). We cannot eliminate the possibility that low levels of *ptc1* are present in cardiac progenitors, so this question deserves future

study. In future work, we could utilize more sensitive hybridization methods, such as RNAscope, to determine whether *ptc1* is present in cardiac progenitors (Wang et al., 2012). If *ptc1* were absent from the ALPM using sensitive detection methods, this would suggest Hh signaling acts indirectly in a different tissue to enforce limits on IFT specification. For instance, perhaps Hh signaling in the midline induces release of a secondary factor that signals within the ALPM and patterns the heart fields. Once we attain a more detailed understanding of where Hh signaling is required, we could then use this knowledge to design blastomere transplantation experiments that would facilitate mosaic analyses (as in Thomas et al., 2008) to definitively determine whether Hh signaling acts autonomously or non-autonomously to restrict IFT specification.

We are also interested in understanding whether the dosage of Hh activity is an important element in cardiac patterning. We have shown that the size of the atrial chamber, ventricular chamber, and OFT populations change in conjunction with the amount of Hh activity (Figures 3.4 and 3.5, and Thomas et al., 2008), which is consistent with a dose-dependent mechanism. However, increasing Hh activity through overexpression of *shh* leaves the IFT population unchanged (Figure 3.4), indicating that high levels of Hh signaling are not sufficient to inhibit IFT formation, even though Hh signaling is required to limit the size of the IFT. This results hints at the possibility of an indirect mechanism for the involvement of Hh signaling during IFT patterning.

However, we cannot rule out the possibility that levels of Hh activity higher than those generated through injection of *shh* mRNA could depress IFT size. Perhaps overexpression of *shh* is does not generate uniformly high Hh activity, due to the influence of endogenous modifiers of Shh and Patched activity (Ramsbottom and Pownall, 2016). Direct modulation of Smo activity could potentially increase Hh signaling to a higher degree or with greater uniformity. Future experiments could utilize the small molecule Smo agonist SAG (Chen et al., 2002) or a constitutively-active *smoM2* construct (Hynes et al., 2000) to induce excess Hh activity and then evaluate the effect on IFT size. If we see a reciprocal relationship between Hh activity and IFT size when Smo activity is increased, it would support a model in which the dosage of Hh activity patterns the heart fields. However, if high levels of Hh activity never affect the IFT population, it would favor an indirect mechanism in which Hh activity is necessary for IFT restriction but does not actively suppress IFT fate.

Finally, we remain curious about potential downstream effectors of Hh activity. We have considered both Nkx2.5 and Isl1 as potential candidates, but neither one seems to be primarily responsible for expanded IFT specification in *smo* mutants. Our data show that IFT expansion is only modestly attenuated in Hh-deficient embryos that overexpress *nkx2.5* (Figure 3.7), and *isl1* expression seems to be normal in the heart fields of *smo* embryos (data not shown). Therefore, we wonder whether new candidate effectors could be identified, perhaps by analyzing published datasets of Hh-responsive genes.

Many groups have used gene expression profiling methods to identify Hh-responsive genes in various embryonic contexts (Lee et al., 2010; Lewandowski et al., 2015; Peterson et al., 2012; Vokes et al., 2008, 2007; Wang et al., 2013; Xu et al., 2006). These datasets could be used to generate a group of candidates for further study. Once we determine where Hh signaling is required to restrict IFT specification, candidates can be screened for expression in that tissue during early somitogenesis stages. Ultimately, the long-term goal in extending this work will be to understand what factors act downstream of Hh signaling to create different progenitor populations within the heart fields.

How does Bmp signaling promote production of IFT cardiomyocytes?

We have also shown in Chapter 3 that Bmp signaling is required for IFT development. Bmp signaling plays a potent early role in promoting specification of IFT cardiomyocytes and also seems to contribute to maintenance of differentiated IFT cardiomyocytes (Figure 3.9). We propose that Bmp signaling acts cell autonomously in cardiac progenitors, with high levels of Bmp signaling promoting IFT specification. After differentiation, we hypothesize that Bmp signaling in IFT cardiomyocytes promotes cell survival and/or reinforces cell fate. Future work dedicated to testing these models will enhance our understanding of IFT development.

To understand how Bmp signaling promotes specification of IFT cardiomyocytes, we would first like to understand where Bmp activity is required. Blastomere transplantation or similar mosaic analyses can be used to ask whether Bmp activity is required cell autonomously in the IFT lineage. If Bmp signaling is required in IFT cells for their specification, we would expect to see that cells that lack Bmp signaling fail to contribute to the IFT after transplantation into a wild-type embryo. Indeed, we have previously shown that cells deficient in Bmp signaling are highly unlikely to contribute to any cardiac population in mosaic assays (Marques and Yelon, 2009). If Bmp-responsive reporters are active in IFT progenitors, that would also be consistent with a cell-autonomous role for Bmp signaling in this population. It has already been shown that Bmp signaling is active in differentiating cardiac cells prior to heart tube formation (de Pater et al., 2012; Strate et al., 2015). In our preliminary experiments analyzing the Bmp reporter *Tg(BRE:dsGFP)* (Collery and Link, 2011), we observe Bmp activity in the lateral portions of the ALPM at 10s, with some overlap between Bmp activity and *nkx2.5*-expressing cardiac progenitors (data not shown). Because we cannot currently mark IFT progenitors specifically, we cannot determine with certainty whether Bmp signaling is active in IFT progenitors. However, once an IFT progenitor marker is identified, it will be important to analyze whether IFT progenitors exhibit Bmp activity. These published results and preliminary data support a model of cell-

autonomous Bmp activity promoting IFT specification, and it will be worthwhile to continue testing this model in extensions of our work.

In considering this model, we are also very curious about how this newly identified role for Bmp signaling during IFT development relates to our previous finding that Bmp signaling promotes atrial specification. Does Bmp signaling promote formation of the entire atrial pool, encompassing both IFT and atrial chamber progenitors? Or does Bmp signaling strongly favor IFT specification with a less potent role in atrial chamber specification? It is difficult to distinguish between these possibilities in the diminished *laf* heart because both the IFT population and the atrial chamber population are reduced. However, in future experiments examining the locations of *Tg(BRE:dsGFP)* expression within the heart fields, it will be interesting to note whether there is differential Bmp activity present in the IFT progenitors and the atrial chamber progenitors. Further analysis could determine how elevated Bmp activity affects the IFT population. In previous work, we have shown that elevating Bmp activity enlarges the atrium (Marques and Yelon, 2009), but we did not distinguish between atrial chamber and IFT cells in those original experiments. Future experiments could overexpress the constitutively active Bmp receptor *alk8CA* and then analyze the number of IFT cells along with the number of atrial chamber cells. We hypothesize that overexpression of *alk8CA* will cause the atrium will contain a greater number of IFT cardiomyocytes than in control embryos, but a more interesting aspect of this phenotype will be the ratio

between atrial chamber cardiomyocytes and IFT cardiomyocytes. If the enlarged atrium retains its usual proportions, then our data would support a model in which Bmp activity expands the atrial pool indiscriminately. Conversely, if the enlarged atrium contains proportionally more IFT cardiomyocytes than atrial chamber cardiomyocytes, that would support a model in which Bmp signaling promotes IFT fate to a greater degree than atrial chamber fate. Discerning between these possibilities will strengthen our understanding of how Bmp activity patterns cardiac progenitors.

We propose that Bmp signaling is also required cell autonomously for maintenance of differentiated IFT cardiomyocytes, although the precise cellular mechanism of IFT maintenance is still unclear. After IFT differentiation, Bmp signaling seems to be active in the venous pole (Laux et al., 2011), and *bmp4* is expressed in IFT cells (Figure 2.1 and Chin et al., 1997). Therefore, it seems likely that Bmp activity acts cell autonomously to maintain the IFT cardiomyocyte population. This hypothesis can be tested through mosaic analysis using reagents that allow temporal control of Bmp activity, in combination with rigorous analysis of reporters of Bmp signaling. Intriguingly, it remains unknown how IFT maintenance is aberrant in embryos with reduced Bmp activity. Are IFT cardiomyocytes lost through apoptosis? Do IFT cardiomyocytes lose expression of IFT markers and transform into atrial chamber cells? These possibilities can be tested through direct analysis of apoptosis indicators and by following IFT marker expression over time in Bmp-

deficient embryos. It is also possible that Bmp signaling drives proliferation in the IFT cardiomyocyte population, although that seems unlikely because differentiated cardiomyocytes show limited proliferation during this timeframe (de Pater et al., 2009). Evaluating these possibilities will provide important information about how the IFT population is maintained.

How do Hh and Bmp interact with each other?

We are very intrigued by the finding that IFT specification relies on interactions between Hh and Bmp signaling. We have observed that reducing both Hh and Bmp signaling through mutations in *smo* and *laf* results in an IFT that is very similar to the wild-type IFT in size (Figure 3.10). This rescue raises an interesting question: how do Hh and Bmp signaling interact? It is possible that Hh and Bmp signaling could converge directly onto the same target genes: perhaps there are certain transcription factors that direct IFT specification and whose expression is negatively regulated by Hh activity and positively regulated by Bmp activity. Alternatively, or additionally, it is possible that Hh and Bmp signaling interact through a less straightforward mechanism. For example, one signaling pathway could influence the signal reception or activity of the other pathway. Perhaps Hh signaling drives expression of Bmp antagonists in the midline, and these Bmp antagonists diffuse into the heart fields such that medial cardiac progenitors are exposed to limited Bmp activity and only lateral IFT progenitors experience high levels of Bmp signaling. This

exciting possibility could be tested by analyzing expression of Bmp antagonists in *smo* or evaluating Bmp activity in Hh-deficient embryos. It is also possible that this relationship goes in the other direction or is reciprocal. Perhaps Bmp signaling affects receipt or transduction of Hh signaling. One first step toward testing this would be to analyze Hh activity using a Hh reporter in dorsomorphin-treated embryos. If we see higher Hh activity in Bmp-deficient embryos, it would support the notion that Bmp activity alters Hh signal reception. In the long term, it will be exciting to determine how these signaling pathways interact in the network of signals that generates highly specialized progenitor populations from within the heart fields.

How do Hh and Bmp interact with other signals?

We envision that cardiac patterning relies on a complex network of interacting signaling pathways. Therefore, another major topic for future investigation is asking how Hh and Bmp interact with other pathways. In addition to Hh and Bmp signaling, cardiac patterning relies on Wnt signaling, retinoic acid (RA) signaling, and fibroblast growth factor signaling (Dohn and Waxman, 2012; Keegan et al., 2005; Marques et al., 2008; Pradhan et al., 2017; Waxman et al., 2008). Therefore, it is intuitive that other signaling pathways could participate in IFT development. In future work, it will be interesting to assimilate information about these pathways into a network in order to more deeply understand cardiac patterning.

The most exciting avenue for further studies of the zebrafish IFT is to integrate our work with an understanding of the role of the Wnt pathway. Experiments in chick embryos have shown that Wnt signaling promotes production of pacemaker progenitors in the ALPM (Bressan et al., 2013). In zebrafish, Wnt signaling is highly dynamic in its effects on cardiac development (Dohn and Waxman, 2012). Eliminating Wnt activity in the ALPM does not seem to negatively affect production of atrial cells, but increasing Wnt signaling during cardiac fusion expands expression of a marker expressed in both IFT and atrial chamber cardiomyocytes (Dohn and Waxman, 2012). These data suggest that Wnt signaling may promote formation of IFT cardiomyocytes during differentiation stages. In future experiments, it will be valuable to test this hypothesis by examining IFT size in embryos where Wnt signaling has been manipulated both positively and negatively. It will also be interesting to compare the role of Wnt signaling to that of Bmp signaling; for example, do Bmp and Wnt activity act during the same timeframe, or are their dynamics different? Is either Bmp or Wnt signaling upstream of the other pathway? Understanding how these pathways promote IFT development will be particularly important for advancing efforts to generate pacemaker cardiomyocytes in vitro; therefore, these questions certainly deserve further study.

Future experiments could also explore the role of RA signaling in IFT development. RA signaling seems to delimit IFT size, as embryos with

increased RA signaling have reduced *isl1* expression in the venous pole (Witzel et al., 2012). Furthermore, the atrial progenitor population is sensitive to RA signaling during gastrulation and early somitogenesis (Waxman et al., 2008), suggesting that RA signaling may act during cardiac patterning to restrict IFT specification. However, open questions remain: how does RA signaling restrict IFT size? Does RA signaling act cell autonomously or non-autonomously? Previously, we have shown that the RA-responsive effector Hoxb5b acts non-autonomously to restrict the size of the atrial progenitor population (Waxman et al., 2008), suggesting that RA signaling is likely to limit production of IFT cardiomyocytes non-autonomously. On the other hand, there is also evidence that RA signaling may limit IFT size autonomously: the RA-responsive transcription factor Ajuba limits *isl1* expression upon binding to Isl1 (Witzel et al., 2012), suggesting that RA and Ajuba may act autonomously in *isl1*-expressing cardiac progenitors. Future experiments could distinguish between these possibilities using mosaic analysis techniques, in addition to more thoroughly evaluating how the IFT population is altered in embryos with altered RA signaling. Incorporating those data into the broader context of IFT patterning could further elevate the findings. Perhaps RA and Hh signaling cooperate to establish the boundaries of the heart fields, with RA signaling setting the posterior boundary and Hh signaling setting the lateral boundary. Over the long term, elucidating this network will be highly interesting to the

scientific community and will deepen our insight into the mechanisms of cardiac specification and the possible etiologies of congenital heart disease.

What is the broader significance of understanding IFT specification?

The data presented in this dissertation represent several novel findings that contribute substantially to our understanding of IFT development. Prior to these studies, very little was known about early patterning of pacemaker cardiomyocytes. Here, we identify two factors that act during the earliest stages of cardiac patterning to influence IFT size. We have also generated a biography of wild-type IFT cardiomyocytes that sets the stage for future studies of this population. These studies add new insight into cardiac development and shed light on how a complex network of signaling activity is deciphered to create specialized populations during cardiac patterning. These ideas should also be of interest to the broader developmental biology community.

Furthermore, these findings could advance regenerative medicine. A major goal in translational research is to create cell-based therapies that can replace invasive surgical interventions. In this context, generation of pacemaker cardiomyocytes in vitro has the potential to replace implanted electrical pacemakers. Electrical pacemakers are commonly used in patients who experience arrhythmia after cardiac injury or disease, but these pacemakers are associated with health risks (Mulpuru et al., 2017; Tjong and

Reddy, 2017; Zhan et al., 2008). In the search for a cell-based alternative, several groups have sought to create pacemaker cells in vitro (Husse and Franz, 2016; Vedantham, 2015; Xiao, 2011). Various approaches have been tested, and each approach is associated with both successes and challenges.

In vitro production of pacemaker cells can be broadly divided into two strategies: transdifferentiation of mature cells into pacemaker-like cells, and differentiation of pluripotent cells into pacemaker-like cells. The transdifferentiation strategy manipulates expression of transcription factors to induce expression of the pacemaker genetic program in quiescent adult cardiomyocytes or fibroblasts. Tbx transcription factors have been used for reprogramming, specifically Tbx18, Tbx3, and Tbx5, and the initial tissue has included explanted cardiomyocytes, in vivo cardiomyocytes, and fibroblasts (Bakker et al., 2012; Hu et al., 2014; Kapoor et al., 2013; Nam et al., 2014). Alternatively, the differentiation strategy begins with pluripotent cells and generates pacemaker-like cells in vitro. Pluripotent cells can be pushed toward a pacemaker-like fate by induced expression of transcription factors like Tbx3 or Shox2 (Ionta et al., 2015; Jung et al., 2014; Rimmbach et al., 2015), or pluripotent cells can be cultured to give rise to mixed cardiac fates and then sorted to enrich for pacemaker cells (Hashem and Claycomb, 2013; Protze et al., 2017; Scavone et al., 2013). A recently developed protocol has been particularly successful by imitating in vivo development of pacemaker cells. This protocol dynamically modulates Bmp, RA, and FGF signaling to generate

pacemaker-like cardiomyocytes from human pluripotent stem cells with impressive efficiency and without inducing any genetic changes (Protze et al., 2017). This exciting advance suggests that patient-specific pacemaker cells could be adopted for therapeutic use. Indeed, some implanted biological pacemakers have been shown to pace the heartbeat in animal models (Kehat et al., 2004; Protze et al., 2017). Implanting these biological pacemakers could replicate normal pacemaking, if biological pacemakers prove safe, effective, and stable.

Though these strategies represent significant advances toward biological pacemakers, some challenges remain, and further study is necessary to develop an optimal biological pacemaker. One major challenge is efficiency; current protocols are inefficient and generally rely on transgene-based sorting to isolate pacemaker-like cells (Hashem and Claycomb, 2013; Kojima and Ieda, 2017; Nam et al., 2014; Rimmbach et al., 2015). Furthermore, pacemaker-like cells differentiated in vitro generally fail to reach full maturity comparable with cells that differentiate in vivo, resulting in very rapid beating and failure to create sarcomeric structures (Nam et al., 2014; Protze et al., 2017). Additionally, it is unclear whether implanted pacemaker-like cells would survive in vivo over the long term. Published data has primarily focused on short-term outputs, and pacemaker-like cells seem to be lost over time (Hu et al., 2014; Kapoor et al., 2013). These challenges and others must

be overcome before biologic pacemakers can replace implanted pacemakers in patients with arrhythmia.

Based on our experiments, we have identified two factors that may improve these efforts: antagonism of Hh activity, and continual activation of Bmp activity. Perhaps editing current protocols by adding cyclopamine at early stages could improve efficiency by limiting the production of chamber-like cardiomyocytes in favor of a pacemaker-like fate. Furthermore, increasing Bmp activity throughout differentiation and maintenance could help pacemaker-like cells reach a mature state in vitro and also enhance their survival. These ideas, along with other advances based in developmental biology, are likely to contribute to the creation of a biological alternative to man-made pacemakers. In this way, developmental biology can be harnessed to advance regenerative medicine and to improve treatment of human disease.

References

Ammirabile, G., Tessari, A., Pignataro, V., Szumska, D., Sutera Sardo, F., Benes, J., Balistreri, M., Bhattacharya, S., Sedmera, D., Campione, M., 2012. Pitx2 confers left morphological, molecular, and functional identity to the sinus venosus myocardium. Cardiovasc. Res. 93, 291–301. doi:10.1093/cvr/cvr314

Anderson, K.R., Ho, S.Y., Anderson, R.H., 1979. Location and vascular supply of sinus node in human heart. Br. Heart J. 41, 28–32.

Arrenberg, A.B., Stainier, D.Y.R., Baier, H., Huisken, J., 2010. Optogenetic Control of Cardiac Function. Science 330, 971–974. doi:10.1126/science.1195929

Ayers, K.L., Thérond, P.P., 2010. Evaluating Smoothened as a G-protein-coupled receptor for Hedgehog signalling. Trends Cell Biol. 20, 287–298. doi:10.1016/j.tcb.2010.02.002

Bakker, M.L., Boink, G.J.J., Boukens, B.J., Verkerk, A.O., van den Boogaard, M., den Haan, A.D., Hoogaars, W.M.H., Buermans, H.P., de Bakker, J.M.T., Seppen, J., Tan, H.L., Moorman, A.F.M., 't Hoen, P.A.C., Christoffels, V.M., 2012. T-box transcription factor TBX3 reprogrammes mature cardiac myocytes into pacemaker-like cells. Cardiovasc. Res. 94, 439–449. doi:10.1093/cvr/cvs120

Bandyopadhyay, A., Yadav, P.S., Prashar, P., 2013. BMP signaling in development and diseases: a pharmacological perspective. Biochem. Pharmacol. 85, 857–864. doi:10.1016/j.bcp.2013.01.004

Bauer, H., Lele, Z., Rauch, G.J., Geisler, R., Hammerschmidt, M., 2001. The type I serine/threonine kinase receptor Alk8/Lost-a-fin is required for Bmp2b/7 signal transduction during dorsoventral patterning of the zebrafish embryo. Dev. Camb. Engl. 128, 849–858.

Bauer, H., Meier, A., Hild, M., Stachel, S., Economides, A., Hazelett, D., Harland, R.M., Hammerschmidt, M., 1998. Follistatin and noggin are excluded from the zebrafish organizer. Dev. Biol. 204, 488–507. doi:10.1006/dbio.1998.9003

Begemann, G., Gibert, Y., Meyer, A., Ingham, P.W., 2002. Cloning of zebrafish T-box genes tbx15 and tbx18 and their expression during embryonic development. Mech. Dev. 114, 137–141.

Berdougo, E., Coleman, H., Lee, D.H., Stainier, D.Y.R., Yelon, D., 2003.

Mutation of weak atrium/atrial myosin heavy chain disrupts atrial function and influences ventricular morphogenesis in zebrafish. Dev. Camb. Engl. 130, 6121–6129. doi:10.1242/dev.00838

Bertrand, N., Roux, M., Ryckebüsch, L., Niederreither, K., Dollé, P., Moon, A., Capecchi, M., Zaffran, S., 2011. Hox genes define distinct progenitor sub-domains within the second heart field. Dev. Biol. 353, 266–274. doi:10.1016/j.ydbio.2011.02.029

Blaschke, R.J., Hahurij, N.D., Kuijper, S., Just, S., Wisse, L.J., Deissler, K., Maxelon, T., Anastassiadis, K., Spitzer, J., Hardt, S.E., Scholer, H., Feitsma, H., Rottbauer, W., Blum, M., Meijlink, F., Rappold, G., Gittenberger-de Groot, A.C., 2007. Targeted Mutation Reveals Essential Functions of the Homeodomain Transcription Factor Shox2 in Sinoatrial and Pacemaking Development. Circulation 115, 1830–1838. doi:10.1161/CIRCULATIONAHA.106.637819

Bleeker, W.K., Mackaay, A.J., Masson-Pévet, M., Bouman, L.N., Becker, A.E., 1980. Functional and morphological organization of the rabbit sinus node. Circ. Res. 46, 11–22.

Boink, G.J.J., Christoffels, V.M., Robinson, R.B., Tan, H.L., 2015. The past, present, and future of pacemaker therapies. Trends Cardiovasc. Med. 25, 661–673. doi:10.1016/j.tcm.2015.02.005

Brazil, D.P., Church, R.H., Surae, S., Godson, C., Martin, F., 2015. BMP signalling: agony and antagony in the family. Trends Cell Biol. 25, 249–264. doi:10.1016/j.tcb.2014.12.004

Bressan, M., Liu, G., Mikawa, T., 2013. Early Mesodermal Cues Assign Avian Cardiac Pacemaker Fate Potential in a Tertiary Heart Field. Science 340, 744–748. doi:10.1126/science.1232877

Briggs, L.E., Phelps, A.L., Brown, E., Kakarla, J., Anderson, R.H., van den Hoff, M.J.B., Wessels, A., 2013. Expression of the BMP receptor Alk3 in the second heart field is essential for development of the dorsal mesenchymal protrusion and atrioventricular septation. Circ. Res. 112, 1420–1432. doi:10.1161/CIRCRESAHA.112.300821

Bumcrot, D.A., Takada, R., McMahon, A.P., 1995. Proteolytic processing yields two secreted forms of sonic hedgehog. Mol. Cell. Biol. 15, 2294–2303.

Cai, C.-L., Liang, X., Shi, Y., Chu, P.-H., Pfaff, S.L., Chen, J., Evans, S., 2003. Isl1 identifies a cardiac progenitor population that proliferates prior to differentiation and contributes a majority of cells to the heart. Dev. Cell 5, 877–889.

Chen, J.K., Taipale, J., Young, K.E., Maiti, T., Beachy, P.A., 2002. Small molecule modulation of Smoothened activity. Proc. Natl. Acad. Sci. U. S. A. 99, 14071–14076. doi:10.1073/pnas.182542899

Chen, W., Burgess, S., Hopkins, N., 2001. Analysis of the zebrafish smoothened mutant reveals conserved and divergent functions of hedgehog activity. Dev. Camb. Engl. 128, 2385–2396.

Chi, N.C., Shaw, R.M., Jungblut, B., Huisken, J., Ferrer, T., Arnaout, R., Scott, I., Beis, D., Xiao, T., Baier, H., Jan, L.Y., Tristani-Firouzi, M., Stainier, D.Y.R., 2008. Genetic and Physiologic Dissection of the Vertebrate Cardiac Conduction System. PLoS Biol. 6, e109. doi:10.1371/journal.pbio.0060109

Chin, A.J., Chen, J.-N., Weinberg, E.S., 1997. Bone morphogenetic protein-4 expression characterizes inductive boundaries in organs of developing zebrafish. Dev. Genes Evol. 207, 107–114. doi:10.1007/s004270050097

Choudhury, M., Boyett, M.R., Morris, G.M., 2015. Biology of the Sinus Node and its Disease. Arrhythmia Electrophysiol. Rev. 4, 28.

Christoffels, V.M., 2006. Formation of the Venous Pole of the Heart From an Nkx2-5-Negative Precursor Population Requires Tbx18. Circ. Res. 98, 1555–1563. doi:10.1161/01.RES.0000227571.84189.65

Christoffels, V.M., Hoogaars, W.M.H., Tessari, A., Clout, D.E.W., Moorman, A.F.M., Campione, M., 2004. T-box transcription factor Tbx2 represses differentiation and formation of the cardiac chambers. Dev. Dyn. 229, 763–770. doi:10.1002/dvdy.10487

Collery, R.F., Link, B.A., 2011. Dynamic Smad-mediated BMP signaling revealed through transgenic zebrafish. Dev. Dyn. Off. Publ. Am. Assoc. Anat. 240, 712–722. doi:10.1002/dvdy.22567

Concordet, J.P., Lewis, K.E., Moore, J.W., Goodrich, L.V., Johnson, R.L., Scott, M.P., Ingham, P.W., 1996. Spatial regulation of a zebrafish patched homologue reflects the roles of sonic hedgehog and protein

kinase A in neural tube and somite patterning. Dev. Camb. Engl. 122, 2835–2846.

Cooper, M.K., Porter, J.A., Young, K.E., Beachy, P.A., 1998. Teratogen-mediated inhibition of target tissue response to Shh signaling. Science 280, 1603–1607.

Currie, P.D., Ingham, P.W., 1996. Induction of a specific muscle cell type by a hedgehog-like protein in zebrafish. Nature 382, 452–455. doi:10.1038/382452a0

Dal-Pra, S., Fürthauer, M., Van-Celst, J., Thisse, B., Thisse, C., 2006. Noggin1 and Follistatin-like2 function redundantly to Chordin to antagonize BMP activity. Dev. Biol. 298, 514–526. doi:10.1016/j.ydbio.2006.07.002

de Pater, E., Ciampricotti, M., Priller, F., Veerkamp, J., Strate, I., Smith, K., Lagendijk, A.K., Schilling, T.F., Herzog, W., Abdelilah-Seyfried, S., Hammerschmidt, M., Bakkers, J., 2012. Bmp signaling exerts opposite effects on cardiac differentiation. Circ. Res. 110, 578–587. doi:10.1161/CIRCRESAHA.111.261172

de Pater, E., Clijsters, L., Marques, S.R., Lin, Y.-F., Garavito-Aguilar, Z.V., Yelon, D., Bakkers, J., 2009. Distinct phases of cardiomyocyte differentiation regulate growth of the zebrafish heart. Development 136, 1633–1641. doi:10.1242/dev.030924

Dobrzynski, H., Boyett, M.R., Anderson, R.H., 2007. New insights into pacemaker activity: promoting understanding of sick sinus syndrome. Circulation 115, 1921–1932. doi:10.1161/CIRCULATIONAHA.106.616011

Dohn, T.E., Waxman, J.S., 2012. Distinct phases of Wnt/β-catenin signaling direct cardiomyocyte formation in zebrafish. Dev. Biol. 361, 364–376. doi:10.1016/j.ydbio.2011.10.032

Domínguez, J.N., Meilhac, S.M., Bland, Y.S., Buckingham, M.E., Brown, N.A., 2012. Asymmetric fate of the posterior part of the second heart field results in unexpected left/right contributions to both poles of the heart. Circ. Res. 111, 1323–1335. doi:10.1161/CIRCRESAHA.112.271247

Dyer, L.A., Kirby, M.L., 2009. Sonic hedgehog maintains proliferation in secondary heart field progenitors and is required for normal arterial pole formation. Dev. Biol. 330, 305–317. doi:10.1016/j.ydbio.2009.03.028

Dyer, L.A., Makadia, F.A., Scott, A., Pegram, K., Hutson, M.R., Kirby, M.L., 2010. BMP signaling modulates hedgehog-induced secondary heart field proliferation. Dev. Biol. 348, 167–176. doi:10.1016/j.ydbio.2010.09.021

Ekker, S.C., Ungar, A.R., Greenstein, P., von Kessler, D.P., Porter, J.A., Moon, R.T., Beachy, P.A., 1995. Patterning activities of vertebrate hedgehog proteins in the developing eye and brain. Curr. Biol. CB 5, 944–955.

Espinoza-Lewis, R.A., Liu, H., Sun, C., Chen, C., Jiao, K., Chen, Y., 2011. Ectopic expression of Nkx2.5 suppresses the formation of the sinoatrial node in mice. Dev. Biol. 356, 359–369. doi:10.1016/j.ydbio.2011.05.663

Espinoza-Lewis, R.A., Yu, L., He, F., Liu, H., Tang, R., Shi, J., Sun, X., Martin, J.F., Wang, D., Yang, J., Chen, Y., 2009. Shox2 is essential for the differentiation of cardiac pacemaker cells by repressing Nkx2-5. Dev. Biol. 327, 376–385. doi:10.1016/j.ydbio.2008.12.028

Fürthauer, M., Thisse, B., Thisse, C., 1999. Three different noggin genes antagonize the activity of bone morphogenetic proteins in the zebrafish embryo. Dev. Biol. 214, 181–196. doi:10.1006/dbio.1999.9401

Garavito-Aguilar, Z.V., Riley, H.E., Yelon, D., 2010. Hand2 ensures an appropriate environment for cardiac fusion by limiting Fibronectin function. Dev. Camb. Engl. 137, 3215–3220. doi:10.1242/dev.052225

Garcia-Frigola, C., Shi, Y., Evans, S.M., 2003. Expression of the hyperpolarization-activated cyclic nucleotide-gated cation channel HCN4 during mouse heart development. Gene Expr. Patterns 3, 777–783. doi:10.1016/S1567-133X(03)00125-X

George, V., Colombo, S., Targoff, K.L., 2015. An early requirement for nkx2.5 ensures the first and second heart field ventricular identity and cardiac function into adulthood. Dev. Biol. 400, 10–22. doi:10.1016/j.ydbio.2014.12.019

Goddeeris, M.M., Rho, S., Petiet, A., Davenport, C.L., Johnson, G.A., Meyers, E.N., Klingensmith, J., 2008. Intracardiac septation requires hedgehog-dependent cellular contributions from outside the heart. Dev. Camb. Engl. 135, 1887–1895. doi:10.1242/dev.016147

Goddeeris, M.M., Schwartz, R., Klingensmith, J., Meyers, E.N., 2007.

Independent requirements for Hedgehog signaling by both the anterior heart field and neural crest cells for outflow tract development. Dev. Camb. Engl. 134, 1593–1604. doi:10.1242/dev.02824

Gritli-Linde, A., Lewis, P., McMahon, A.P., Linde, A., 2001. The whereabouts of a morphogen: direct evidence for short- and graded long-range activity of hedgehog signaling peptides. Dev. Biol. 236, 364–386. doi:10.1006/dbio.2001.0336

Hami, D., Grimes, A.C., Tsai, H.-J., Kirby, M.L., 2011. Zebrafish cardiac development requires a conserved secondary heart field. Development 138, 2389–2398. doi:10.1242/dev.061473

Hammerschmidt, M., Serbedzija, G.N., McMahon, A.P., 1996. Genetic analysis of dorsoventral pattern formation in the zebrafish: requirement of a BMP-like ventralizing activity and its dorsal repressor. Genes Dev. 10, 2452–2461.

Hans, S., Scheer, N., Riedl, I., v Weizsäcker, E., Blader, P., Campos-Ortega, J.A., 2004. her3, a zebrafish member of the hairy-E(spl) family, is repressed by Notch signalling. Dev. Camb. Engl. 131, 2957–2969. doi:10.1242/dev.01167

Hashem, S.I., Claycomb, W.C., 2013. Genetic isolation of stem cell-derived pacemaker-nodal cardiac myocytes. Mol. Cell. Biochem. 383, 161–171. doi:10.1007/s11010-013-1764-x

Hegarty, S.V., O'Keeffe, G.W., Sullivan, A.M., 2013. BMP-Smad 1/5/8 signalling in the development of the nervous system. Prog. Neurobiol. 109, 28–41. doi:10.1016/j.pneurobio.2013.07.002

Hild, M., Dick, A., Rauch, G.J., Meier, A., Bouwmeester, T., Haffter, P., Hammerschmidt, M., 1999. The smad5 mutation somitabun blocks Bmp2b signaling during early dorsoventral patterning of the zebrafish embryo. Dev. Camb. Engl. 126, 2149–2159.

Hoffmann, A.D., Peterson, M.A., Friedland-Little, J.M., Anderson, S.A., Moskowitz, I.P., 2009. sonic hedgehog is required in pulmonary endoderm for atrial septation. Development 136, 1761–1770. doi:10.1242/dev.034157

Hoffmann, S., Berger, I.M., Glaser, A., Bacon, C., Li, L., Gretz, N., Steinbeisser, H., Rottbauer, W., Just, S., Rappold, G., 2013. Islet1 is a

direct transcriptional target of the homeodomain transcription factor Shox2 and rescues the Shox2-mediated bradycardia. Basic Res. Cardiol. 108. doi:10.1007/s00395-013-0339-z

Hoogaars, W.M., Tessari, A., Moorman, A.F., de Boer, P.A., Hagoort, J., Soufan, A.T., Campione, M., Christoffels, V.M., 2004. The transcriptional repressor Tbx3 delineates the developing central conduction system of the heart. Cardiovasc. Res. 62, 489–499. doi:10.1016/j.cardiores.2004.01.030

Hoogaars, W.M.H., Engel, A., Brons, J.F., Verkerk, A.O., de Lange, F.J., Wong, L.Y.E., Bakker, M.L., Clout, D.E., Wakker, V., Barnett, P., Ravesloot, J.H., Moorman, A.F.M., Verheijck, E.E., Christoffels, V.M., 2007. Tbx3 controls the sinoatrial node gene program and imposes pacemaker function on the atria. Genes Dev. 21, 1098–1112. doi:10.1101/gad.416007

Hu, Y.-F., Dawkins, J.F., Cho, H.C., Marbán, E., Cingolani, E., 2014. Biological pacemaker created by minimally invasive somatic reprogramming in pigs with complete heart block. Sci. Transl. Med. 6, 245ra94. doi:10.1126/scitranslmed.3008681

Huang, C.-J., Tu, C.-T., Hsiao, C.-D., Hsieh, F.-J., Tsai, H.-J., 2003. Germ-line transmission of a myocardium-specific GFP transgene reveals critical regulatory elements in the cardiac myosin light chain 2 promoter of zebrafish. Dev. Dyn. Off. Publ. Am. Assoc. Anat. 228, 30–40. doi:10.1002/dvdy.10356

Huang, P., Xiong, F., Megason, S.G., Schier, A.F., 2012. Attenuation of Notch and Hedgehog signaling is required for fate specification in the spinal cord. PLoS Genet. 8, e1002762. doi:10.1371/journal.pgen.1002762

Hui, C.-C., Angers, S., 2011. Gli proteins in development and disease. Annu. Rev. Cell Dev. Biol. 27, 513–537. doi:10.1146/annurev-cellbio-092910-154048

Husse, B., Franz, W.-M., 2016. Generation of cardiac pacemaker cells by programming and differentiation. Biochim. Biophys. Acta 1863, 1948–1952. doi:10.1016/j.bbamcr.2015.12.004

Hynes, M., Ye, W., Wang, K., Stone, D., Murone, M., Sauvage, F. d, Rosenthal, A., 2000. The seven-transmembrane receptor smoothened cell-autonomously induces multiple ventral cell types. Nat. Neurosci. 3,

41–46. doi:10.1038/71114

Ingham, P.W., 1998. The patched gene in development and cancer. Curr. Opin. Genet. Dev. 8, 88–94.

Ingham, P.W., McMahon, A.P., 2001. Hedgehog signaling in animal development: paradigms and principles. Genes Dev. 15, 3059–3087. doi:10.1101/gad.938601

Ionta, V., Liang, W., Kim, E.H., Rafie, R., Giacomello, A., Marbán, E., Cho, H.C., 2015. SHOX2 overexpression favors differentiation of embryonic stem cells into cardiac pacemaker cells, improving biological pacing ability. Stem Cell Rep. 4, 129–142. doi:10.1016/j.stemcr.2014.11.004

Jung, J.J., Husse, B., Rimmbach, C., Krebs, S., Stieber, J., Steinhoff, G., Dendorfer, A., Franz, W.-M., David, R., 2014. Programming and isolation of highly pure physiologically and pharmacologically functional sinus-nodal bodies from pluripotent stem cells. Stem Cell Rep. 2, 592–605. doi:10.1016/j.stemcr.2014.03.006

Kamino, K., Hirota, A., Fujii, S., 1981. Localization of pacemaking activity in early embryonic heart monitored using voltage-sensitive dye. Nature 290, 595–597.

Kapoor, N., Liang, W., Marbán, E., Cho, H.C., 2013. Direct conversion of quiescent cardiomyocytes to pacemaker cells by expression of Tbx18. Nat. Biotechnol. 31, 54–62. doi:10.1038/nbt.2465

Karlstrom, R.O., Talbot, W.S., Schier, A.F., 1999. Comparative synteny cloning of zebrafish you-too: mutations in the Hedgehog target gli2 affect ventral forebrain patterning. Genes Dev. 13, 388–393.

Karlstrom, R.O., Tyurina, O.V., Kawakami, A., Nishioka, N., Talbot, W.S., Sasaki, H., Schier, A.F., 2003. Genetic analysis of zebrafish gli1 and gli2 reveals divergent requirements for gli genes in vertebrate development. Dev. Camb. Engl. 130, 1549–1564.

Katagiri, T., Watabe, T., 2016. Bone Morphogenetic Proteins. Cold Spring Harb. Perspect. Biol. 8. doi:10.1101/cshperspect.a021899

Ke, Z., Emelyanov, A., Lim, S.E.S., Korzh, V., Gong, Z., 2005. Expression of a novel zebrafish zinc finger gene, gli2b, is affected in Hedgehog and Notch signaling related mutants during embryonic development. Dev.

Dyn. Off. Publ. Am. Assoc. Anat. 232, 479–486. doi:10.1002/dvdy.20242

Ke, Z., Kondrichin, I., Gong, Z., Korzh, V., 2008. Combined activity of the two Gli2 genes of zebrafish play a major role in Hedgehog signaling during zebrafish neurodevelopment. Mol. Cell. Neurosci. 37, 388–401. doi:10.1016/j.mcn.2007.10.013

Keegan, B.R., Feldman, J.L., Begemann, G., Ingham, P.W., Yelon, D., 2005. Retinoic acid signaling restricts the cardiac progenitor pool. Science 307, 247–249. doi:10.1126/science.1101573

Keegan, B.R., Meyer, D., Yelon, D., 2004. Organization of cardiac chamber progenitors in the zebrafish blastula. Development 131, 3081–3091. doi:10.1242/dev.01185

Kehat, I., Khimovich, L., Caspi, O., Gepstein, A., Shofti, R., Arbel, G., Huber, I., Satin, J., Itskovitz-Eldor, J., Gepstein, L., 2004. Electromechanical integration of cardiomyocytes derived from human embryonic stem cells. Nat. Biotechnol. 22, 1282–1289. doi:10.1038/nbt1014

Kikuchi, K., Holdway, J.E., Major, R.J., Blum, N., Dahn, R.D., Begemann, G., Poss, K.D., 2011. Retinoic acid production by endocardium and epicardium is an injury response essential for zebrafish heart regeneration. Dev. Cell 20, 397–404.

Kishimoto, Y., Lee, K.H., Zon, L., Hammerschmidt, M., Schulte-Merker, S., 1997. The molecular nature of zebrafish swirl: BMP2 function is essential during early dorsoventral patterning. Dev. Camb. Engl. 124, 4457–4466.

Klaus, A., Saga, Y., Taketo, M.M., Tzahor, E., Birchmeier, W., 2007. Distinct roles of Wnt/beta-catenin and Bmp signaling during early cardiogenesis. Proc. Natl. Acad. Sci. U. S. A. 104, 18531–18536. doi:10.1073/pnas.0703113104

Kojima, H., Ieda, M., 2017. Discovery and progress of direct cardiac reprogramming. Cell. Mol. Life Sci. CMLS. doi:10.1007/s00018-017-2466-4

Koudijs, M.J., den Broeder, M.J., Groot, E., van Eeden, F.J., 2008. Genetic analysis of the two zebrafish patched homologues identifies novel roles for the hedgehog signaling pathway. BMC Dev. Biol. 8, 15.

doi:10.1186/1471-213X-8-15

Krauss, S., Concordet, J.P., Ingham, P.W., 1993. A functionally conserved homolog of the Drosophila segment polarity gene hh is expressed in tissues with polarizing activity in zebrafish embryos. Cell 75, 1431–1444.

Kumar, S., Balczarek, K.A., Lai, Z.C., 1996. Evolution of the hedgehog gene family. Genetics 142, 965–972.

Kurata, T., Nakabayashi, J., Yamamoto, T.S., Mochii, M., Ueno, N., 2001. Visualization of endogenous BMP signaling during Xenopus development. Differ. Res. Biol. Divers. 67, 33–40. doi:10.1046/j.1432-0436.2001.067001033.x

Laux, D.W., Febbo, J.A., Roman, B.L., 2011. Dynamic analysis of BMP-responsive smad activity in live zebrafish embryos. Dev. Dyn. Off. Publ. Am. Assoc. Anat. 240, 682–694. doi:10.1002/dvdy.22558

Lazic, S., Scott, I.C., 2011. Mef2cb regulates late myocardial cell addition from a second heart field-like population of progenitors in zebrafish. Dev. Biol. 354, 123–133. doi:10.1016/j.ydbio.2011.03.028

Lee, E.Y., Ji, H., Ouyang, Z., Zhou, B., Ma, W., Vokes, S.A., McMahon, A.P., Wong, W.H., Scott, M.P., 2010. Hedgehog pathway-regulated gene networks in cerebellum development and tumorigenesis. Proc. Natl. Acad. Sci. U. S. A. 107, 9736–9741. doi:10.1073/pnas.1004602107

Lee, K.H., Xu, Q., Breitbart, R.E., 1996. A new tinman-related gene, nkx2.7, anticipates the expression of nkx2.5 and nkx2.3 in zebrafish heart and pharyngeal endoderm. Dev. Biol. 180, 722–731. doi:10.1006/dbio.1996.0341

Lenhart, K.F., Holtzman, N.G., Williams, J.R., Burdine, R.D., 2013. Integration of nodal and BMP signals in the heart requires FoxH1 to create left-right differences in cell migration rates that direct cardiac asymmetry. PLoS Genet. 9, e1003109. doi:10.1371/journal.pgen.1003109

Lepilina, A., Coon, A.N., Kikuchi, K., Holdway, J.E., Roberts, R.W., Burns, C.G., Poss, K.D., 2006. A dynamic epicardial injury response supports progenitor cell activity during zebrafish heart regeneration. Cell 127, 607–619. doi:10.1016/j.cell.2006.08.052

Lescroart, F., Mohun, T., Meilhac, S.M., Bennett, M., Buckingham, M., 2012. Lineage Tree for the Venous Pole of the Heart: Clonal Analysis Clarifies Controversial Genealogy Based on Genetic Tracing. Circ. Res. 111, 1313–1322. doi:10.1161/CIRCRESAHA.112.271064

Lewandowski, J.P., Du, F., Zhang, S., Powell, M.B., Falkenstein, K.N., Ji, H., Vokes, S.A., 2015. Spatiotemporal regulation of GLI target genes in the mammalian limb bud. Dev. Biol. 406, 92–103. doi:10.1016/j.ydbio.2015.07.022

Lewis, K.E., Concordet, J.P., Ingham, P.W., 1999. Characterisation of a second patched gene in the zebrafish Danio rerio and the differential response of patched genes to Hedgehog signalling. Dev. Biol. 208, 14–29. doi:10.1006/dbio.1998.9169

Liang, X., Evans, S.M., Sun, Y., 2017. Development of the cardiac pacemaker. Cell. Mol. Life Sci. CMLS 74, 1247–1259. doi:10.1007/s00018-016-2400-1

Liang, X., Zhang, Q., Cattaneo, P., Zhuang, S., Gong, X., Spann, N.J., Jiang, C., Cao, X., Zhao, X., Zhang, X., Bu, L., Wang, G., Chen, H.S.V., Zhuang, T., Yan, J., Geng, P., Luo, L., Banerjee, I., Chen, Y., Glass, C.K., Zambon, A.C., Chen, J., Sun, Y., Evans, S.M., 2015. Transcription factor ISL1 is essential for pacemaker development and function. J. Clin. Invest. 125, 3256–3268. doi:10.1172/JCI68257

Lin, L., Bu, L., Cai, C.-L., Zhang, X., Evans, S., 2006. Isl1 is upstream of sonic hedgehog in a pathway required for cardiac morphogenesis. Dev. Biol. 295, 756–763. doi:10.1016/j.ydbio.2006.03.053

Mandel, Y., Weissman, A., Schick, R., Barad, L., Novak, A., Meiry, G., Goldberg, S., Lorber, A., Rosen, M.R., Itskovitz-Eldor, J., Binah, O., 2012. Human embryonic and induced pluripotent stem cell-derived cardiomyocytes exhibit beat rate variability and power-law behavior. Circulation 125, 883–893. doi:10.1161/CIRCULATIONAHA.111.045146

Mangoni, M.E., Nargeot, J., 2008. Genesis and regulation of the heart automaticity. Physiol. Rev. 88, 919–982. doi:10.1152/physrev.00018.2007

Marigo, V., Scott, M.P., Johnson, R.L., Goodrich, L.V., Tabin, C.J., 1996. Conservation in hedgehog signaling: induction of a chicken patched homolog by Sonic hedgehog in the developing limb. Dev. Camb. Engl.

122, 1225–1233.

Marques, S.R., Lee, Y., Poss, K.D., Yelon, D., 2008. Reiterative roles for FGF signaling in the establishment of size and proportion of the zebrafish heart. Dev. Biol. 321, 397–406. doi:10.1016/j.ydbio.2008.06.033

Marques, S.R., Yelon, D., 2009. Differential requirement for BMP signaling in atrial and ventricular lineages establishes cardiac chamber proportionality. Dev. Biol. 328, 472–482. doi:10.1016/j.ydbio.2009.02.010

Martinez-Barbera, J.P., Toresson, H., Da Rocha, S., Krauss, S., 1997. Cloning and expression of three members of the zebrafish Bmp family: Bmp2a, Bmp2b and Bmp4. Gene 198, 53–59. doi:10.1016/S0378-1119(97)00292-8

McCulley, D.J., Kang, J.-O., Martin, J.F., Black, B.L., 2008. BMP4 is required in the anterior heart field and its derivatives for endocardial cushion remodeling, outflow tract septation, and semilunar valve development. Dev. Dyn. Off. Publ. Am. Assoc. Anat. 237, 3200–3209. doi:10.1002/dvdy.21743

Miller-Bertoglio, V.E., Fisher, S., Sánchez, A., Mullins, M.C., Halpern, M.E., 1997. Differential regulation of chordin expression domains in mutant zebrafish. Dev. Biol. 192, 537–550. doi:10.1006/dbio.1997.8788

Mintzer, K.A., Lee, M.A., Runke, G., Trout, J., Whitman, M., Mullins, M.C., 2001. Lost-a-fin encodes a type I BMP receptor, Alk8, acting maternally and zygotically in dorsoventral pattern formation. Dev. Camb. Engl. 128, 859–869.

Mishina, Y., Suzuki, A., Ueno, N., Behringer, R.R., 1995. Bmpr encodes a type I bone morphogenetic protein receptor that is essential for gastrulation during mouse embryogenesis. Genes Dev. 9, 3027–3037.

Mommersteeg, M.T.M., Brown, N.A., Prall, O.W.J., de Gier-de Vries, C., Harvey, R.P., Moorman, A.F.M., Christoffels, V.M., 2007a. Pitx2c and Nkx2-5 are required for the formation and identity of the pulmonary myocardium. Circ. Res. 101, 902–909. doi:10.1161/CIRCRESAHA.107.161182

Mommersteeg, M.T.M., Dominguez, J.N., Wiese, C., Norden, J., de Gier-de Vries, C., Burch, J.B.E., Kispert, A., Brown, N.A., Moorman, A.F.M.,

Christoffels, V.M., 2010. The sinus venosus progenitors separate and diversify from the first and second heart fields early in development. Cardiovasc. Res. 87, 92–101. doi:10.1093/cvr/cvq033

Mommersteeg, M.T.M., Hoogaars, W.M.H., Prall, O.W.J., de Gier-de Vries, C., Wiese, C., Clout, D.E.W., Papaioannou, V.E., Brown, N.A., Harvey, R.P., Moorman, A.F.M., Christoffels, V.M., 2007b. Molecular Pathway for the Localized Formation of the Sinoatrial Node. Circ. Res. 100, 354–362. doi:10.1161/01.RES.0000258019.74591.b3

Monfredi, O., Dobrzynski, H., Mondal, T., Boyett, M.R., Morris, G.M., 2010. The anatomy and physiology of the sinoatrial node--a contemporary review. Pacing Clin. Electrophysiol. PACE 33, 1392–1406. doi:10.1111/j.1540-8159.2010.02838.x

Moosmang, S., Stieber, J., Zong, X., Biel, M., Hofmann, F., Ludwig, A., 2001. Cellular expression and functional characterization of four hyperpolarization-activated pacemaker channels in cardiac neuronal tissues. Eur. J. Biochem. 268, 1646–1652.

Mori, A.D., Zhu, Y., Vahora, I., Nieman, B., Koshiba-Takeuchi, K., Davidson, L., Pizard, A., Seidman, J.G., Seidman, C.E., Chen, X.J., Henkelman, R.M., Bruneau, B.G., 2006. Tbx5-dependent rheostatic control of cardiac gene expression and morphogenesis. Dev. Biol. 297, 566–586. doi:10.1016/j.ydbio.2006.05.023

Motoyama, J., Takabatake, T., Takeshima, K., Hui, C., 1998. Ptch2, a second mouse Patched gene is co-expressed with Sonic hedgehog. Nat. Genet. 18, 104–106. doi:10.1038/ng0298-104

Mullins, M.C., Hammerschmidt, M., Kane, D.A., Odenthal, J., Brand, M., van Eeden, F.J., Furutani-Seiki, M., Granato, M., Haffter, P., Heisenberg, C.P., Jiang, Y.J., Kelsh, R.N., Nüsslein-Volhard, C., 1996. Genes establishing dorsoventral pattern formation in the zebrafish embryo: the ventral specifying genes. Dev. Camb. Engl. 123, 81–93.

Mulpuru, S.K., Madhavan, M., McLeod, C.J., Cha, Y.-M., Friedman, P.A., 2017. Cardiac Pacemakers: Function, Troubleshooting, and Management: Part 1 of a 2-Part Series. J. Am. Coll. Cardiol. 69, 189–210. doi:10.1016/j.jacc.2016.10.061

Nam, Y.-J., Lubczyk, C., Bhakta, M., Zang, T., Fernandez-Perez, A., McAnally, J., Bassel-Duby, R., Olson, E.N., Munshi, N.V., 2014. Induction of

diverse cardiac cell types by reprogramming fibroblasts with cardiac transcription factors. Development 141, 4267–4278. doi:10.1242/dev.114025

Niederreither, K., Vermot, J., Messaddeq, N., Schuhbaur, B., Chambon, P., Dollé, P., 2001. Embryonic retinoic acid synthesis is essential for heart morphogenesis in the mouse. Dev. Camb. Engl. 128, 1019–1031.

Nikaido, M., Tada, M., Saji, T., Ueno, N., 1997. Conservation of BMP signaling in zebrafish mesoderm patterning. Mech. Dev. 61, 75–88.

Pathi, S., Pagan-Westphal, S., Baker, D.P., Garber, E.A., Rayhorn, P., Bumcrot, D., Tabin, C.J., Blake Pepinsky, R., Williams, K.P., 2001. Comparative biological responses to human Sonic, Indian, and Desert hedgehog. Mech. Dev. 106, 107–117.

Payne, T.L., Postlethwait, J.H., Yelick, P.C., 2001. Functional characterization and genetic mapping of alk8. Mech. Dev. 100, 275–289.

Peterson, K.A., Nishi, Y., Ma, W., Vedenko, A., Shokri, L., Zhang, X., McFarlane, M., Baizabal, J.-M., Junker, J.P., van Oudenaarden, A., Mikkelsen, T., Bernstein, B.E., Bailey, T.L., Bulyk, M.L., Wong, W.H., McMahon, A.P., 2012. Neural-specific Sox2 input and differential Gli-binding affinity provide context and positional information in Shh-directed neural patterning. Genes Dev. 26, 2802–2816. doi:10.1101/gad.207142.112

Poon, K.L., Brand, T., 2013. The zebrafish model system in cardiovascular research: A tiny fish with mighty prospects. Glob. Cardiol. Sci. Pract. 2013, 9–28. doi:10.5339/gcsp.2013.4

Poon, K.-L., Liebling, M., Kondrychyn, I., Brand, T., Korzh, V., 2016. Development of the cardiac conduction system in zebrafish. Gene Expr. Patterns 21, 89–96. doi:10.1016/j.gep.2016.08.003

Pradhan, A., Zeng, X.-X.I., Sidhwani, P., Marques, S.R., George, V., Targoff, K.L., Chi, N.C., Yelon, D., 2017. FGF signaling enforces cardiac chamber identity in the developing ventricle. Dev. Camb. Engl. doi:10.1242/dev.143719

Prall, O.W.J., Menon, M.K., Solloway, M.J., Watanabe, Y., Zaffran, S., Bajolle, F., Biben, C., McBride, J.J., Robertson, B.R., Chaulet, H., Stennard, F.A., Wise, N., Schaft, D., Wolstein, O., Furtado, M.B., Shiratori, H.,

Chien, K.R., Hamada, H., Black, B.L., Saga, Y., Robertson, E.J., Buckingham, M.E., Harvey, R.P., 2007. An Nkx2-5/Bmp2/Smad1 Negative Feedback Loop Controls Heart Progenitor Specification and Proliferation. Cell 128, 947–959. doi:10.1016/j.cell.2007.01.042

Protze, S.I., Liu, J., Nussinovitch, U., Ohana, L., Backx, P.H., Gepstein, L., Keller, G.M., 2017. Sinoatrial node cardiomyocytes derived from human pluripotent cells function as a biological pacemaker. Nat. Biotechnol. 35, 56–68. doi:10.1038/nbt.3745

Puskaric, S., Schmitteckert, S., Mori, A.D., Glaser, A., Schneider, K.U., Bruneau, B.G., Blaschke, R.J., Steinbeisser, H., Rappold, G., 2010. Shox2 mediates Tbx5 activity by regulating Bmp4 in the pacemaker region of the developing heart. Hum. Mol. Genet. 19, 4625–4633. doi:10.1093/hmg/ddq393

Ramsbottom, S.A., Pownall, M.E., 2016. Regulation of Hedgehog Signalling Inside and Outside the Cell. J. Dev. Biol. 4, 23.

Rana, M.S., Théveniau-Ruissy, M., De Bono, C., Mesbah, K., Francou, A., Rammah, M., Domínguez, J.N., Roux, M., Laforest, B., Anderson, R.H., Mohun, T., Zaffran, S., Christoffels, V.M., Kelly, R.G., 2014. Tbx1 coordinates addition of posterior second heart field progenitor cells to the arterial and venous poles of the heart. Circ. Res. 115, 790–799. doi:10.1161/CIRCRESAHA.115.305020

Ribeiro, I., Kawakami, Y., Büscher, D., Raya, Á., Rodríguez-León, J., Morita, M., Rodríguez Esteban, C., Izpisúa Belmonte, J.C., 2007. Tbx2 and Tbx3 Regulate the Dynamics of Cell Proliferation during Heart Remodeling. PLoS ONE 2, e398. doi:10.1371/journal.pone.0000398

Rimmbach, C., Jung, J.J., David, R., 2015. Generation of murine cardiac pacemaker cell aggregates based on ES-cell-programming in combination with Myh6-promoter-selection. J. Vis. Exp. JoVE e52465. doi:10.3791/52465

Robbins, D.J., Fei, D.L., Riobo, N.A., 2012. The Hedgehog signal transduction network. Sci. Signal. 5, re6. doi:10.1126/scisignal.2002906

Sánchez-Quintana, D., Cabrera, J.A., Farré, J., Climent, V., Anderson, R.H., Ho, S.Y., 2005. Sinus node revisited in the era of electroanatomical mapping and catheter ablation. Heart Br. Card. Soc. 91, 189–194. doi:10.1136/hrt.2003.031542

Scavone, A., Capilupo, D., Mazzocchi, N., Crespi, A., Zoia, S., Campostrini, G., Bucchi, A., Milanesi, R., Baruscotti, M., Benedetti, S., Antonini, S., Messina, G., DiFrancesco, D., Barbuti, A., 2013. Embryonic stem cell-derived CD166+ precursors develop into fully functional sinoatrial-like cells. Circ. Res. 113, 389–398. doi:10.1161/CIRCRESAHA.113.301283

Schier, A.F., Talbot, W.S., 2005. Molecular genetics of axis formation in zebrafish. Annu. Rev. Genet. 39, 561–613. doi:10.1146/annurev.genet.37.110801.143752

Schindler, Y.L., Garske, K.M., Wang, J., Firulli, B.A., Firulli, A.B., Poss, K.D., Yelon, D., 2014. Hand2 elevates cardiomyocyte production during zebrafish heart development and regeneration. Development 141, 3112–3122. doi:10.1242/dev.106336

Schlange, T., Andrée, B., Arnold, H.H., Brand, T., 2000. BMP2 is required for early heart development during a distinct time period. Mech. Dev. 91, 259–270.

Schoenebeck, J.J., Keegan, B.R., Yelon, D., 2007. Vessel and Blood Specification Override Cardiac Potential in Anterior Mesoderm. Dev. Cell 13, 254–267. doi:10.1016/j.devcel.2007.05.012

Schulte-Merker, S., Lee, K.J., McMahon, A.P., Hammerschmidt, M., 1997. The zebrafish organizer requires chordino. Nature 387, 862–863. doi:10.1038/43092

Schumacher, J.A., Bloomekatz, J., Garavito-Aguilar, Z.V., Yelon, D., 2013. tal1 Regulates the formation of intercellular junctions and the maintenance of identity in the endocardium. Dev. Biol. 383, 214–226. doi:10.1016/j.ydbio.2013.09.019

Shi, Y., Katsev, S., Cai, C., Evans, S., 2000. BMP signaling is required for heart formation in vertebrates. Dev. Biol. 224, 226–237. doi:10.1006/dbio.2000.9802

Sieber, C., Kopf, J., Hiepen, C., Knaus, P., 2009. Recent advances in BMP receptor signaling. Cytokine Growth Factor Rev. 20, 343–355. doi:10.1016/j.cytogfr.2009.10.007

Staudt, D., Stainier, D., 2012. Uncovering the molecular and cellular mechanisms of heart development using the zebrafish. Annu. Rev.

Genet. 46, 397–418. doi:10.1146/annurev-genet-110711-155646

Stickney, H.L., Imai, Y., Draper, B., Moens, C., Talbot, W.S., 2007. Zebrafish bmp4 functions during late gastrulation to specify ventroposterior cell fates. Dev. Biol. 310, 71–84. doi:10.1016/j.ydbio.2007.07.027

Stieber, J., Herrmann, S., Feil, S., Löster, J., Feil, R., Biel, M., Hofmann, F., Ludwig, A., 2003. The hyperpolarization-activated channel HCN4 is required for the generation of pacemaker action potentials in the embryonic heart. Proc. Natl. Acad. Sci. 100, 15235–15240.

Strate, I., Tessadori, F., Bakkers, J., 2015. Glypican4 promotes cardiac specification and differentiation by attenuating canonical Wnt and Bmp signaling. Dev. Camb. Engl. 142, 1767–1776. doi:10.1242/dev.113894

Sun, Y., Liang, X., Najafi, N., Cass, M., Lin, L., Cai, C.-L., Chen, J., Evans, S.M., 2007. Islet 1 is expressed in distinct cardiovascular lineages, including pacemaker and coronary vascular cells. Dev. Biol. 304, 286–296. doi:10.1016/j.ydbio.2006.12.048

Tessadori, F., van Weerd, J.H., Burkhard, S.B., Verkerk, A.O., de Pater, E., Boukens, B.J., Vink, A., Christoffels, V.M., Bakkers, J., 2012. Identification and Functional Characterization of Cardiac Pacemaker Cells in Zebrafish. PLoS ONE 7, e47644. doi:10.1371/journal.pone.0047644

Thisse, B., Thisse, C., 2004. Fast Release Clones: A High Throughput Expression Analysis. [WWW Document]. ZFIN Direct Data Submiss. Httpzfinorg. URL http://zfin.org/ZDB-PUB-040907-1 (accessed 4.17.17).

Thomas, N.A., Koudijs, M., van Eeden, F.J.M., Joyner, A.L., Yelon, D., 2008. Hedgehog signaling plays a cell-autonomous role in maximizing cardiac developmental potential. Dev. Camb. Engl. 135, 3789–3799. doi:10.1242/dev.024083

Thomas, P.S., Rajderkar, S., Lane, J., Mishina, Y., Kaartinen, V., 2014. AcvR1-mediated BMP signaling in second heart field is required for arterial pole development: implications for myocardial differentiation and regional identity. Dev. Biol. 390, 191–207. doi:10.1016/j.ydbio.2014.03.008

Tirosh-Finkel, L., Zeisel, A., Brodt-Ivenshitz, M., Shamai, A., Yao, Z., Seger, R., Domany, E., Tzahor, E., 2010. BMP-mediated inhibition of FGF

signaling promotes cardiomyocyte differentiation of anterior heart field progenitors. Dev. Camb. Engl. 137, 2989–3000. doi:10.1242/dev.051649

Tjong, F.V.Y., Reddy, V.Y., 2017. Permanent Leadless Cardiac Pacemaker Therapy: A Comprehensive Review. Circulation 135, 1458–1470. doi:10.1161/CIRCULATIONAHA.116.025037

Tucker, J.A., Mintzer, K.A., Mullins, M.C., 2008. The BMP signaling gradient patterns dorsoventral tissues in a temporally progressive manner along the anteroposterior axis. Dev. Cell 14, 108–119. doi:10.1016/j.devcel.2007.11.004

Tyurina, O.V., Guner, B., Popova, E., Feng, J., Schier, A.F., Kohtz, J.D., Karlstrom, R.O., 2005. Zebrafish Gli3 functions as both an activator and a repressor in Hedgehog signaling. Dev. Biol. 277, 537–556. doi:10.1016/j.ydbio.2004.10.003

van den Berg, G., Abu-Issa, R., de Boer, B.A., Hutson, M.R., de Boer, P.A.J., Soufan, A.T., Ruijter, J.M., Kirby, M.L., van den Hoff, M.J.B., Moorman, A.F.M., 2009. A caudal proliferating growth center contributes to both poles of the forming heart tube. Circ. Res. 104, 179–188. doi:10.1161/CIRCRESAHA.108.185843

van Weerd, J.H., Christoffels, V.M., 2016. The formation and function of the cardiac conduction system. Dev. Camb. Engl. 143, 197–210. doi:10.1242/dev.124883

Varga, Z.M., Amores, A., Lewis, K.E., Yan, Y.L., Postlethwait, J.H., Eisen, J.S., Westerfield, M., 2001. Zebrafish smoothened functions in ventral neural tube specification and axon tract formation. Dev. Camb. Engl. 128, 3497–3509.

Vedantham, V., 2015. New Approaches to Biological Pacemakers: Links to Sinoatrial Node Development. Trends Mol. Med. 21, 749–761. doi:10.1016/j.molmed.2015.10.002

Verheijck, E.E., van Kempen, M.J., Veereschild, M., Lurvink, J., Jongsma, H.J., Bouman, L.N., 2001. Electrophysiological features of the mouse sinoatrial node in relation to connexin distribution. Cardiovasc. Res. 52, 40–50.

Vicente-Steijn, R., Passier, R., Wisse, L.J., Schalij, M.J., Poelmann, R.E.,

Gittenberger-de Groot, A.C., Jongbloed, M.R.M., 2011. Funny current channel HCN4 delineates the developing cardiac conduction system in chicken heart. Heart Rhythm Off. J. Heart Rhythm Soc. 8, 1254–1263. doi:10.1016/j.hrthm.2011.03.043

Vokes, S.A., Ji, H., McCuine, S., Tenzen, T., Giles, S., Zhong, S., Longabaugh, W.J.R., Davidson, E.H., Wong, W.H., McMahon, A.P., 2007. Genomic characterization of Gli-activator targets in sonic hedgehog-mediated neural patterning. Dev. Camb. Engl. 134, 1977–1989. doi:10.1242/dev.001966

Vokes, S.A., Ji, H., Wong, W.H., McMahon, A.P., 2008. A genome-scale analysis of the cis-regulatory circuitry underlying sonic hedgehog-mediated patterning of the mammalian limb. Genes Dev. 22, 2651–2663. doi:10.1101/gad.1693008

Wang, F., Flanagan, J., Su, N., Wang, L.-C., Bui, S., Nielson, A., Wu, X., Vo, H.-T., Ma, X.-J., Luo, Y., 2012. RNAscope: a novel in situ RNA analysis platform for formalin-fixed, paraffin-embedded tissues. J. Mol. Diagn. JMD 14, 22–29. doi:10.1016/j.jmoldx.2011.08.002

Wang, J., Klysik, E., Sood, S., Johnson, R.L., Wehrens, X.H.T., Martin, J.F., 2010. Pitx2 prevents susceptibility to atrial arrhythmias by inhibiting left-sided pacemaker specification. Proc. Natl. Acad. Sci. 107, 9753–9758. doi:10.1073/pnas.0912585107

Wang, X., Zhao, Z., Muller, J., Iyu, A., Khng, A.J., Guccione, E., Ruan, Y., Ingham, P.W., 2013. Targeted inactivation and identification of targets of the Gli2a transcription factor in the zebrafish. Biol. Open 2, 1203–1213. doi:10.1242/bio.20136262

Washington Smoak, I., Byrd, N.A., Abu-Issa, R., Goddeeris, M.M., Anderson, R., Morris, J., Yamamura, K., Klingensmith, J., Meyers, E.N., 2005. Sonic hedgehog is required for cardiac outflow tract and neural crest cell development. Dev. Biol. 283, 357–372. doi:10.1016/j.ydbio.2005.04.029

Waxman, J.S., Keegan, B.R., Roberts, R.W., Poss, K.D., Yelon, D., 2008. Hoxb5b acts downstream of retinoic acid signaling in the forelimb field to restrict heart field potential in zebrafish. Dev. Cell 15, 923–934. doi:10.1016/j.devcel.2008.09.009

Wharton, K.A., Serpe, M., 2013. Fine-tuned shuttles for bone morphogenetic

proteins. Curr. Opin. Genet. Dev. 23, 374–384. doi:10.1016/j.gde.2013.04.012

Wiese, C., Grieskamp, T., Airik, R., Mommersteeg, M.T.M., Gardiwal, A., de Gier-de Vries, C., Schuster-Gossler, K., Moorman, A.F.M., Kispert, A., Christoffels, V.M., 2009. Formation of the Sinus Node Head and Differentiation of Sinus Node Myocardium Are Independently Regulated by Tbx18 and Tbx3. Circ. Res. 104, 388–397. doi:10.1161/CIRCRESAHA.108.187062

Witzel, H.R., Cheedipudi, S., Gao, R., Stainier, D.Y.R., Dobreva, G.D., 2017. Isl2b regulates anterior second heart field development in zebrafish. Sci. Rep. 7, 41043. doi:10.1038/srep41043

Witzel, H.R., Jungblut, B., Choe, C.P., Crump, J.G., Braun, T., Dobreva, G., 2012. The LIM Protein Ajuba Restricts the Second Heart Field Progenitor Pool by Regulating Isl1 Activity. Dev. Cell 23, 58–70. doi:10.1016/j.devcel.2012.06.005

Xiao, Y.-F., 2011. Cell and gene therapy for arrhythmias: Repair of cardiac conduction damage. J. Geriatr. Cardiol. JGC 8, 147–158. doi:10.3724/SP.J.1263.2011.00147

Xu, J., Srinivas, B.P., Tay, S.Y., Mak, A., Yu, X., Lee, S.G.P., Yang, H., Govindarajan, K.R., Leong, B., Bourque, G., Mathavan, S., Roy, S., 2006. Genomewide expression profiling in the zebrafish embryo identifies target genes regulated by Hedgehog signaling during vertebrate development. Genetics 174, 735–752. doi:10.1534/genetics.106.061523

Yadin, D., Knaus, P., Mueller, T.D., 2016. Structural insights into BMP receptors: Specificity, activation and inhibition. Cytokine Growth Factor Rev. 27, 13–34. doi:10.1016/j.cytogfr.2015.11.005

Yang, L., Xie, G., Fan, Q., Xie, J., 2010. Activation of the hedgehog-signaling pathway in human cancer and the clinical implications. Oncogene 29, 469–481. doi:10.1038/onc.2009.392

Ye, W., Wang, J., Song, Y., Yu, D., Sun, C., Liu, C., Chen, F., Zhang, Y., Wang, F., Harvey, R.P., Schrader, L., Martin, J.F., Chen, Y., 2015. A common Shox2-Nkx2-5 antagonistic mechanism primes the pacemaker cell fate in the pulmonary vein myocardium and sinoatrial node. Development 142, 2521–2532. doi:10.1242/dev.120220

Yelon, D., Horne, S.A., Stainier, D.Y., 1999. Restricted expression of cardiac myosin genes reveals regulated aspects of heart tube assembly in zebrafish. Dev. Biol. 214, 23–37. doi:10.1006/dbio.1999.9406

Yu, P.B., Hong, C.C., Sachidanandan, C., Babitt, J.L., Deng, D.Y., Hoyng, S.A., Lin, H.Y., Bloch, K.D., Peterson, R.T., 2008. Dorsomorphin inhibits BMP signals required for embryogenesis and iron metabolism. Nat. Chem. Biol. 4, 33–41. doi:10.1038/nchembio.2007.54

Zeng, X.-X.I., Yelon, D., 2014. Cadm4 restricts the production of cardiac outflow tract progenitor cells. Cell Rep. 7, 951–960. doi:10.1016/j.celrep.2014.04.013

Zhan, C., Baine, W.B., Sedrakyan, A., Steiner, C., 2008. Cardiac Device Implantation in the United States from 1997 through 2004: A Population-based Analysis. J. Gen. Intern. Med. 23, 13–19. doi:10.1007/s11606-007-0392-0

Zhang, X.M., Ramalho-Santos, M., McMahon, A.P., 2001. Smoothened mutants reveal redundant roles for Shh and Ihh signaling including regulation of L/R symmetry by the mouse node. Cell 106, 781–792.

Zhou, Y., Cashman, T.J., Nevis, K.R., Obregon, P., Carney, S.A., Liu, Y., Gu, A., Mosimann, C., Sondalle, S., Peterson, R.E., Heideman, W., Burns, C.E., Burns, C.G., 2011. Latent TGFβ binding protein 3 identifies a second heart field in zebrafish. Nature 474, 645–648. doi:10.1038/nature10094

Appendix: Utilizing zebrafish to understand second heart field development

Reprinted from: Knight, H.G., Yelon, D., 2016. Utilizing Zebrafish to Understand Second Heart Field Development, in: Nakanishi, T., Markwald, R.R., Baldwin, H.S., Keller, B.B., Srivastava, D., Yamagishi, H. (Eds.), Etiology and Morphogenesis of Congenital Heart Disease: From Gene Function and Cellular Interaction to Morphology. Springer Japan, Tokyo, pp. 193–199.

Abstract

Heart formation relies on two sources of cardiomyocytes: the first heart field (FHF), which gives rise to the linear heart tube, and the second heart field (SHF), which gives rise to the right ventricle, the outflow tract, parts of the atria, and the inflow tract. The development of the SHF is of particular importance due to its relevance to common congenital heart defects. However, it remains unclear how the SHF is maintained in a progenitor state while the FHF differentiates. Likewise, the factors that trigger SHF differentiation into specific cardiac cell types are poorly understood. Investigation of SHF development can benefit from the utilization of multiple model organisms. Here, we review the experiments that have identified the SHF in zebrafish and investigated its contribution to the poles of the zebrafish heart. Already, zebrafish research has illuminated novel positive and negative regulators of SHF development, cementing the utility of zebrafish in this context.

Keywords: Second heart field, zebrafish, outflow tract, inflow tract

H.G. Knight and D. Yelon, Ph.D.*

Division of Biological Sciences, University of California, San Diego, La Jolla, CA 92093 USA

*email: dyelon@ucsd.edu

Introduction

The embryonic origins of the heart have been a topic of intense interest due to the prevalence of congenital heart defects [1]. Cardiac progenitors (CPs) from the first heart field (FHF) form the initial heart tube, and CPs from the second heart field (SHF) contribute to most of the structures of the mature heart including the outflow tract, right ventricle, and much of the atria [2]. The SHF is generally defined as a population of CPs that originates adjacent to the FHF, differentiates after the initial heart tube has formed, and is responsible for cardiomyocyte accretion at both poles of the heart tube [2]. The SHF is particularly significant to congenital heart disease: many common cardiac abnormalities are caused by defects in SHF-derived tissues, including ventricular and atrial septal defects, transposition of the great arteries, and double outlet right ventricle [3]. Despite the importance of the SHF, the mechanisms that distinguish FHF and SHF development remain unclear. What signals or factors prevent the SHF from differentiating while the FHF is deployed, and what eventual change triggers SHF differentiation? Recent advances in zebrafish research offer new approaches that can complement work in mouse to deepen our comprehension of SHF regulation.

Several lines of evidence indicate the presence of a population of late-differentiating CPs in zebrafish that is likely to be analogous to the mammalian SHF. The conservation of the SHF provides exciting opportunities to advance our understanding using the distinct advantages of zebrafish embryos [4].

Zebrafish embryos develop rapidly and have small hearts that are particularly tractable for cellular resolution of cardiogenesis. Furthermore, the transparency of the zebrafish embryo facilitates exceptional opportunities for time-lapse imaging of heart formation and tracking of cardiac cell fates. Finally, zebrafish are particularly well suited for conducting both genetic and chemical screens, which have the potential to identify novel regulators of heart development. Here, we review the studies that support the existence of a zebrafish SHF and demonstrate the utility of the zebrafish for opening new avenues in SHF research.

Late-differentiating cardiomyocytes originate from the SHF in zebrafish

Two types of assays have demonstrated that late-differentiating cardiomyocytes are recruited to the poles of the zebrafish heart tube. First, a developmental timing assay that relies on the different kinetics of GFP and DsRed fluorescence was used to visualize the dynamics of cardiomyocyte differentiation. Analysis of *Tg(myl7:GFP); Tg(myl7:DsRed)* embryos showed that newly-differentiated cardiomyocytes populate the cardiac poles at 48 hours post-fertilization (hpf), whereas cardiomyocytes in the middle of the heart differentiate at an earlier stage (Fig. 31.1A; [5]). Second, photoconversion assays have consistently revealed late-differentiating cardiomyocytes in the outflow tract. UV exposure of *Tg(myl7:kaede)* or *Tg(myl7:KikGR)* embryos after the heart tube has formed, followed by imaging

at 48 hpf, showed addition of cardiomyocytes to the outflow tract after the time of photoconversion (Fig. 31.1B, [5, 6]). Together, these experiments revealed the existence of late-differentiating cardiomyocytes at the arterial pole of the zebrafish heart that seem to be analogous to SHF-derived cardiomyocytes in mammals.

Fate mapping in zebrafish has shown that early SHF precursors seem to neighbor the FHF. Prior to gastrulation, arterial pole progenitors are found adjacent to ventricular progenitors at the embryonic margin (Fig. 31.1C; [7]). After gastrulation, arterial pole progenitors map to a medial cranial region next to the FHF in the anterior lateral plate mesoderm (ALPM) (Fig. 31.1C; [7]). Finally, DiI labeling has shown that the SHF resides adjacent to the heart tube in older embryos: pericardial cells just outside the outflow tract at 24 hpf move into the arterial pole at later stages [7]. The SHF has also been identified using Cre-mediated lineage tracing: this technique has shown that arterial pole progenitors express both *gata4* and *nkx2.5* during somitogenesis, confirming that SHF progenitors originate in the ALPM [8]. Furthermore, Cre-mediated lineage tracing has confirmed that cells from the pericardial mesenchyme adjacent to the heart tube migrate into the outflow tract [9]. Taken together, these analyses show that the late-differentiating cardiomyocytes at the zebrafish arterial pole meet the criteria that define the SHF. Outflow tract cells remain undifferentiated until after the linear heart tube has formed, are recruited to the arterial pole from outside the heart, and map to an area

adjacent to the FHF. These data, combined with conserved molecular mechanisms regulating mouse and zebrafish arterial pole development, suggest that the SHF is a conserved vertebrate feature.

Mechanisms regulating outflow tract development in zebrafish

Studies of the regulation of outflow tract formation have demonstrated conservation of the transcription factors utilized in zebrafish and mouse. Zebrafish embryos deficient in *mef2cb* lack late-differentiating cells that form the outflow tract [6], which is strikingly similar to the phenotype of *Mef2c* mutant mice that lack the SHF-derived outflow tract and right ventricle [10]. Zebrafish *tbx1* mutants have several outflow tract defects, including reduced migration of cells into the heart [7] and reduced proliferation of cells at the arterial pole, resulting in a small outflow tract [11]. This phenotype is reminiscent of mouse *Tbx1* mutants, which also display outflow tract abnormalities due to severely reduced proliferation in the SHF [12].

Signaling pathways also seem to have conserved roles in the mouse and zebrafish SHF. Hedgehog signaling is important for zebrafish SHF development: migration of cells into the heart is impaired in *smoothened* mutants, resulting in a small outflow tract [7]. Similarly, Hedgehog signaling is crucial for mammalian SHF survival and outflow tract septation [13]. In zebrafish, reduced Fgf signaling eliminates accretion of cardiomyocytes at the arterial pole [5] and blocks *mef2cb* expression in the SHF [6]. This requirement

for Fgf signaling mimics mouse *Fgf8* mutants, which have a severely hypoplastic outflow tract and right ventricle [13]. These findings underscore the conserved mechanisms regulating outflow tract development and suggest that new discoveries in the zebrafish SHF are likely to be relevant to mammals.

Importantly, novel insights into outflow tract development have emerged through studies in zebrafish. The role of Ltbp3, a secreted protein that regulates TGF-β ligand availability, has been of particular interest. *ltbp3* is expressed in the zebrafish SHF, and Cre-mediated lineage tracing has shown that *ltbp3*-expressing cells give rise to outflow tract cardiomyocytes [9]. Ltbp3-deficient embryos lack an outflow tract due to reduced SHF proliferation, a consequence of reduced TGF-β signaling [9]. This work not only illuminated Ltbp3 as a new SHF regulator but also uncovered a novel role for TGF-β signaling in SHF development. Additional studies have revealed that Nkx2.5 promotes maintenance of *ltbp3* expression [8]. This is exciting, as it elucidates a new pathway downstream of Nkx2.5: Nkx2.5 facilitates the activation of TGF-β signaling through regulation of *ltbp3* and thereby drives SHF proliferation. Since Nkx2.5 is highly relevant to congenital heart disease, factors downstream of Nkx2.5 are excellent candidates for translational research. Thus, investigations in zebrafish can lead to the discovery of novel regulators of SHF development and provide new insight into connections between important factors.

Mechanisms regulating inflow tract development in zebrafish

In mouse, the SHF has been shown to contribute to the venous pole in addition to the arterial pole [2]. The mammalian SHF is thought to be subdivided into the anterior SHF, which gives rise to the right ventricle and outflow tract, and the posterior SHF, which gives rise to the atria and the inflow tract [2]. The zebrafish heart has a distinct population of inflow tract cells that express the canonical SHF marker Isl1 [14]. In addition, developmental timing assays have shown that the zebrafish inflow tract contains a population of late-differentiating cardiomyocytes (Fig. 31.1A; [5]). However, the degree of overlap between these two populations has not been examined, and the precise timing of when inflow tract cells are added to the heart is unclear. Furthermore, it is not known where zebrafish inflow tract cells originate in the early embryo and if inflow and outflow tract progenitors share a common lineage. Future experiments will be valuable to elucidate the zebrafish equivalent of the mammalian posterior SHF.

Studies of inflow tract development in zebrafish have revolved around the role of Isl1. Zebrafish *isl1* mutants lack late-differentiating cardiomyocytes at the venous pole [5]. This phenotype is similar to that of *Isl1* null mouse embryos, which lack SHF-derived atrial cardiomyocytes [15]. Interestingly, studies in zebrafish have identified a novel requirement for the LIM domain protein Ajuba, which directly interacts with Isl1 [14]. Ajuba-deficient embryos have large hearts with an excess of Isl1-expressing cells and an expansion of

SHF markers in the ALPM. Conversely, Ajuba overexpression eliminates Isl1 in the inflow tract [14]. Ajuba is one of the first factors that has been shown to limit SHF development, and the presence of Ajuba may determine whether Isl1 activity promotes or limits cardiomyocyte formation. The identification of Ajuba as a negative regulator of inflow tract formation further illustrates the utility of zebrafish for the discovery of novel factors involved in SHF development.

Future directions and clinical implications

Altogether, the studies summarized here support the value of the zebrafish for the investigation of SHF development. It will be particularly exciting for future work in zebrafish to probe important open questions in this area. For example, zebrafish studies may be valuable for elucidating the mechanisms that pattern the SHF into its anterior and posterior subdivisions. In addition, it will be interesting to use zebrafish to examine the factors that control differentiation of multipotent SHF cells into myocardial, endocardial, and smooth muscle lineages [9]. Zebrafish will also be valuable for exploring whether multipotent SHF cells are maintained after embryogenesis, perhaps to be deployed after injury. In the long term, use of the zebrafish for analysis of SHF development is likely to illuminate pathways that facilitate our understanding of the etiology of congenital heart disease.

Acknowledgments

Research in the Yelon laboratory is supported by grants from the NIH/NHLBI, American Heart Association, and March of Dimes. H.G.A. is supported by the UCSD Training Program in Cell and Molecular Genetics (NIH T32 GM007240).

References

1. Hoffman JIE, Kaplan S (2002) The incidence of congenital heart disease. J Am Coll Cardiol 39:1890–1900.

2. Kelly RG (2012) The Second Heart Field. Curr Top Dev Biol 100:33–65.

3. Gittenberger-de Groot AC, Bartelings MM, Poelmann RE, Haak MC, Jongbloed MR. (2013) Embryology of the heart and its impact on understanding fetal and neonatal heart disease. Semin Fetal Neonatal Med 18:237–244.

4. Scott IC, Yelon D (2010) Cardiac Development in the Zebrafish. In: Rosenthal N, Harvy RP (eds) Heart Development and Regeneration, Academic Press, Oxford, p 103-120.

5. De Pater E, Clijsters L, Marques SR, Lin YF, Garavito-Aguilar ZV, Yelon D, Bakkers J. (2009) Distinct phases of cardiomyocyte differentiation regulate growth of the zebrafish heart. Development 136:1633–1641.

6. Lazic S, Scott IC (2011) Mef2cb regulates late myocardial cell addition from a second heart field-like population of progenitors in zebrafish. Dev Biol 354:123–133.

7. Hami D, Grimes AC, Tsai H-J, Kirby ML. (2011) Zebrafish cardiac development requires a conserved secondary heart field. Development 138:2389–2398.

8. Guner-Ataman B, Paffett-Lugassy N, Adams MS, Nevis KR, Jahangiri L, Obregon P, Kikuchi K, Poss KD, Burns CE, Burns CG. (2013) Zebrafish second heart field development relies on progenitor specification in anterior lateral plate mesoderm and nkx2.5 function. Development 140:1353–1363.

9. Zhou Y, Cashman TJ, Nevis KR, Obregon P, Carney SA, Liu Y, Gu A, Moismann C, Sondalle S, Peterson RE, Heiderman W, Burns CE, Burns CG. (2011) Latent TGF-β binding protein 3 identifies a second heart field in zebrafish. Nature 474:645–648.

10. Lin Q, Schwarz J, Bucana C, Olson EN. (1997) Control of Mouse Cardiac Morphogenesis and Myogenesis by Transcription Factor MEF2C. Science 276:1404–1407.

11. Nevis K, Obregon P, Walsh C, Guner-Ataman B, Burns CG, Burns CE. (2013) Tbx1 is required for second heart field proliferation in zebrafish.

Dev Dyn 242:550–559.

12. Greulich F, Rudat C, Kispert A (2011) Mechanisms of T-box gene function in the developing heart. Cardiovasc Res 91:212–222.

13. Rochais F, Mesbah K, Kelly RG (2009) Signaling Pathways Controlling Second Heart Field Development. Circ Res 104:933–942.

14. Witzel H, Jungblut B, Choe CP, Crump JG, Braun T, Dobreva G. (2012) The LIM Protein Ajuba Restricts the Second Heart Field Progenitor Pool by Regulating Isl1 Activity. Dev Cell 23:58-70.

15. Cai C-L, Liang X, Shi Y, Chu PH, Pfaff SL, Chen J, Evans S. (2003) Isl1 identifies a cardiac progenitor population that proliferates prior to differentiation and contributes a majority of cells to the heart. Dev Cell 5:877–889.

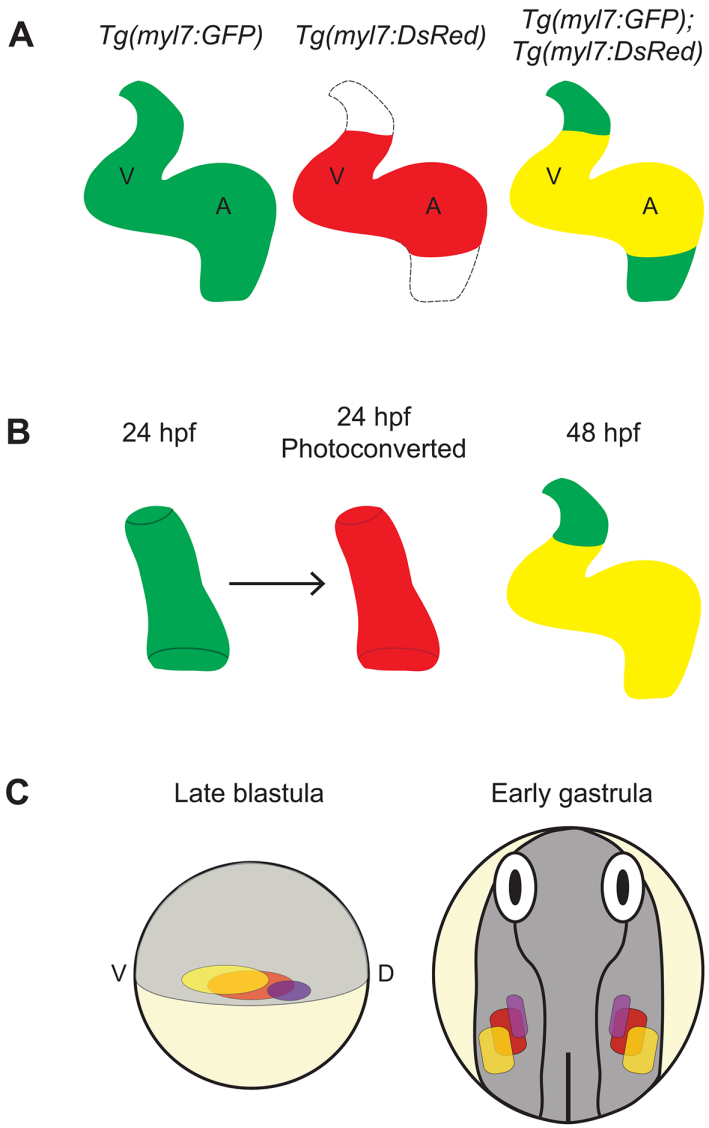

Figure A.1 *Late-differentiating cardiomyocytes originate from the zebrafish SHF.* (A) A developmental timing assay reveals late-differentiating cardiomyocytes displaying GFP, but not DsRed [5]. (B) Green-to-red conversion of photoconvertible proteins expressed in differentiated cardiomyocytes at 24 hpf, followed by imaging at 48 hpf, reveals newly-added green cardiomyocytes in the outflow tract [6]. (C) Fate mapping in the late blastula shows that outflow tract progenitors (purple) are located close to the margin, adjacent to ventricular progenitors (red) and separate from atrial progenitors (yellow) [7]. In the early gastrula, outflow tract progenitors are located in a medial cranial portion of the ALPM [7].

ACKNOWLEDGMENTS

This appendix, in full, is a reformatted reprint of the following book chapter: Knight, H.G., Yelon, D., 2016. Utilizing Zebrafish to Understand Second Heart Field Development, in: Nakanishi, T., Markwald, R.R., Baldwin, H.S., Keller, B.B., Srivastava, D., Yamagishi, H. (Eds.), Etiology and Morphogenesis of Congenital Heart Disease: From Gene Function and Cellular Interaction to Morphology. Springer Japan, Tokyo, pp. 193–199. Hannah Knight was the primary author of this paper.